UNIVERSIDAD AUTÓNOMA DE MADRID

Programa de Doctorado en Biociencias Moleculares

Endoglin, a novel biomarker and therapeutic target in malignant peripheral nerve sheath tumors

Teresa González Muñoz

Madrid, 2022

Universidad Autónoma de Madrid

CENTRO NACIONAL DE INVESTIGACIONES ONCOLÓGICAS

UNIVERSIDAD AUTÓNOMA DE MADRID

Departamento de Bioquímica, Facultad de Medicina.

Programa de Doctorado en Biociencias Moleculares

Endoglin, a novel biomarker and therapeutic target in malignant peripheral nerve sheath tumors

Teresa González Muñoz

Bachelor Degree in Biotechnology

Master in Advanced Therapies

Thesis Director

Dr. Héctor Peinado Selgas

Microenvironment and Metastasis group, Molecular Oncology Programme

Spanish National Cancer Research Centre

Madrid, 2022

Dr. Héctor Peinado Selgas, head of the Microenvironment and Metastasis Group at the Spanish National Cancer Research Centre (CNIO).

CERTIFIES:

That the study "**Endoglin, a novel biomarker and therapeutic target in malignant peripheral nerve sheath tumors**" developed by Teresa González Muñoz meets the necessary requirements to obtain the PhD degree in Molecular Biosciences. To this purpose, she will defend her Doctoral Thesis at the Universidad Autónoma de Madrid. This work has been carried out under my direction, and hereby I authorize its defense to an appropriate Thesis Committee.

I hereby issue this certificate in Madrid on January 24th, 2022

Héctor Peinado Selgas, PhD
Thesis Director

cnïo CENTRO NACIONAL DE INVESTIGACIONES ONCOLÓGICAS

This thesis, submitted for the degree of Doctor in Philosophy in Molecular Biosciences at the Universidad Autónoma de Madrid, has been completed in the Microenvironment and Metastasis Laboratory at the Spanish National Cancer Research Centre (CNIO), under the supervision of Dr. Héctor Peinado Selgas.

This work was supported by the following fellowships and grants:

- FPU PhD Fellowship. 2017-2022.
- United States Department of Defense. W81XWH-16-1-0131.
- Fundación Proyecto Asociación de Afectados de Neurofibromatosis.

A mis padres.

ACKNOWLEDGEMENTS

AGRADECIMIENTOS

Por fin, después de unos meses largos de escritura intensa sobre los tumores malignos de la vaina del nervio periférico y la endoglina, llega la hora de abordar mi parte preferida de esta tesis doctoral. En ella, quiero agradecer al tesoro más grande que me llevo de estos seis largos años, es decir, a todas las personas que me han acompañado durante este tiempo y cuyos nombres ya forman parte especial de mi vida. No sé si seré capaz de plasmar en tan sólo unas líneas todo lo que siento, pero, una cosa tengo clara, saldrá directo del corazón.

En primer lugar, quiero dar las GRACIAS a **Héctor**, mi director de tesis y constante apoyo y acompañante. Me has enseñado muchísimo a nivel científico: a preguntarme el por qué de las cosas y hacer que me atreviera a dar respuestas, a aportar y ejecutar ideas propias en el proyecto, a enfrentarme a charlas algo lejos de España con público bastante mayor que yo y, sobre todo, a disfrutar mucho mucho de la ciencia. Además de todo ello, nos has transmitido algo que me ha llegado muy dentro: tus ganas inmensas de disfrutar de la vida. Gracias Héctor por mostrarnos que, aunque a veces las circunstancias se vuelvan duras, la fuerza, el coraje, la valentía y la ilusión te hacen seguir adelante. Gracias por tu SÍ de aquel día hace ya unos siete años que me permitió comenzar esta aventura, la cual ha sido un auténtico regalo para mí.

Durante este tiempo, he tenido la oportunidad de conocer a compañeros de viaje extraordinarios con los que he compartido muchas, muchísimas horas. Fueron llegando poco a poco al laboratorio y a mi vida, formando la gran familia M&M.

Ana, fuiste la primera persona que me recibió en el laboratorio y, aunque parecías “muy apañá”, en ese momento no me podía hacer ni una idea de todo lo bueno que llevas dentro. Te doy las gracias por haberme permitido descubrirte y conocerte a fondo. Ani, estás llena de luz, de paz, de bondad, de coraje, de estabilidad, de generosidad y de un amor que te hace muy especial. Recuerda: “el mejor de tus sentidos es tu sentido del amor”. Ya sabes lo importante que eres para mí y pido seguir compartiendo contigo mucho bueno. **Susana**, gracias por todo lo que me has enseñado desde tu gran experiencia. Fuiste la que me diste la mano para empezar a experimentar en este laboratorio y me presentaste los primeros datos de mi proteína preferida, endoglina. Gracias por ayudarme siempre que lo he necesitado y hacerlo con tanto cariño. **Crisme**, la alegría de mi huerta, de mi poyata, de mi mesa, de mi día en el laboratorio y de mil aventuras juntas. Gracias por tu constante ayuda y por enseñarme que la vida con optimismo e ilusión es mucho más bonita. Que nunca te falten esas ganas de comerte el mundo que tanto te caracterizan. **Luci**, mi Lusssi, mi Pepi, mi Mili, mi compañera de tesis

y mi amiga del alma. Tuve la suerte de que fueras tú, que eres de esos regalos con los que la vida te premia a veces. Nos hemos hecho más de un 24/5 juntas y, en varias ocasiones, tu familia, tan maja como es, me invitaba a pasar el fin de semana con vosotros para que no nos echáramos de menos en esos dos días. Gracias por nuestras cómicas discusiones, nuestras largas horas en CNIO, nuestras aventuras exteriores (como "tu borrachera" en Barcelona jeje) y, sobre todo, por tu amistad fiel y enorme cariño. No me imagino esta tesis sin ti a mi lado, menos mal que nos queda pendiente Pekín Express. **Marta**, me ganaste el primer día cuando me dijiste que habías estudiado y vivido en nuestra querida Córdoba. Gracias por haberme escuchado y ayudado siempre que lo he necesitado. He podido disfrutar a través de ti de una de mis asignaturas pendientes preferidas, la maternidad ;) **Marina**, gracias por llenarnos de orden y de colores todas las poyatas y todo el laboratorio, por tu gran apoyo y cariño. Te deseo que la vida te premie con todo lo bueno que te mereces, que es mucho. **Sara**, que lo que ha unido un experimento de 50 ratones, no lo separe el hombre. Gracias por tu enorme ayuda, por hacerme una "oral gavage machine" y por ser la mejor amiga invisible del mundo. Ha sido una suerte conocerte y compartir trabajo y vida contigo. **Albert**, a estas alturas de la vida, la tesis me ha regalado algo muy grande: un hermanito. No, sangre no tenemos la misma y pensamientos iguales, en muchos casos, tampoco. Es el cariño tan grande, verdadero y puro que hay entre nosotros el que nos convierte en familia. Gracias por compartir conmigo alegrías, discusiones, confidencias, sufrimientos, reflexiones, bromas, risas, casa, comida y hasta padres (mis "padres adoptivos" en Madrid). Gracias por cuidarme y apoyarme como lo haces. Lo que se ha formado entre nosotros es un tesoro y espero que los dos lo cuidemos y mantengamos vivo siempre. **Claudia**, gracias por tu ayuda y por acompañarme en el camino de la endoglina. Te deseo lo mejor en el trabajo y en la vida. **Alberto III**, nuestro médico preferido. Gracias por la alegría que desprendías en el laboratorio con tus bromas y ocurrencias. Ha sido genial coincidir contigo y aprender de ti la parte más clínica de este campo. Espero que te vaya fenomenal en tu etapa estadounidense. **Ali**, gracias por acompañarme durante los primeros años de tesis y por permitirme descubrir toda la bondad y generosidad que llevas dentro. Eres una persona excelente y serás una doctora brillante. **Laura**, qué alegría que a mitad de mi tesis te incorporaras al laboratorio. Recuerdo que conectamos desde el primer momento y, a pesar de mis dotes de marquesa, se estableció entre nosotros una relación muy especial. Gracias por cuidarme y querer siempre lo mejor para mí, por hacerme ver lo importante y lo bonito de la vida cuando yo lo veo negro, por organizar momentos únicos que se quedarán siempre con nosotros y por nuestras charlas eternas que me llenan de energía. A seguir sumando mucho juntas, Lau. Ya sabes que, aunque no seas mi primera amiga doctora, eres una amiga a la que quiero

mucho. **Elena**, gracias por llevar el título “Paquito” con el mismo orgullo que yo y por acompañarme en estos años de tesis. Me ha encantado conocerte, descubrir tu ahínco, fortaleza y ganas de cambiar el mundo. Aunque ya no esté en el día a día del laboratorio, me tienes para lo que necesites y espero que sigamos compartiendo momentos juntas. **Vane**, un ángel que cayó del cielo en mi último año de tesis. Gracias por las miles de horas juntas haciendo de cirujanas de nervio ciático, por transmitirme paz y serenidad, por tu enorme bondad y por estar siempre dispuesta a ayudarme aunque no te cupieran más cosas en el día. **Juan**, ha sido genial conocerte en la última etapa de tesis. Gracias por apoyarme sobre todo en los meses de escritura que han sido los más duros y reservarme siempre la mesa de la biblioteca. Disfruta mucho y sácale el máximo partido a esta experiencia porque luego la vas a recordar con mucho cariño. **Kike**, mi compañero de poyata en los últimos meses, aunque te la he dejado bastante libre. Te quedas al cargo de ese lado, aprovecha mucho todo. Gracias por cerrar conmigo tantas tardes de viernes de la mejor forma posible (aún con percances de centrífuga incluidos) y por estar a mi lado en la recta final.

Además, por nuestro laboratorio han pasado excelentes estudiantes y magníficas personas: **Iñaki**, **Silvia**, **Ainhoa**, **Olwen**, **Eva**, **Raúl**, **JC**, **Ariane**, **Bélen**, **Ane**, **Edu**. Gracias a todos, cada uno de vosotros dejasteis una huella especial en el laboratorio, en mi etapa pre-doctoral y en mi vida.

A compañeros de otros laboratorios del CNIO también les debo profundos y sinceros agradecimientos. A **Vero**, gracias por compartir conmigo crisis tésicas pero también muchas alegrías y platos riquísimos ;) Espero que la vida nos siga regalando muchos más momentos juntas. A **Ana Belén**, mi cordobesa preferida en el CNIO. A veces los momentos duros de la vida dejan mucho bueno. Yo doy gracias por haberte descubierto y conocido a fondo, eres estupenda. Nos quedan muchas ferias y aventuras pendientes. A **Nerea**, **Celia**, **Ana** y **Cris** con las que he disfrutado de más de una cerveza, risa y fiesta. A **Laura**, gracias por deleitarnos con tus cantos en el karaoke y con tu simpatía constate. A los chicos de Valiente Lab: **Peter**, con el que además de unos ratones endoglina *flox*, he compartido viajes, vivencias, fiestas y mucho cariño; **Mariam**, gracias por la enorme paciencia que tuviste enseñándome tus habilidades quirúrgicas; **Ana**, **Laura**, **Neibla** y **Lucía**, siempre tan serviciales, generosas y cariñosas conmigo. A **Xavi**, **Marta**, **Cris** y **Davide,** con los he tenido interesantes charlas científicas y personales e incluso divertidos bailes. Y gracias a nuestros vecinos más cercanos, **Patri**, **Elena**, **Dani**, **Sergio**, **Miriam**, **Magali**, **Carmen**, por aguantar nuestros gritos y dejarnos lo que necesitábamos en todo momento.

Este trabajo tampoco hubiera sido posible sin la ayuda de todas las personas de las Unidades del CNIO. Quiero agradecer especialmente a **Patri** y **Eduardo**, de la Unidad de Histopatología; a **Isabel**, **Gema Luque**, **Gema Iglesias**, **Virginia** y **Flor**, de la Unidad de Animalario; a **Diego**, **Manu**, **Jesús** y **Gadea**, de la Unidad de Microscopía Confocal; a **Paqui** y **Guillermo**, de la Unidad de Imagen Molecular, y a **Osvaldo** y **Héctor**, de la Unidad de Bioinformática. Gracias a todos por atenderme siempre con tanta amabilidad y cercanía. Vuestra contribución a este proyecto ha sido enorme. Gracias también a **Paloma Olave** por facilitarnos los trámites y las asistencias a todos los viajes y congresos. Tampoco me puedo olvidar de todo el personal de limpieza, cafetería y seguridad, que con tanto cariño me han tratado durante estos años. Me es imposible nombraros a todos, pero os llevo en el corazón.

También me gustaría agradecer a los miembros de mi comité de tesis: **Carmen Blanco, Eduard Serra** y **Manuel Valiente**. Gracias por interesaros por este proyecto, aportar excelentes ideas desde vuestra enorme experiencia y, sin duda, dar un fuerte impulso a esta tesis.

Asimismo, quiero hacer una mención especial a la **Fundación de Afectados de Neurofibromatosis**, que me ha permitido conocer en persona la realidad y la fortaleza de estos pacientes. No tengo duda de que seguiremos trabajando para conseguir entre todos que la esperanza y calidad de vida siga mejorando.

Y, por supuesto, yo no hubiera llegado hasta aquí sin el apoyo de los de siempre. Gracias a mis tíos y primos bujalanceños, lucentinos, madrileños y malagueños por cuidarme y quererme tanto desde pequeñita. Siempre me he considerado una afortunada por tener una familia tan unida y maravillosa como la nuestra. Gracias a mis amigos de toda la vida, **Águeda**, **Celina**, **Jesús**, **Jose**, **María**, **Martina**, **Miguel**, **Melchor**, que tienen un arte especial para hacerme sonreír y disfrutar de la vida a pesar de mis agobios. Con vosotros me siento siempre en familia. Doy gracias infinitas por nuestra amistad. Gracias a mis amigos mayores de Bujalance y Córdoba, que me acompañan y me dan fuerzas en todas mis aventuras y con los que tan a gusto me siento siempre.

Tengo un hueco especial reservado para **mis padres**. Qué deciros: que me emociono al empezar a escribir estas líneas. Gracias por confiar en mí y por apoyarme constantemente durante estos años de tesis doctoral y siempre. Gracias por enseñarme a vivir con sentido amando a los demás. Gracias por la relación que hemos ido construyendo entre los tres, la cual es cada vez más madura, más estrecha, más sólida.

Uno de los grandes motivos por los que yo hoy estoy aquí sois vosotros. Papá, mamá, os quiero mucho.

Y gracias al regalo deseado durante mucho tiempo, real en la última etapa de tesis. Gracias **Fran** por tu compresión, tu ayuda, tu paciencia, tu cercanía y tu cariño. Me dijiste que esta tesis la acabaríamos juntos y así ha sido literalmente. Menos mal que no me tiraste el ordenador por la ventana. Que sigamos viviendo mucho más de la mano. Eres el mejor compañero de camino que podía tener.

Termino dando gracias a la **FUERZA**, que, sin ser nuestra, está en nuestro interior y es la que nos sostiene, nos da sentido en el vivir y energías para ser libres y para amar.

SUMMARY

Malignant peripheral nerve sheath tumors (MPNSTs) are highly aggressive soft tissue sarcomas that represent an important clinical challenge due to their high tendency to relapse and metastasize and their relatively poor response to conventional therapies. Likewise, targeted agents have thus far failed to demonstrate clinical efficacy in MPNSTs. Therefore, there is a significant lack of known effective treatments for these patients, which underscores the urgent need for new therapeutic strategies.

In this PhD thesis, we attempted to identify mediators of MPNST pathogenesis, aiming to find novel therapeutic opportunities. Based on preliminary data from our laboratory, we focused on investigating the potential role of the TGF-β coreceptor endoglin (ENG) in MPNST malignancy and progression.

We have discovered that ENG is upregulated in both tumor and endothelial cells of human MPNSTs and, its expression correlates with advanced stages of the disease (i.e. local recurrence and distant metastasis). Moreover, we observed increased ENG levels in plasma circulating small extracellular vesicles from patients with MPNSTs. Mechanistically, we revealed that ENG modulates the activation of the SMAD1/5 and MAPK/ERK signaling pathways and the expression of pro-metastatic and pro-angiogenic genes in the STS26T and ST88-14 human MPNST cell lines. Our data also demonstrate an active role for tumor cell-specific ENG in MPNST progression *in vivo*, positively regulating both tumor cell proliferation and tumor-associated angiogenesis in STS26T tumors. Therapeutically, we found that the anti-ENG antibodies TRC105 and M1043 impair tumor growth and lymph node metastasis in STS26T and ST88-14 xenograft models, reducing tumor cell proliferation, metastatic ability and angiogenesis. Notably, the combination of these anti-ENG therapies with the MEK inhibitor PD-901 synergistically inhibited tumor growth, and almost abolished spontaneous and experimental metastasis in STS26T xenograft models. The analysis of the mechanisms involved showed that ENG targeting cooperates with MEK inhibition to block the activation of the Smad1/5 and MAPK/ERK pathways in both STS26T and ST88-14 cells and to decrease tumor cell proliferation and angiogenesis in primary tumors.

Overall, our data unveil a tumor-promoting function of ENG in MPNSTs and support the use of this protein as a novel biomarker and a promising therapeutic target for this disease. Notably, we also provide preclinical evidence that dual pharmacological inhibition of ENG and MEK represents an attractive approach for the treatment of these tumors.

RESUMEN

Los tumores malignos de la vaina del nervio periférico (MPNSTs, por sus siglas en inglés) son sarcomas de tejidos blandos muy agresivos, que suponen un reto clínico importante debido a su alta tendencia a recurrir y metastatizar y, a su escasa respuesta a las terapias convencionales. Asimismo, los agentes dirigidos que han sido estudiados hasta ahora en ensayos clínicos de pacientes con MPNSTs no han demostrado eficacia. Por tanto, hay una falta notable de tratamientos efectivos para estos pacientes, lo que pone de relieve la necesidad urgente de nuevas estrategias terapéuticas. En esta tesis doctoral, hemos tratado de identificar mediadores de la patogénesis de MPNSTs, con el objetivo de encontrar nuevas opciones farmacológicas. Basándonos en datos preliminares de nuestro laboratorio, nos centramos en analizar el papel de endoglina (ENG) en la malignidad y la progresión de MPNSTs. Hemos descubierto que la expresión de ENG está aumentada tanto en células tumorales como en células endoteliales de muestras humanas de MPNSTs, y correlaciona con estadios avanzados de la enfermedad (i.e. recurrencia local y metástasis distal). Además, observamos que los pacientes con MPNSTs presentan niveles elevados de ENG en vesículas extracelulares pequeñas circulantes en plasma. Asimismo, desde un punto de vista mecanístico, revelamos que ENG promueve la activación de las rutas de señalización Smad1/5 y MAPK/ERK así como la expresión de genes pro-angiogénicos y pro-metastásticos en las líneas celulares de MPNST humano STS26T y ST88-14. Nuestros datos también indican que ENG desempeña un papel activo en la progresión de MPNSTs *in vivo*, promoviendo tanto la proliferación de las células cancerígenas como la angiogénesis en tumores de células STS26T. Desde un punto de vista terapéutico, demostramos que los anticuerpos anti-ENG TRC105 y M1043 reducen el crecimiento tumoral y la metástasis a nódulo linfático en xenoinjertos derivados de células STS26T y ST88-14, al disminuir la proliferación y habilidad metastásica de las células tumorales y la angiogénesis. De manera importante, la combinación de estos anticuerpos anti-ENG con el inhibidor de MEK PD-901 redujo de manera sinérgica el crecimiento tumoral y eliminó casi por completo la metástasis espontánea y experimental en xenoinjertos de STS26T. El análisis de los mecanismos implicados mostró que la inhibición dual de MEK y ENG actúa de forma cooperativa bloqueando la activación de las vías Smad1/5 y MAPK/ERK en las células STS26T y ST88-14 y, disminuyendo la proliferación de las células tumorales y la angiogénesis en tumores primarios. En su conjunto, nuestros datos demuestran que ENG funciona como un promotor tumoral en MPNSTs y apoyan su uso como un nuevo biomarcador y una diana terapéutica para esta enfermedad. También, proporcionamos evidencia preclínica de que la combinación de terapias anti-ENG y anti-MEK es una estrategia atractiva para el tratamiento de estos tumores.

INDEX

ABBREVIATIONS

ADC	Antibody-drug conjugate
ADCC	Antibody-dependent-cell-mediated cytotoxicity
ADM	Adrenomedullin
AGPC	Acid guanidinium thiocyanate-phenol-chloroform
AKT	Protein kinase B
ALK	Activin receptor-like kinase
ANNUBP	Atypical neurofibromatosis neoplasm of uncertain biological potential
ATCC	American Type Culture Collection
BALB/c	Bagg albino
BCA	Bicinchoninic acid
BLI	Bioluminescence imaging
BMP	Bone morphogenetic protein
Breg	B regulatory cell
BSA	Bovine serum albumin
BW	Body weight
CAF	Cancer-associated fibroblast
CAM	Comunidad Autónoma de Madrid
CBR	Clinical benefit rate
CD	Cluster of differentiation
CDKN2A	Cyclin-dependent kinase inhibitor 2A
CEIyBA	Institutional Ethics Committee for Research and Animal Welfare
cfDNA	Cell-free DNA
CNIO	Spanish National Cancer Research Centre
CRC	Colorectal cancer
CSF1	Colony stimulating factor 1
CSRD	Cysteine-serine-rich domain
CTC	Circulating tumor cell
CTD	C-terminal domain
DAB	3, 30-diaminobenzidine tetrahydrochloride
DAPI	4’, 6-diamidino-2-phenylindole
DCR	Disease control rate
DMEM	Dulbecco’s modified Eagle’s medium
DN	Dermal neurofibroma
EC	Endothelial cell
ECM	Extracellular matrix
EDTA	Ethylenediamine tetraacetic acid
EED	Embryonic ectoderm development
EGFR	Epidermal growth factor receptor
ELISA	Enzyme-linked immunosorbent assay
EMT	Epithelial-mesenchymal transition
ENG	Endoglin
ERBB	Erb-B2 receptor tyrosine kinase
ERK	Extracellular signal-regulated protein kinase
ETP	Experimental Therapeutics Unit
EV	Extracellular vesicle
FACS	Fluorescence-Activated Cell Sorting

FAK	Focal adhesion kinase
FBS	Fetal bovine serum
FDA	Food and Drug Administration
FDG	Fluorodeoxyglucose
FDR	False discovery rate
FGF	Fibroblast growth factor
FGFR	Fibroblast growth factor receptor
FSC	Forward scatter
GAP	GTPase activating protein
GDF	Growth differentiation factor
gDNA	Genomic DNA
GEM	Genetically engineered mouse
GFP	Green fluorescence protein
GIST	Gastrointestinal stromal tumor
GRD	GAP-related domain
GSEA	Gene Set Enrichment Analysis
H&E	Hematoxylin and eosin
H3K27me3	H3K27 trimethylation
HCC	Hepatocellular carcinoma
HHT1	Hereditary hemorrhagic telangiectasia type 1
HIF1A	Hypoxia inducible factor 1 subunit alpha
HRP	Horseradish peroxidase
HSC	Hematopoietic stem cell
HSP90	Heat shock protein 90
i.p.	Intraperitoneally
IGF1R	Insulin-like growth factor 1 receptor
IGFBP1	Insulin like growth factor-binding protein 1
IGTP	Institute for Health Science Research Germans Trias i Pujol
IHC	Immunohistochemistry
IL2RG	Interleukin 2 receptor subunit gamma
IMVD	Intratumoral microvessel density
ISCIII	Instituto de Salud Carlos III
ITGA1	Integrin subunit alpha 1
ITGB1	Integrin subunit beta 1
IVIS	*In vivo* Imaging System
L-ENG	Long-endoglin
lEV	Large extracellular vesicle
LN	Lymph node
LOH	Loss of heterozygosity
mAb	Monoclonal antibodies
MAPK	Mitogen-activated protein kinase
MDSC	Myeloid-derived suppressor cell
MEK	Mitogen-activated protein kinase kinase
MEKi	MEK inhibitors
MMP14	Matrix metalloproteinase
MOI	Multiplicity of infection
MPNST	Malignant peripheral nerve sheath tumor
MSC	Mesenchymal stem cell

MSigDB	Molecular Signatures Database
mTOR	Mechanistic target of rapamycin
NF1	Neurofibromatosis type 1
NF1	Neurofibromin 1
NFATC4	Nuclear factor of activated T cells 4
NSG	NOD scid gamma
NTA	Nanoparticle tracking analysis
OS	Overall survival
p.o.	Oral gavage
p-AKT	Phospho-AKT
PBS	Phosphate-buffered saline
PDGF	Platelet-derived growth factor
PDGFR	Platelet-derived growth factor receptor
PDGFRA	Platelet-derived growth factor receptor alpha
PDGFRB	Platelet-derived growth factor receptor beta
PD-L1	Programmed death-ligand 1
p-ERK	Phospho-ERK
PET/CT	Positron emission tomography/computerized tomography
PFA	Paraformaldehyde
PFS	Progression-free survival
PI3K	Phosphatidylinositol-3-kinase
PIGF	Placental growth factor
PLXDC1	Plexin domain containing 1
p-MEK	Phospho-MEK
PMN	Pre-metastatic niche
p-mTOR	Phospho-mTOR
PN	Plexiform neurofibroma
PNST	Peripheral nerve sheath tumor
POSTN	Periostin
PR	Partial response
PRC2	Polycomb repressive complex 2
Prkdc	Protein kinase, DNA-activated, catalytic subunit
PTEN	Phosphatase and tensin homolog
qRT-PCR	Real-time quantitative polymerase chain reaction
RB1	RB transcriptional corepressor 1
RCC	Renal cell carcinoma
RECIST	Response Evaluation Criteria in Solid Tumors
RGD	Arginine–glycine–aspartic acid
Rho	Ras homologous
RIN	RNA Integrity Number
RIPA	Radioimmunoprecipitation assay
RNA-seq	RNA sequencing
ROI	Region of interest
RR	Response rate
R-Smad	Receptor-regulated Smad
RT	Room temperature
RTK	Receptor tyrosine kinase
S100A1	S100 calcium-binding protein A1

SC	Schwann cell
SCF	Stem cell factor
SCID	Severe combined immunodeficiency
SD	Stable disease
SDS-PAGE	Sodium dodecyl sulfate–polyacrylamide gel electrophoresis
SecPH	Sec14-pleckstrim homology
SEM	Standard error mean
SEMA5	Semaphorin-5A
S-ENG	Short-endoglin
sEV	Smal extracellular vesicle
shRNA	Short hairpin RNA
siRNA	Small interfering RNA
Sol-ENG	Soluble endoglin
SOX10	SRY-box transcription factor 10
SSC	Side scatter
STAT3	Signal transducer and activator of transcription 3
STS	Soft tissue sarcoma
SUZ12	Suppressor of zeste 12 homolog
TAM	Tumor-associated macrophages
TBD	Tubulin-binding domain
TBS-T	Tris-buffered saline with Tween
TGF-β	Transforming growth factor beta
THBS1	Thrombospondin 1
THBS2	Thrombospondin 2
TKI	Tyrosine kinase inhibitor
TMA	Tissue microarray
TME	Tumor microenvironment
TP53	Tumor protein 53
TRAMP	Transgenic adenocarcinoma mouse prostate
Treg	Regulatory T cell
TβRI	TGFβ type-I receptor
TβRII	TGFβ type-II receptor
VEGF	Vascular endothelial growth factor
VEGFR	Vascular endothelial growth factor receptor
Wnt	Wingless-related integration site
ZP	Zona pellucida

INTRODUCTION

1. Malignant Peripheral Nerve Sheath Tumors, a complicated clinical scenario

1.1. Etiology and epidemiology

Sarcomas represent a heterogeneous and clinically challenging family of cancers that affect the body's connective tissues [1,2]. Historically, they have been classified into two large subgroups, according to the anatomical site of occurrence: bone sarcomas and soft tissue sarcomas (STS) [3]. This last subgroup comprises around 70-80% of all sarcomas and consists of tumors derived from non-epithelial extraskeletal tissues including muscle, fat, fibrous tissue, blood and lymph vessels and peripheral nervous system [4,5]. Among STS, malignant peripheral nerve sheath tumor (MPNST) is the sixth most common subtype, accounting for approximately 5-10% of cases [6]. It is a poorly differentiated malignant neoplasm derived from cells of the Schwann cell (SC) lineage in the peripheral nerves [7].

SCs are neural crest-derived glial cells that produce the myelin sheath around neuronal axons, being crucial for the proper function and maintenance of peripheral nerves [8,9]. Axons with associated SCs are surrounded by a connective tissue layer, the endoneurium, forming nerve fibers [10]. Several nerve fibers cluster into nerve fascicles and each fascicle is then encircled by concentric layers of perineurial cells [11]. Multiple fascicles are contained within a peripheral nerve surrounded by a connective tissue layer called the epineurium [11]. During MPNST development, this normal structure of peripheral nerves is lost; transformed SCs are dissociated from axons and interact with fibroblasts, perineurial cells, endothelial cells (ECs) and immune cells, thus contributing to the establishment of a tumor niche [12] (**Figure 1**).

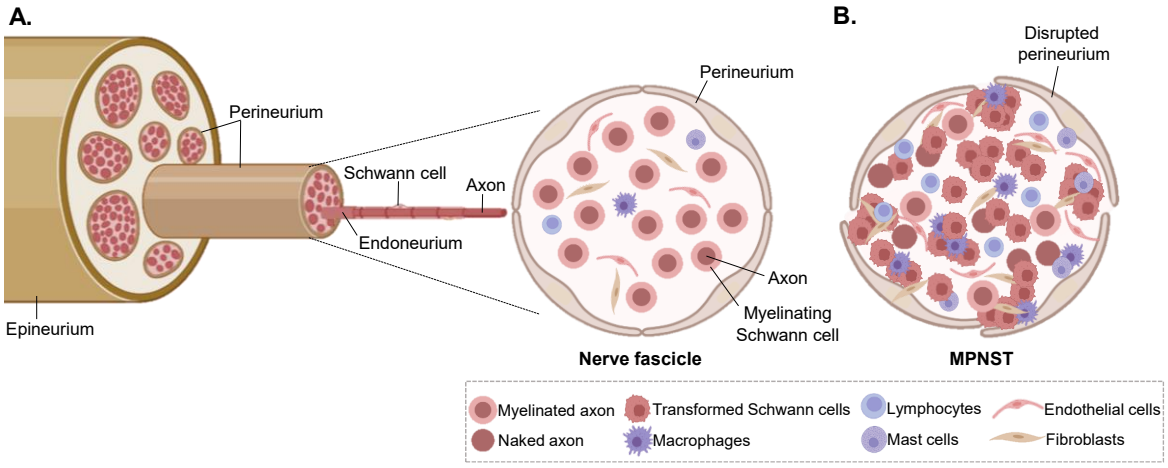

Figure 1. Structure of normal peripheral nerves and MPNSTs. A) Scheme showing the normal structure of a peripheral nerve with a cross-section of a nerve fascicle, and **B)** the aberrant structure of nerve fascicles found in MPNSTs.

MPNSTs can develop anywhere in the body but they are most common on the extremities (33-46%), the trunk (34-41%) and head and neck (17-25%), arising mainly from major nerve trunks, such as the brachial plexus, the sacral plexus or the sciatic nerve [13,14]. These tumors occur principally in adults between 20 and 60 years of age without gender predilection [15]. However, approximately 20% of cases are diagnosed in children [16]. Indeed, although the occurrence of MPNSTs is rare in the general population with an incidence of 0,001%, they are one of the most frequent non-rhabdomyosarcoma childhood tumors [16,17].

MPNSTs are encountered in three different clinical settings [18]. About 40% to 50% of MPNSTs arise in patients with neurofibromatosis type 1 (NF1), while the other 40-47% of cases are sporadic, with the remaining 10% to 13% occurring at sites of previous radiation therapy [19,20].

NF1 is an autosomal dominant disorder caused by inherited or de novo mutations in the neurofibromin 1 (*NF1*) tumor suppressor gene [21,22]. The hallmark manifestation of this disease is the development of peripheral nerve sheath tumors (PNSTs) called neurofibromas derived from the biallelic loss of *NF1* in SCs [21-23]. These tumors include discrete or dermal neurofibromas (DNs) and plexiform neurofibromas (PNs), which are benign forms [21,22]. Unlike DNs, which are associated with a single small peripheral nerve, PNs are larger tumors, usually involving multiple branches of major peripheral nerves or nerve plexuses [21,22,24]. They cause substantial morbidities, such as disfigurement, pain and functional impairment, and can impose pressure on and affect the normal function of surrounding tissues and organs [25]. Importantly, PNs can transform to MPNSTs [26]. Histological and genetic evidence reveals that premalignant lesions, termed atypical neurofibromatosis neoplasms of uncertain biological potential (ANNUBPs, formerly referred to as atypical neurofibromas), represent an intermediate state in the transition of benign PNs to MPNSTs [27]. In fact, ANNUBPs exhibit at least two of the features associated with higher risk of malignant transformation including cytologic atypia, loss of neurofibroma architecture, hypercellularity and high mitotic activity [27,28]. MPNSTs develop in 8% to 13% of NF1 patients, representing the main cause of death in this disease [19,29].

Irrespective of their origin, MPNSTs display similar histological features [30]. They are typically high-grade spindle cell neoplasms, with frequent nuclear pleomorphism, mitotic figures and areas of necrosis [30,31]. Heterologous differentiation to mesenchymal lineages such as skeletal muscle, bone, cartilage and blood vessels is found in approximately 15% of tumors [7]. Likewise, MPNSTs are highly aggressive tumors,

characterized by a high tendency to recur, invade surrounding soft tissues and metastasize to distant organs, especially to lungs and bone [32,33].

1.2. Prognosis

The prognosis of MPNSTs is dismal, with 5-year survival rates ranging from 15% to 50% [34-36]. In patients with advanced and metastatic disease, outcomes are even worse, with a recent study reporting a 5-year survival of 7.3% [37]. Indeed, MPNSTs have the highest risk of sarcoma-specific death compared with other STS [15].

Clinicopathologic features that accurately predict prognosis of patients with MPNSTs are still debated. Large tumor size and high tumor grade have been the most consistent factors associated with worse outcomes [38]. Likewise, several studies have reported many other prognostic variables including primary tumor location, tumor staging and recurrence, histology, age, surgical margin status and association with NF1 and with radiation therapy, among others [13,33,38-40]. However, the small sample size and non-standardized evaluation criteria limit the predictive power of these studies [38,39]. Therefore, future efforts should focus on identifying well-defined or widely reproducible biomarkers for MPNST prognosis.

1.3. Diagnosis

Establishing an accurate diagnosis is a major challenge in managing patients with MPNSTs [41,42]. Unfortunately, MPNSTs are histologically similar to several other types of sarcomas [12,41,43]. Moreover, in the NF1 setting, the distinction between MPNSTs, precursor lesions (ANNUBPs) and benign forms (PNs) is often not clear [27,44].

Thus, the diagnosis of MPNSTs relies on a comprehensive clinicopathologic assessment of ultrastructural, histologic and immunohistochemical findings [45]. Biopsy is necessary for diagnosis but it is often technically challenging due to tumor location and presents limitations, mainly because of inter- and intra- tumor heterogeneity [45,46]. Hence, imaging modalities have been traditionally used to predict malignancy and guide biopsy [47]. However, MPNSTs and their benign counterparts have often overlapping fluorodeoxyglucose (FDG)-positron emission tomography/computerized tomography (PET/CT) appearance [48,49]. Likewise, there are no specific imaging features that differentiate MPNSTs from other high-grade sarcomas [50,51]. Similarly, the immunohistochemical markers that are commonly used to diagnose MPNSTs have demonstrated limited sensitivity and specificity [41,52]. These markers include S100

protein, SRY-box transcription factor 10 (SOX10), marker of proliferation Ki-67, tumor protein 53 (TP53), cluster of differentiation (CD) 34, cyclin-dependent kinase inhibitor 2A (CDKN2A) and cytokeratins [43,45]. The finding that a substantial subset of MPNSTs exhibits mutations in the polycomb repressive complex 2 (PRC2), which is responsible for trimethylation of Lys 27 on histone H3, has resulted in the emergence of H3K27 trimethylation (H3K27me3) as a new biomarker for MPNSTs [53,54]. However, considerable controversy remains about the diagnostic value of this marker in MPNSTs [30]. Indeed, some reports have demonstrated that mutations in the PCR2 complex and the subsequent loss of H3K27me3 also occurs in other types of sarcomas, such as radiation-associated angiosarcomas and dedifferentiated chondrosarcomas and liposarcomas [55-57]. Therefore, there is a significant lack of adequate tools for early and accurate diagnosis of MPNSTs. In fact, the majority of patients are diagnosed with high-grade MPNSTs [41].

Importantly, a recent study has shown for the first time that a liquid biopsy test is able to differentiate MPNSTs from their benign precursor lesions (i.e. PNs) with high specificity and sensitivity [58]. Specifically, these authors revealed that plasma from MPNST patients was enriched for cell-free DNA (cfDNA), which harbored a significantly shorter fragmentation profile and higher tumor genomic instability compared to PN patients or healthy subjects [58]. In line with these data, two additional reports have demonstrated that serum concentrations of insulin like growth factor-binding protein 1 (IGFBP1) and adrenomedullin (ADM) can help distinguish MPNST patients from those with benign tumors or healthy controls [59,60]. These data suggest that liquid biopsy is emerging as a promising tool for MPNST diagnosis and that the identification of novel biomarkers would greatly facilitate the early detection of these tumors.

1.4. MPNSTs: a significant unmet therapeutic need

Current treatment of MPNSTs is essentially similar to treatment of STS as a whole and relies mainly on local control measures [61]. The only known effective therapy for MPNSTs is complete surgical resection with wide negative margins to reduce local recurrence and improve survival [62,63]. However, this is often not feasible due to factors such as tumor size, location and/or presence of metastases [62,63]. In fact, the local recurrence rate after surgery is high, ranging from 32 to 65% [62]. The role of radiation in MPNST management is still being defined but it is generally recommended for patients with large high-grade lesions (>5cm in size) or with positive resection margins as a measure to improve local control [64]. However, it has no effect on overall survival (OS) [65,66]. Unfortunately, radiotherapy has been associated with the development of

secondary malignancies, including MPNSTs [67,68]. Therefore, an exhaustive risk-benefit evaluation must be conducted, especially in NF1 patients who present increased risk for malignant transformation of surrounding benign tumors [69]. The use of chemotherapy for the treatment of MPNSTs is also not clear, since several studies showed that these tumors are relatively chemoresistant [13,70,71]. Most chemotherapeutic regimens are based on the use of an anthracycline (doxorubicin or epirubicin), which can be combined with alkylating agents (ifosfamide or cyclophosphamide) [72,73]. Some evidence suggests that neoadjuvant cytotoxic therapy may make surgery possible in some localized MPNSTs deemed initially inoperable [74,75]. Unfortunately, around 40-60% of patients receiving curative-intend treatment for localized disease ultimately develop metastases and another 10% of patients present with *de novo* metastatic disease [33,71,76,77]. Clinical outcomes associated with chemotherapy in patients with advanced or metastatic MPNSTs are poor, with only a response rate (RR) of 21% according to the Response Evaluation Criteria in Solid Tumors (RECIST) [73]. Furthermore, initial responses to therapy are often transient, followed by a rapid progression and, ultimately, death [41]. Therefore, patients with recurrent, unresectable or metastatic disease do not currently have effective treatment options, and development of novel therapeutic approaches is needed.

To date, targeted, non-cytotoxic treatments have generally demonstrated little success in MPNST patients [78]. **Table 1** summarizes data from published clinical trials using targeted therapies in individuals with MPNSTs. Particularly, phase II studies investigating the effect of tyrosine kinase inhibitor (TKI) monotherapy (e.g. erlotinib [79], sorafenib [80], dasatinib [81], alisertib [82] and imatinib [83]) showed limited clinical response in MPNST patients, with a median progression-free survival (PFS) of less than 2 months and stable disease (SD) in only 0-20% of the patients. Likewise, combinations of mechanistic target of rapamycin (mTOR) inhibitors with the anti-vascular endothelial growth factor (VEGF) antibody bevacizumab or the heat shock protein 90 (HSP90) inhibitor ganetespib did not demonstrated efficacy in phase II trials involving patients with refractory sporadic or NF1-associated MPNSTs [84,85].

Thus, there is an urgent need to uncover effective therapies for this disease. Importantly, other targeted agents, including mitogen-activated protein kinase kinase (MEK) inhibitors (MEKi) and some anti-angiogenics (e.g. pazopanib), may represent promising strategies for the treatment of MPNSTs (see sections 2.2 and 3.3). Therefore, exploration of crucial mediators for MPNST pathogenesis is an important area of research in this field, aiming to provide novel therapeutic targets and design efficient combination approaches that include the aforementioned therapies.

Table 1. Published data from clinical trials of targeted therapies for MPNSTs.

Drug	Pathway	Phase	Disease	MPNST patients (n)	Outcome	Adverse effects	Study
Erlotininb	EGFR	II	Unresectable or metastatic MPNST	20	SD:5% PFS: 2 mo. OS: 4 mo.	Grade 3 in 31.6%	[79]
Sorafenib.	Multikinase (incl. VEGFR, RAF)	II	Metastatic or recurrent sarcoma (incl. MPNST)	12	SD:25% PFS: 1.7 mo. OS: 4.9 mo.	Most common AEs: grade 2 and 3 skin reactions	[80]
Dasatinib	Multikinase (incl. C-KIT, BCR/ABL)	II	High-grade, advanced sarcoma (incl. MPNST)	14	Non-responses 2-mo PFS: 14% 4-mo PFS: 7%	Severe grade 3–4: <5%.	[81]
Alisertib	Aurora kinase A	II	Advanced or metastatic sarcoma (incl. MPNST)	10	Non-responses 3-mo PFS: 60% OS: 17.25 mo.	Most common grade 3-4 AEs: neutropenia (42%), leucopenia (22%)	[82]
Imatinib	Multikinase (incl. C-KIT, PDGFR, VEGFR)	II	Metastatic or recurrent sarcoma (incl. MPNST)	7	SD:14.28% PFS: 1.92 mo.	NR. Toxicity in 1 patient (14%)	[83]
Pazopanib	Multikinase (inl. VEGFR, PDGFR, FGFR)	II	Advanced MPNST	12	CBR.: 50% PFS: 5.4 mo. OS: 10.6 mo.	Well-tolerated. Only grade 4 neutropenia and lipase elevation in one patient each	[86]
Everolimus + bevacizumab	mTOR, VEGF	II	Recurrent or metastatic MPNST	25	SD: 12%	Most AEs graded as 1 and 2.	[84]
Sirolimus + ganetespib	mTOR, Hsp90	II	Unresectable or metastatic MPNST	20	Non-responses	Acceptable. Most common AEs: diarrhea, transaminitis, fatigue	[85]

SD, stable disease; PFS, progression-free survival; OS, overall survival; CBR, clinical benefit rate; AEs, adverse effects; NR, not reported; mo., months.

2. Cell-intrinsic drivers of MPNST pathogenesis

2.1. Genetic and genomics of MPNSTs

MPNSTs harbor highly complex karyotypes with multiple chromosome abnormalities including aneuploidies (from hypodiploidy to near-tetraploidy), frequent deletions and duplications and, extensive chromosomal rearrangements [87,88]. Previous studies demonstrated common losses on chromosomes 1p, 9p, 11, 12p and focal gains on chromosomes 7, 8q, and 15q [89,90]. However, accumulating data reveal that MPNSTs are characterized by a high genomic heterogeneity [91,92]. Thus, research over the last three decades has focused on identifying the main driver genes of MPNST pathogenesis.

Multiple next-generation sequencing studies have reported recurrent mutations in similar genes across the distinct subtypes of MPNSTs (sporadic, NF1- and radiation-associated), suggesting that all MPNSTs are driven by similar genetic or epigenetic mechanisms [93-95]. Indeed, biallelic loss of the *NF1* tumor suppressor gene is a common event in the majority of MPNTs, regardless of their origin [53,96]. NF1-associated MPNSTs undergo loss of heterozygosity (LOH) or “second-hit” somatic mutations in the remaining wild-type

NF1 allele, while sporadic and radiation-induced tumors not arising in the context of NF1 display somatically acquired mutations in both alleles [93,97]. In this respect, some publications have shown considerable differences between the germline and somatic *NF1* mutational spectrum in NF1-derived MPNSTs [94,98]. However, the somatic events share similar characteristics in both NF1-associated and sporadic tumors [94,98]. Specifically, the majority of reported germline alterations (80-90%) are intragenic point mutations such as missense, nonsense, frameshift and splicing anomalies, whereas large genomic deletions are the most common type of somatic mutation found in MPNSTs [92,94,98]. Taken together, these findings strengthen the crucial role of *NF1* in MPNST development.

The *NF1* gene is located on the long (q) arm of chromosome 17, at band 11.2 (17q11.2) [21,99]. It spans approximately 300 kb and contains 60 exons (57 constitutive exons and 3 tissue-specific alternatively spliced exons (9a, 23a and 48a)) [21,99]. There may be different splice variants but the main gene product codes for a protein of 2818 aa called neurofibromin [21,99,100]. It is widely expressed in different organs and tissues, with high levels in the nervous system, especially in neurons, astrocytes, oligodendrocytes, microglia, and SCs [21,99,100]. Neurofibromin contains several domains: an N-terminal cysteine-serine-rich domain (CSRD), a central GTPase activating protein (GAP)-related domain (GRD), including a tubulin-binding domain (TBD) at its N-terminus, followed by a phospholipid- and protein-interaction Sec14-pleckstrim homology (SecPH) domain, and a C-terminal domain (CTD) [101]. However, the GRD is the most-well studied domain and functions by stimulating the intrinsic GTPase activity of RAS, thus promoting the conversion of active RAS-GTP to inactive RAS-GDP [101,102]. Indeed, neurofibromin has been identified as a RAS-GAP [101,102]. RAS proteins control cellular signaling pathways responsible for growth, migration, adhesion, cytoskeletal integrity, survival and differentiation [103]. The main RAS-induced signaling pathways are the mitogen-activated protein kinase (MAPK)/extracellular signal-regulated protein kinase (ERK) and phosphatidylinositol-3-kinase (PI3K)/protein kinase B (AKT) pathways [103]. Loss of neurofibromin in MPNST cells therefore leads to aberrant activation of RAS and its downstream effector pathways [104] **(Figure 2**).

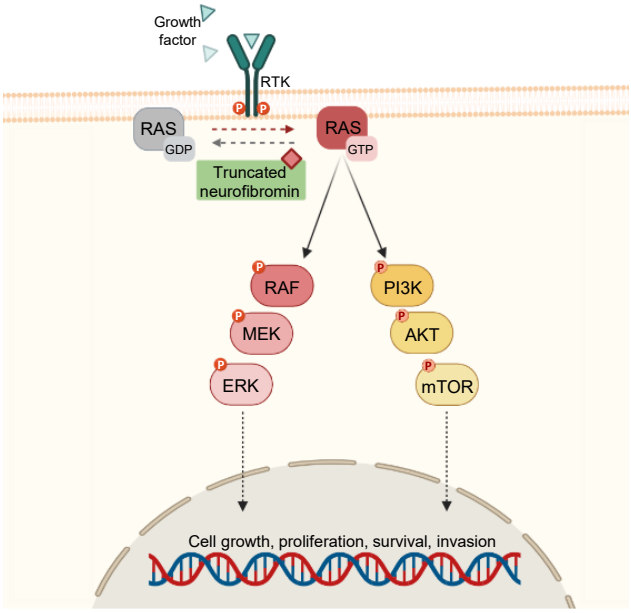

Figure 2. Effect of neurofibromin deficiency on RAS signaling in MPNST cells. Neurofibromin acts as a RAS-GAP, since it negatively regulates RAS activation by accelerating the conversion of RAS-GTP to RAS-GDP. Therefore, lack of functional neurofibromin, due to *NF1* mutations, in MPNST cells leads to increased activation of RAS and downstream MAPK/ERK and PI3K/AKT signaling pathways, promoting dysregulated cell growth and tumorigenesis.

Mounting evidence suggests that mutations in additional driver genes are also required for MPNST pathogenesis [87,91,92]. In fact, MPNSTs are typified by the loss of other tumor suppressor loci [87,91,105]. Specifically, deletions of the *CDKN2A* gene, which encodes the cell-cycle inhibitors p16INK4A and p14ARF, are recurrent in MPNSTs, occurring in approximately 75% of cases [106-108]. Frequent somatic alterations of *NF1* and *CDKN2A* significantly co-occur with loss-of-function mutations in the suppressor of zeste 12 homolog (*SUZ12*) and embryonic ectoderm development (*EDD*) genes encoding components of the PRC2, a histone methyltransferase involved in epigenetic silencing [53,96,109]. These mutations are observed in 55% and 30% of MPNSTs, respectively, in a mutually exclusive manner [53,92]. Likewise, *TP53* point mutations or deletions have been associated with MPNST development, with several series reporting mutations of this tumor suppressor gene in up to 75% of patients [110-112]. As in the case of many other malignancies, loss of the phosphatase and tensin homolog (*PTEN*) and RB transcriptional corepressor 1 (*RB1*) tumor suppressor genes has also been identified in a subset of MPNSTs [112-115]. The amplification of oncogenes encoding receptor tyrosine kinases (RTKs), such as *c-KIT*, epidermal growth factor receptor (*EGFR*), Erb-B2 receptor tyrosine kinase 2 (*ERBB2*), platelet-derived growth factor receptor (*PDGFR*), insulin-like growth factor 1 receptor (*IGF1R*), and *MET* and *KIT* proto-oncogenes, is another frequent event in MPNST pathogenesis [45,91,116].

Although alterations in the mentioned genes have been identified in many series of MPNST patients [91,92], the precise order and timing of these changes need to be clarified in order to gain a better understanding of the early stages of MPNST tumorigenesis.

2.2. Aberrant signaling pathways in MPNSTs: defining the relevance of the MAPK/ERK pathway

Dysregulation of different signaling pathways, including the MAPK/ERK, PI3K/AKT, Wingless-related integration site (Wnt) and Hippo pathways, has been reported to be involved in the pathogenesis of MPNSTs [117]. Among them, the RAS-induced MAPK/ERK and PI3K/AKT pathways have been the most extensively studied, since they are commonly upregulated in MPNSTs due to the hyperactivation of RAS which results from *NF1* loss [93,104,117]. Interestingly, a study examining the activation profiles of these pathways in a cohort of human MPNSTs showed that the MAPK/ERK signaling cascade is more frequently activated than the PI3K/AKT/mTOR pathway [118]. Specifically, expression of phospho-MEK (p-MEK) and p–ERK was found in the majority of MPNST samples (93.4% and 81.3%, respectively), while only 58.2% and 47.3% of tumors expressed p-AKT and p-mTOR, respectively [118]. Moreover, a significantly higher expression of p-MEK was found in human MPNSTs compared to their benign counterparts, which supports the importance of this pathway for MPNST development [20].

As RAS-directed therapies have largely been unsuccessful [119,120], efforts to target the MAPK/ERK pathway in MPNSTs have focused on MEK inhibition. In fact, several studies have proved that the MEKi PD325901 (PD-901) effectively decreases tumor growth in different MPNST xenograft and genetically engineered mouse models (GEMMs) [121-124]. This anti-tumor activity was associated with a significant reduction in tumor cell proliferation and vessel density [121,122]. These findings provide additional evidence for the crucial role of the MAPK/ERK pathway in MPNST progression and suggest that MEK-targeting approaches could be an effective treatment for MPNST patients. Indeed, MEKi have demonstrated clinical therapeutic efficacy against PNs, benign lesions that can transform into MPNSTs [125,126]. Of note, the Food and Drug Administration (FDA) has recently approved the MEKi selumetinib for the treatment of pediatric patients with NF1 and symptomatic inoperable PNs, thus becoming the first ever approved therapy for these patients [127,128].

In MPNSTs, preclinical evidence indicates that MEKi could prove more useful in combination with other therapies [78]. Particularly, a high-throughput study of multiple FDA-approved and promising therapies for MPNSTs showed that MEKi at very low doses were the drugs leading to the strongest synergism and efficacy in combination with other agents [129]. These authors proposed that MEK inhibition sensitizes MPNST cells to other therapies that may not be effective when used as a single-agent [129]. Accordingly, the

combination of MEKi with many different strategies significantly improved therapeutic efficacy, when compared with single-agent treatment, in several NF1-associated and sporadic MPNST mouse models [109,130-136].

To date, however, there is only one ongoing clinical study investigating combination treatments that include MEKi in MPNST patients (SARC031; NCT03433183). Specifically, this Phase II trial is examining the effect of the MEKi selumetinib plus the mTORi sirolimus in patients with unresectable or metastatic NF1-associated or sporadic MPNSTs. Further clinical studies should test novel combinations of MEKi with therapies targeting other key and complementary pathways in MPNSTs, thus opening new options for the treatment of these tumors.

3. Role of the tumor microenvironment in cancer progression

3.1. Importance of the tumor microenvironment in tumor progression and metastasis

In addition to tumor-cell-intrinsic mechanisms (genetic/epigenetic changes), alterations in the tumor microenvironment (TME) are now recognized as critical elements influencing tumor progression [137-140]. The TME typically comprises different cell types, including mesenchymal stem cells (MSCs), cancer-associated fibroblasts (CAFs), immune cells and ECs, and non-cellular components such as extracellular matrix (ECM) or secreted molecules [138,139]. Interactions between non-malignant TME and primary neoplastic cells are crucial during tumor progression, leading to the corruption of the TME along tumor evolution [140,141].

More precisely, initial tumors acquire the ability to circumvent normalizing cues of the microenvironment, and, in turn, the microenvironment evolves to accommodate the growing tumor [137,139]. This dynamic and cooperative crosstalk supports key aspects of primary tumor progression, particularly the capability to evade immune system, to induce proliferation and angiogenesis, to stimulate ECM remodeling and to activate cancer-associated immune cells in order to support tumor migration, invasion and metastasis [137,139].

Indeed, the TME has an active role in metastasis, as first described by Stephen Paget in 1889 [142]. He noticed that the organ distribution of metastases was not random, and proposed that some tumor cells (the “seed”) preferentially grow in specific organs (the “soil”) where the local microenvironment is favorable [142]. Since then, numerous investigations regarding environmental factors influencing metastatic colonization were

carried out and a novel concept arose with fundamental discoveries from Lyden and colleagues [143]. They revealed that primary tumors induce the formation of specific microenvironments at distant organs that are conducive to the survival and outgrowth of tumor cells prior to their arrival at these sites [143-146]. These microenvironments were termed “pre-metastatic niches (PMNs)” [143]. Vascular leakiness, alteration of local stromal cells, recruitment of immune cells or ECM remodeling are some of the key processes that occur during PMN formation [144,147]. Collectively, these findings demonstrate a pivotal role for host microenvironment in promoting all stages of tumorigenesis and metastasis.

3.2. Extracellular vesicles: crucial intercellular delivery vehicles

It is widely known that tumor-host interactions discussed above can occur through the secretion of specific molecules [144,147]. Although soluble factors operate as key players of this crosstalk, more recently, extracellular vesicle (EV) shedding has emerged as another critical mediator of intercellular communication between tumor cells and stromal cells [148]. EVs are small lipid membrane vesicles secreted constitutively by most cells [149]. A recent classification based on size divided them in large EVs (lEVs), comprising microvesicles (200 nm – 1 μm), apoptotic bodies (1-5 μm) and oncosomes (1-10 μm), and small EVs (sEVs), among them exosomes (30-150 nm) and exomeres (~35nm) [150-152]. Importantly, EVs carry a variety of molecular cargo, including nucleic acids (DNA, mRNA, microRNA, and non-coding RNAs), proteins (receptors, transcription factors, enzymes, ECM proteins) and lipids, which is representative of their cell of origin and can redirect the phenotype of the recipient cell [149,153-155].

Indeed, tumor-secreted EVs promote molecular and cellular changes in local and distant microenvironments by transferring their cargo, thus favoring tumor growth, PMN formation, and, ultimately, metastasis [148,156-158]. During intercellular communication processes, EVs are released as stable entities that can travel over long distances within the extracellular spaces and biofluids of the organism [159]. In fact, they can be efficiently isolated from nearly all body fluids (e.g. blood, saliva and urine) [159,160]. Because of their tumor-specific content, stability and ease of accessibility, tumor-derived EVs, among them sEVs, are emerging as a potent source of biomarkers for liquid biopsy in the clinical setting [161,162]. This rapidly advancing field is contributing to the generation of new tools for early diagnosis, patient stratification, disease monitoring and treatment decisions in many types of cancer [162,163]. Therefore, finding novel tumor-derived EV biomarkers (e.g. proteins) could be especially valuable in those cases where the ability to conduct a tissue biopsy is limited, such as MPNSTs.

3.3. Role of the TME in MPNST progression

Increasing evidence reveals that dysregulated SCs, the cell type of origin for MPNSTs, closely interact with specific local microenvironments influencing MPNST formation and progression [164-167] (**Figure 3**). In fact, *NF1*-deficient SCs are hypersensitive to environmental signaling (e.g. growth factors or ECM stimuli) that is required for their neoplastic transformation [168].

Likewise, loss of *NF1* in SCs leads to increased production of growth factors and cytokines (e.g. stem cell factor (SCF), colony stimulating factor 1 (CSF1), transforming growth factor beta (TGF-β), platelet-derived growth factor (PDGF), fibroblast growth factor (FGF), placental growth factor (PIGF), VEGF) that induce the recruitment of immune cells (e.g. mast cells, macrophages and lymphocytes), fibroblasts and ECs [169-171]. Specifically, macrophage recruitment into PNSTs correlates with malignant progression, which is also linked to a shift of macrophages toward protumoral phenotypes [172]. In addition, it was also reported that the MPNST microenvironment shows a significant infiltration of CD8+ T cells, which is associated with increased, albeit variable, expression of programmed death-ligand 1 (PD-L1) [173]. Although these findings suggest the presence of an immunosuppressive TME, the specific interaction mechanisms between MPNST cells and their surrounding microenvironment are still poorly defined. However, considerable attention has been paid to an essential component of the MPNST microenvironment: ECs.

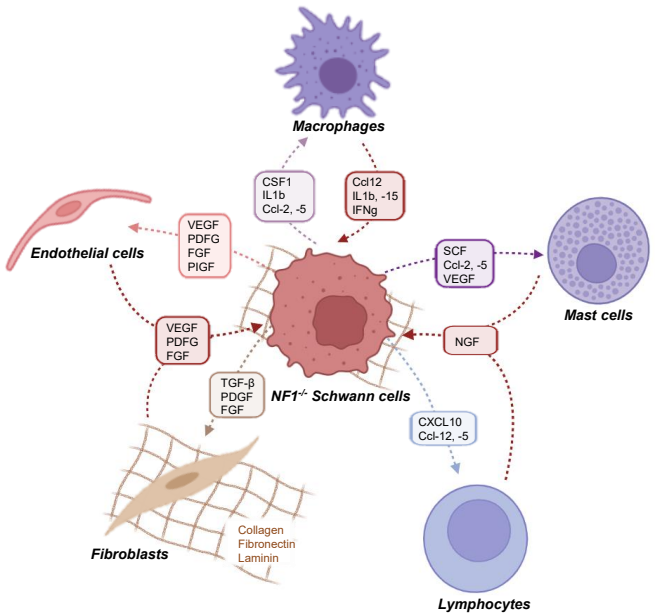

Figure 3. Crosstalk between *NF1*-deficient SCs and their microenvironment. Loss of *NF1* in SCs results in increased secretion of growth factors and cytokines that induce the recruitment of different cell types into the TME. In turn, these *NF1*-deficient SCs are extremely sensitive to microenvironment signals (e.g. cell-derived mediators and ECM stimuli), thus promoting tumor development and progression.

3.3.1. Tumor angiogenesis, a key step in MPNST progression

Tumor angiogenesis is widely considered as a critical event in the transformation and progression of MPNSTs [174,175]. Indeed, several reports demonstrated that VEGF expression and vessel density are significantly higher in human MPNSTs compared to their benign counterparts (PNs) [176-178]. Importantly, increased VEGF levels and vascularization were correlated with a worse prognosis in patients with MPNSTs [177,179]. In line with these data, a study of Gesundheit and colleagues suggested that the development and progression of MPNSTs depend, at least in part, on their ability to induce an “angiogenic switch” [180]. They evaluated the vascular architecture of benign PNs and MPNSTs from the same patients, which allowed the identification of changes associated with malignant transformation in each case [180]. While a well-defined and mature vascular pattern was observed in benign forms, MPNSTs exhibited a structure composed of numerous irregular and immature vessels that was suggestive of “sprouting angiogenesis” [180]. Interestingly, it was also shown that common EC receptors (e.g. vascular endothelial growth factor receptor (VEGFR), platelet-derived growth factor receptor alpha (PDGFRA), platelet-derived growth factor receptor beta (PDGFRB)) are not only expressed by ECs but also by tumor cells from human MPNST specimens, being therefore potential targets for tumor cell- and stroma-directed therapy [180-182].

Several works have shed light on signaling pathways governing MPNST angiogenesis. For example, the activation of certain RTKs, including fibroblast growth factor receptor (FGFR), MET, EGFR or ERBB4, in tumor cells indirectly stimulates neovascularization in different MPNST mouse models, via the induction of soluble angiogenic factors (e.g. VEGF) [183-186]. Moreover, since the loss of *NF1* in MPNST cells enhances the activation of downstream effectors of RTKs, such as the MAPK/ERK and PI3K/AKT pathways [181], it could also contribute to RTK-mediated angiogenesis. Indeed, *NF1* deficiency in SCs is associated with increased secretion of soluble factors known to stimulate proliferation and migration of ECs (e.g. VEGF, FGF, PIGF, PDGF) [187-189]. In this respect, signal transducer and activator of transcription 3 (STAT3) has been identified as a common nexus of convergence for RTKs involved in angiogenic signaling in MPNSTs, coordinating the angiogenic response through the hypoxia inducible factor 1 subunit alpha (HIF1A)/VEGF axis [190]. In fact, STAT3 knockdown was sufficient to completely inhibit expression of HIF1A and VEGF in multiple MPNST cell lines [190]. Despite these findings, the specific molecular mechanisms modulating MPNST angiogenesis remain incompletely understood and need to be further analyzed.

Additional evidence of the importance of angiogenesis in MPNST progression is provided by studies demonstrating that several anti-angiogenics suppress tumor growth in various MPNST mouse models [78]. Indeed, a comprehensive review, comparing the efficacy of the targeted-therapies that have so far been tested in MPNST preclinical *in vivo* models, identified angiogenesis inhibitors as one of the most promising therapeutic approaches, highlighting that combination drug regimens are more efficient than monotherapy [78]. Accordingly, in a recent phase II trial involving patients with unresectable or metastatic MPNSTs, the anti-angiogenic TKI pazopanib has demonstrated encouraging outcomes with a clinical benefit rate (CBR) at 12 weeks of 50% [86]. Of note, these results are better than those achieved with any of the targeted therapies previously tested in MPNST patients [86] (see **Table 1**). Interestingly, pazopanib was particularly effective against more advanced-stage MPNSTs [86]. Taken together, these data reveal that anti-angiogenic therapy may be an attractive treatment option for patients with MPNSTs.

Therefore, finding novel key players of MPNST angiogenesis would be of interest to better understand the mechanisms underlying the pathogenesis of this disease and to identify new therapeutic targets.

4. Endoglin: a novel player in MPNST progression?

The TGF-β coreceptor endoglin (ENG) has been widely described to be highly expressed in proliferating ECs, promoting angiogenesis in many types of solid tumors [191]. Preliminary data from our laboratory suggested that ENG could play a role in MPNST pathogenesis, however, whether ENG is involved in MPNST angiogenesis and progression is a question that remains to be answered. In this PhD thesis, we will analyze and discuss the role of ENG in MPNST malignancy.

4.1. Molecular features and physiological function

ENG, also known as CD105, is a transmembrane glycoprotein that functions as a coreceptor for the TGF-β superfamily [192]. It is expressed mainly in activated ECs [193], but also in other cell types such as MSCs [194], neural crest stem cells [195], fibroblasts [196], hematopoietic stem cells (HSCs) [197], mesangial cells [198], chondrocytes [199], keratinocytes [200], periodontal ligament cells [201], hepatic stellate cells [202] and diverse subpopulations of immune cells [203-206]. ENG is composed of two identical 90- to 95-kDa subunits that associate through disulfide bonds to form a homodimer [207]. Each subunit comprises a 561 aa extracellular region (ectodomain), a 25 aa hydrophobic transmembrane domain, and a serine/threonine/tyrosine-rich cytoplasmic short domain

[208] (**Figure 4A**). There are two alternatively spliced isoforms that vary in the length of the intracellular domain: long- (L) and short- (S) ENG, containing 47 and 14 aa, respectively [209]. These isoforms also differ in cellular localization and in the modulation of TGF-β signaling [209,210]. L-ENG is the predominantly expressed isoform and promotes signaling via the activin receptor-like kinase (ALK)-1 pathway, whereas S-ENG is induced in senescent ECs and myeloid cells and activates the ALK5 pathway [210-212].

TGF-β signaling regulates crucial cellular processes such as proliferation, migration, differentiation and apoptosis [213]. The members of the TGF-β superfamily, including TGF-βs, bone morphogenetic proteins (BMPs), activins and growth differentiation factors (GDFs), exert their effects by binding to a complex of type-I and type-II transmembrane receptors [214,215]. Seven type-I receptors (TβRI), also known as ALKs, and five ligand-binding type-II receptors (TβRII) have been identified [214,215]. Upon ligand binding, activated TβRII transphosphorylates ALK, which subsequently transduces the signal by phosphorylating the downstream receptor-regulated Smad (R-Smad) molecules [214,215]. The involvement of different ALKs determines the signaling specificity by provoking the induction of different R-Smads, as detailed below [214]. Activated R-Smads associate with their common partner Smad4 and these complexes are translocated to the nucleus, where they modulate the transcription of specific target genes [215]. It is known that ENG (a type-III receptor) interacts with ALKs and TβRII and plays an important role in balancing the TGF-β signal [216-218]. The most well-known ligands for ENG are TGF-β1, TGF-β3 and BMP-9 [219,220]. The binding of these ligands to ENG in a heterotypic complex with TβRII leads to the recruitment of ALK1 and the subsequent phosphorylation of Smad1 and Smad5 [221,222]. Activation of the ENG-Smad1/5 pathway indirectly inhibits the canonical TGF-β signaling pathway, which involves ALK5 resulting in Smad2 and Smad3 phosphorylation [223,224] (**Figure 4B**). Additionally, the TGF-β family of cytokines and ENG can also regulate non-canonical, non-Smads pathways, including the MAPK/ERK, PI3K/AKT and Ras homologous (Rho)-like GTPase signaling pathways [225-227].

ENG is mainly known for its essential role in angiogenesis and vascular remodeling [222,228-231]. Indeed, genetic deletion of *ENG* in mice causes defective yolk sac vascularization and early embryonic lethality [232,233]. Moreover, mutations in the *ENG* gene are responsible for hereditary hemorrhagic telangiectasia type 1 (HHT1), an autosomal dominant disorder characterized by arteriovenous malformations and frequent hemorrhages [234,235].

Recent studies have reported novel functions for ENG beyond the endothelium, such as the regulation of proper embryonic development or the modulation of immune responses, among others [236].

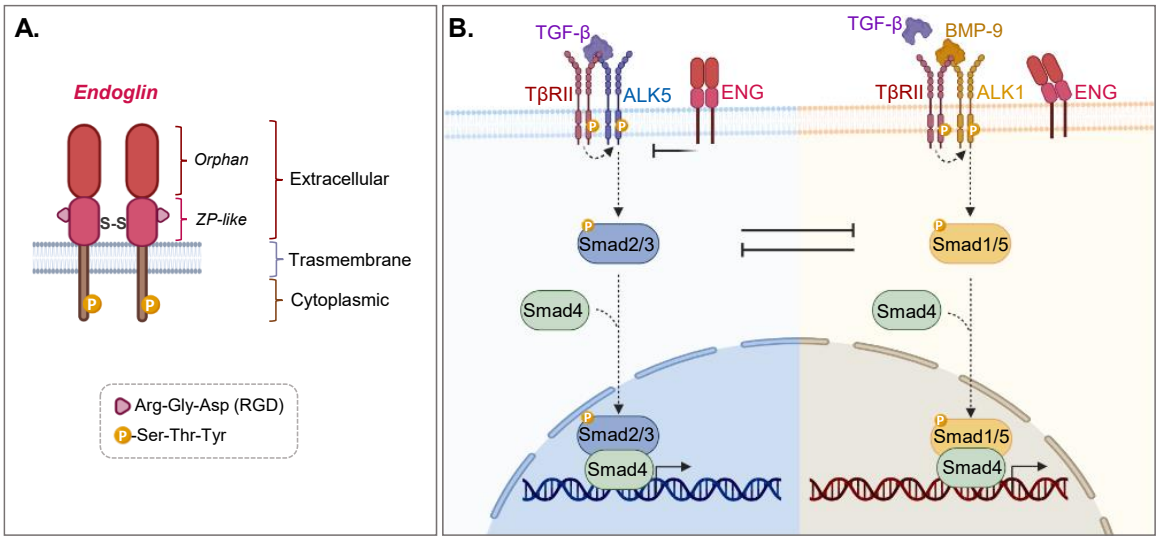

Figure 4. ENG structure and signaling. A) Structural representation of ENG. ENG is a type I transmembrane glycoprotein with a large extracellular domain that contains an NH2-terminal orphan domain followed by a zona pellucida (ZP)-like domain. The orphan domain is involved in binding to TGF-β family members and the ZP domain encodes an arginine–glycine–aspartic acid (RGD) tripeptide, a sequence recognized by integrins that is relevant in cell adhesion. The cytoplasmic domain can be phosphorylated at Ser/Thr/Tyr residues. ENG forms dimers through intermolecular disulfide bonds. **B)** Mechanisms regulating ENG-mediated signaling. When TGF-β binds to TβRII in absence of ENG, the type-I receptor ALK5 is recruited and transphosphorylated, leading to phosphorylation of Smad2/3, which translocates into the nucleus together with their common partner Smad4. The presence of ENG on the cell membrane inhibits this signaling pathway (left panel). In fact, after BMP-9 or TGF-β binding to its type II receptor, ENG favors the recruitment of ALK1 and the subsequent phosphorylation of Smad1/5 (right panel).

4.2. ENG and cancer

4.2.1. Role of ENG on tumor cell behavior

ENG expression has been also detected in cancer cells, where it is involved in a series of biological processes such as proliferation, invasion and metastasis, thus modulating tumor cell behavior [237].

The specific role of ENG in cancer epithelial cells depends on the cell context [238]. In some neoplasms, including hepatocellular carcinoma (HCC), renal cell carcinoma (RCC), and pancreatic, ovarian and endometrial cancer, ENG promotes tumor development and progression, whereas it has been associated with tumor suppression in esophageal squamous cell carcinoma and breast, lung and prostate cancer [237-239].

Importantly, as ENG is a MSC marker [240], it is not surprising that this TGF-β coreceptor is highly expressed in many sarcoma subtypes [238]. In fact, ENG is upregulated in multiple sarcomas cell lines, and its expression correlates with increased proliferation capacity [241]. In this respect, several studies have revealed that ENG regulates malignant phenotypes of sarcomas cells by modulating both Smad-dependent and -independent mechanisms [238]. More specifically, ENG induces Ewing sarcoma cell plasticity by stimulating the BMP-Smad1 signaling cascade and the focal adhesion kinase (FAK) and PI3K non-Smad pathways [242]. Accordingly, *ENG* downregulation hinders invasiveness and abrogates tumor growth in preclinical models of Ewing sarcoma [242]. Importantly, high levels of ENG correlate with worse prognosis in patients with this sarcoma subtype [242]. Likewise, overexpression of ENG predicts poor OS and PFS in uterine leiomyosarcoma patients [243]. Indeed, *ENG* knockdown reduces the invasive and migratory abilities of uterine leiomyosarcoma cells [243]. Similarly, ENG is upregulated in human angiosarcoma and its inhibition with small interfering RNA (siRNA) in tumor cells leads to a less aggressive phenotype, with induction of apoptosis and suppression of migration and invasion [244]. In line with these data, a recent study has suggested that ENG promotes the pro-metastatic phenotype of osteosarcoma cells [245]. In addition, increased ENG expression is associated with malignant progression of two human sarcoma subtypes: chondrosarcoma and gastrointestinal stromal tumor (GIST) [246,247]. Other sarcomas, including fibrosarcoma [248], Kaposi sarcoma [249], malignant fibrous histiocytoma [250], Wilms tumor [251] and rhabdomyosarcoma [252], also express ENG, although its specific function has not yet been defined. Collectively, these data reveal that ENG upregulation is a common event in sarcoma, which is linked to pro-tumoral and pro-metastatic effects. However, whether ENG is involved in the progression of MPNSTs has not yet been investigated.

4.2.2. Impact of ENG on the TME

In addition to being expressed in tumor cells, ENG is also present in various non-malignant cell types within the TME (e.g. ECs, MSCs, CAFs and immune cells), actively regulating their behavior during tumorigenesis [236,237]. However, based on the pivotal function of ENG in angiogenesis, most of the studies examining the role of ENG in the TME have focused on tumor-associated ECs [191,253,254].

In fact, ENG expression has been shown to be upregulated in actively proliferating ECs of tumor-associated vessels in different types of cancer, which has led to the use of ENG as a reliable marker for measuring intratumoral microvessel density (IMVD) [255]. Importantly, high ENG-positive IMVD is closely correlated with poor prognosis in

numerous tumor types [255]. Recently, a potential mechanism was proposed by which high endothelial ENG expression may predict worse outcome in different neoplasms [256]. It was demonstrated that continuous ENG overexpression in mice stimulates EC activation and induces angiogenesis, although it hinders vessel stabilization and maturation, giving rise to more permeable vessels [256]. These alterations promote the intravasation of tumor cells and the subsequent formation of metastases, resulting in a poorer cancer prognosis [256].

There is ample evidence that ENG is a key player in tumor angiogenesis. *ENG* downregulation by siRNA impairs the proliferation and angiogenesis of human ovarian carcinoma-derived ECs [257], and it reduces the number of tumor-associated vessels and the growth of mammary adenocarcinomas *in vivo* [258]. Similarly, allelic or EC-specific deletion of *ENG* in lung carcinoma and breast cancer mouse models, respectively, decreases both tumor volume and vascularization [259,260]. Likewise, *ENG* haploinsufficiency generates smaller, less vascularized and less metastatic tumors in the transgenic adenocarcinoma mouse prostate (TRAMP) model [261]. These data suggest that targeting ENG represents a promising anti-angiogenic and anti-tumor therapeutic strategy as explained in the section 4.2.3.

ENG can be also secreted into the extracellular space, mediating tumor-stroma crosstalk [237]. In fact, a soluble form of ENG (Sol-ENG) has been identified that results from the shedding of the extracellular domain of membrane-associated ENG due to the activity of the matrix metalloproteinase 14 (MMP14) [262]. Some studies showed that the ENG extracellular domain fused to an immunoglobulin Fc domain (ENG-Fc), mimicking Sol-ENG, inhibits *in vitro* and *in vivo* angiogenesis [262,263] and reduces tumor growth in a xenograft model of colorectal cancer (CRC) [263]. These observations suggest an anti-angiogenic and anti-tumor function for Sol-ENG. However, high plasma or serum levels of Sol-ENG have been correlated with poor survival and metastasis in some cancer patients [264,265]. Together, these findings indicate that the role of Sol-ENG in cancer remains unclear. In addition, ENG can be released by cells as a cargo of EVs [266]. In this respect, ENG-expressing EVs derived from human renal cancer stem cells induce angiogenesis and promotes lung PMN formation and metastasis [267]. Accordingly, plasma levels of ENG-positive EVs are significantly higher in metastatic breast cancer patients compared to healthy controls [268], suggesting that EV-associated ENG could be a novel non-invasive biomarker for cancer patients. Nevertheless, the potential diagnostic use of ENG in circulating EVs has not yet been explored in other tumor types.

4.2.3. Targeting ENG for multi-target directed cancer therapy

Given the high expression of ENG in both cancer cells and non-malignant cells (especially activated ECs) from different types of tumors, this TGF-β coreceptor has been exploited as an attractive target for tumor cell- and stroma-directed therapy [237,269]. Indeed, in the last few years, significant progress has been made in the development of ENG-targeting strategies, including monoclonal antibodies (mAbs), antibody-drug conjugates (ADCs), radiolabeled antibodies and vaccines [237,238]. Among them, TRC105 or carotuximab (TRACON Pharmaceuticals, Sand Diego, CA) represents the most successful anti-ENG therapy [238]. TRC105 is a chimeric IgG1 mAb that binds to the extracellular domain of human ENG and prevents BMP-9 binding, thereby inhibiting ENG-mediated downstream signaling (i.e. Smad1/5 phosphorylation) [270]. As well as competing with BMP-9, this drug induces apoptosis via antibody-dependent-cell-mediated cytotoxicity (ADCC) [254].

In order to better explore the effect of anti-ENG treatment in preclinical models, a specific mouse ENG-neutralizing rat IgG1 antibody was developed, M1043. This mAb effectively blocks BMP-9-induced ENG signaling in mice [270]. Multiple studies proved that ENG targeting with TRC105 and M1043 impaired tumor growth and metastasis in different syngeneic and human xenograft mouse tumor models [269]. These therapeutic effects were attributed in large part to the inhibition of tumor angiogenesis, but also to the targeting of ENG on tumor cells, CAFs and immunosuppressive cells (e.g. regulatory T cells (Tregs) and myeloid-derived suppressor cells (MDSCs)) [253,269].

Based on this potent preclinical efficacy, TRC105 was first tested in a phase I clinical trial involving patients with advanced refractory solid tumors [271]. The treatment was well-tolerated and exerted anti-tumor activity, with durable SD in 47% of patients [271]. These data formed the basis for further clinical development and led to phase II trials of single-agent TRC105 in patients with advanced HCC and bladder and prostate cancer [272-274]. These studies revealed that TRC105 monotherapy exhibited preliminary evidence of efficacy, suggesting that combination treatments could enhance clinical benefit [272-274].

Accordingly, several phase II trials evaluated the combination of TRC105 with other agents, such as chemotherapy (e.g. capecitabine) or VEGF/VEGFR-targeted drugs (e.g. bevacizumab, axitinib, pazopanib), in patients with different advanced solid malignancies [269] (see **Table 2** for TRC105 clinical trials). Results from these studies indicated that the combination therapies including TRC105 showed a favorable toxicity profile and were associated with promising outcomes in terms of disease control rate (DCR), PFS and OS [269]. More specifically, TRC105 in combination with pazopanib demonstrated

encouraging efficacy in patients with advanced STS, with a RR of 32% [275]. These data have led to a multicenter phase III trial of TRC105 plus pazopanib in patients with advanced angiosarcoma [276]. Collectively, these findings reveal that TRC105 in monotherapy but, more notably, in combination regimens, could be an attractive treatment option for patients with solid tumors, particularly for those with angiogenesis-dependent neoplasms (e.g. some sarcoma subtypes). Nevertheless, there is a lack of knowledge regarding the effect of TRC105 as single agent or in combination with other drugs in MPNST patients, who have significant unmet therapeutic needs.

Table 2. Published data from clinical trials of TRC105

Treatment	Phase	Disease	Patients (n)	Outcome	Adverse effects	Study
TRC105	I	Advanced or metastatic solid tumors	50	SD:47% (two ongoing responses at 48 and 18 mo.)	Well-tolerated. Most AEs graded as 1 and 2. MTD: 10mg/kg every week 15mg/kg every two weeks.	[271]
TRC105	II	Urothelial carcinoma	13	SD:15.4% 3-mo PFS: 18.2%. OS: 8.3 mo.	Most common AEs: grade 1 telangiectasia and grade 2 anemia	[272]
TRC105	I/II	Metastatic castration-resistant prostate cancer	20	SD: 50%	Favorable toxicity profile. Most common AEs: infusion-related reaction, headache, anemia, epistaxis and fever	[273]
TRC105	II	Hepatocellular carcinoma refractory to sorafenib	11	Confirmed PR: 10% at 32 weeks PFS: 3 mo. OS: 6.6 mo.	Only grade 1 and 2 AEs (headache and epistaxis)	[274]
TRC105+ capecitabine	I/II	Metastatic breast cancer	10	SD: 30% (beyond 9 weeks) PR: 10%	Grade 1 or grade 2 AEs (infusion reaction, epistaxis, telangiectasia, headache, rash, fatigue)	[277]
TRC105+ bevacizumab	II	Glioblastoma	22	OS: 5.75 mo. (exceeding the historical 4-mo. OS with bevacizumab alone)	Well-tolerated	[278]
TRC105+ bevacizumab	Ib	Advanced solid tumors	38	ORR: 58%. More durable responses than reported for bevacizumab alone	Most AEs were graded as 1 or 2	[279]
TRC105+ axitinib	II	Advanced metastatic renal cell carcinoma	18	ORR: 28%	Well-tolerated. Most frequent AEs: headache, epistaxis diarrhea	[280]
TRC105+ pazopanib	Ib/II	Advanced soft tissue sarcoma	81	ORR: 32% (lasting more than 75 weeks)	Well-tolerated. AEs of each drug were not increased in frequency or severity with the combination	[275]

SD, stable disease; PFS, progression-free survival; OS, overall survival; PR, partial response; ORR, overall response rate; AEs, adverse effects; MTD, maximum tolerated dose; mo., months.

In summary, ENG expression in cancer cells, mainly sarcoma cells, and in tumor-associated endothelium has been widely described to promote tumor progression and metastasis. Accordingly, the anti-ENG antibody TRC105, alone and, principally, in combination with other therapies, has shown promising clinical activity in patients with solid tumors, especially in STS patients. However, whether ENG is 1) an important player and 2) a therapeutic target in MPNSTs is still unknown.

OBJECTIVES

In view of the dismal prognosis of MPNSTs and the lack of known effective therapies, in this PhD thesis, we attempted to identify novel mediators of MPNST pathogenesis that may serve as potential therapeutic targets for these tumors.

Based on our preliminary data, we focused on analyzing the role of the TGF-β coreceptor ENG in MPNST progression, evaluating its use as a novel biomarker both in tissue and in plasma, the molecular mechanisms involved, and its potential as a therapeutic target in this disease.

For this purpose, we defined the following specific objectives:

AIM 1: Evaluate the relevance of ENG in MPNST progression.

AIM 2: Determine the role of ENG in MPNST progression.

AIM 3: Examine the use of ENG as a therapeutic target in MPNSTs.

MATERIALS AND METHODS

1. Cell culture studies

1.1. Cell lines

The human NF1-associated MPNST cell lines S462, 90-8, NMS-2, and the sporadic human MPNST cell line STS26T were generously provided by Dr. Eduard Serra (The Institute for Health Science Research Germans Trias i Pujol (IGTP) – PMPPC, Barcelona, Spain). The SNF02.2, SNF96.2 and SNF94.3 cell lines (NF1-derived MPNST) were purchased from the American Type Culture Collection (ATCC). They are among the most commonly used cell lines in MPNST research [91].
All these cells were cultured in high glucose Dulbecco's modified Eagle's medium (DMEM, Sigma, D5796) supplemented with 10% fetal bovine serum (FBS, Gibco, 10270-106), 1 mM sodium pyruvate (Sigma, S8636) and 20 µg/ml gentamicin (Sigma, G1272). All cell lines were maintained in a humidified incubator with 5% CO_2 at 37ºC and routinely tested for mycoplasma contamination (MycoAlert™ Mycoplasma Detection Kit, Lonza, LT07-418).

1.2. Cell model generation

1.2.1. Generation of luciferase-GFP expressing tumor cells

With the aim of monitoring and quantifying MPNST growth and metastasis *in vivo*, lentivirus expressing the firefly luciferase fused to the green fluorescence protein (GFP) were generated and used to infect MPNST cells.

For this purpose, a monolayer of HEK293T cells with 70-80% confluence was co-transfected with the lentiviral vector pFUGW-FerH-ffluc2-eGFP containing the GFP-Luc fusion gene (5 µg) and the packaging plasmids (pLP1 (3.55 µg), pLP2 (1.25 µg), pLP/VSVG (1.75 µg)) using the X-tremeGENE 9 DNA Transfection Reagent (Roche). More specifically, 500 µl of DMEM containing the amounts of plasmids indicated above were mixed 1:1 with the X-tremeGENE 9 DNA Transfection Reagent diluted in DMEM (1:6 ratio). This transfection complex was incubated for 20 min and then added to HEK293T cells. Media was changed 8 hours after transfection and the supernatants containing lentiviruses were collected 24 hours later and passed through a sterile 0.45 µm filter (Celltrics, sysmex).

MPNST cells were transduced with the viral supernatants (3:1 dilution with DMEM) supplemented with 8 µg/ml polybrene (Sigma, H9268) for enhancing infection efficiency.

GFP expression was monitored using an inverted fluorescence microscope (Leica DM IL LED / Cool LED p300 lite). In order to enrich for GFP-Luc expressing cells, cells were sorted for GFP expression on a FACSAria™ IIu sorter (BD). Luciferase activity was measured using a Luciferase Assay System (Promega, E1500) (see *In vitro luciferase activity measurement* section) or an IVIS Spectrum Imaging System (PerkinElmer) after the addition of D-luciferin (Sydlabs, MB102).

1.2.2. *ENG* gene silencing via lentiviral transduction of shRNAs

For short hairpin RNA (shRNA)-mediated knockdown of *ENG* in MPNST cells, lentiviral particles encoding shRNA designed to silence human *ENG* (shENG, Santa Cruz Biotechnology #sc35302-V) or a non-targeting control scrambled sequence (shScramble, Santa Cruz Biotechnology, sc-108080) were used. MPNST cells were transduced with the lentiviruses at a multiplicity of infection (MOI) of 10 in the presence of 8 µg/ml polybrene. Selection of infected cells was started 48 hours after infection with 1 µg/ml puromycin (Sigma, P8833). *ENG* downregulation was determined by real-time quantitative polymerase chain reaction (qRT-PCR), Western blot and immunofluorescence (see *Molecular and cellular biology-related experiments* section).

1.3. Cell sorting

For cell sorting, MPNST cells were harvested with cell dissociation buffer (Gibco, 13151-014), washed and resuspended in Fluorescence-Activated Cell Sorting (FACS) buffer (D-phosphate-buffered saline (PBS), 5 mM ethylenediamine tetraacetic acid (EDTA), 0.1% bovine serum albumin (BSA)) at a concentration of $5x10^6$ cells/ml. Then, cells were passed through a sterile 50 µm disposable filter (Celltrics, sysmex). Viability was assessed by staining with 4', 6-diamidino-2-phenylindole (DAPI) (Sigma, D9542), and cell debris and aggregates were excluded based on forward scatter (FSC) and side scatter (SSC) (pulse width and area). Live GFP-positive cells were subsequently sorted using a 100 µm nozzle and 20 psi on a FACSAria™ IIu sorter (BD) under aseptic conditions. Sorted cell populations were then re-analyzed to ensure high purities after cell sorting and cultured in a humidified incubator with 5% CO_2 at 37ºC.

1.4. Cell signaling assays

To analyze the effects of ENG targeting and/or MEK inhibition on associated signaling pathways in MPNST cells, $2x10^5$ STS26T or ST88-14 cells were seeded in six-well plates. Upon 80-90% confluency, cells were starved overnight in the presence of either the anti-

human ENG mAb TRC105 (TRACON Pharmaceuticals, San Diego, CA, USA) alone, the MEKi PD-901 alone, the combination of the two drugs, or an IgG control (Jackson InmunoResearch Laboratories, INC). PD-901 was synthetized by the Experimental Therapeutics Unit (ETP) of the Spanish National Cancer Research Centre (CNIO) according to the procedure described by Barrett and colleagues [281]. TRC105 and IgG were added to the culture medium at a final concentration of 50 µg/ml and PD-901 at 10nM for STS26T cells or at 1nM for ST88-14 cells. Next day, cells were stimulated with 50 ng/ml recombinant human BMP-9 (R&D Systems, 3209-BP-010) and 150 ng/ml recombinant human VEGF (PeproTech, 100-20) for one hour at 37ºC in a humidified 5% CO_2 atmosphere. Then, cells were lysed, protein content was determined and the activation status of the Smad1/5 and MAPK/ERK signaling pathways was analyzed by Western blot (see *Protein extraction and quantification* and *Western blot analysis* sections). MPNST cells in serum-free DMEM without neither pre-treatment nor stimulation were used as a control.

2. Animal studies

All experiments with mice were performed in accordance with protocols approved by the Institutional Ethics Committee for Research and Animal Welfare (CEIyBA) of the CNIO (IACUC 006-2016), the Instituto de Salud Carlos III (ISCIII, CBA 15_2017) and the Comunidad Autónoma de Madrid (CAM, PROEX 168/17). Hsd:Athymic Nude-Foxn1^{nu} mice were purchased from ENVIGO. NOD. Cg-*Prkdc*^{scid} *Il2rg*^{tm1Wjl}/SzJ mice, commonly known as NOD scid gamma (NSG) mice, were bred in house at specific pathogen-free conditions. Mice were maintained under a regular 12-hour light-dark cycle in a temperature-controlled room (22 ± 1ºC). Details for specific animal experiments are described below.

2.1. *ENG*- and Scramble-shRNA xenograft experiments

To assess the impact of *ENG* knockdown on MPNST progression, 1x10^6 STS26T-shScramble or –shENG cells were resuspended in 100 µl of 1:1 serum-free DMEM/Matrigel (Corning) and injected subcutaneously into both flanks of 7-week old female athymic nude mice. Tumor growth was monitored twice weekly by caliper measurement of the two orthogonal large and small external diameters (a, b). Tumor volume was calculated using the formula V = a x b2 x π/6. In accordance with our animal protocols, mice were sacrificed when tumors reached approximately 1.5 cm^3. Tumors were excised and processed for histological analysis. Sentinel lymph nodes (LNs) were

also collected, fixed in 10% formalin and analyzed for the presence of metastases by hematoxylin and eosin (H&E) staining (see *Immunohistochemical analyses*).

2.2. Drug treatments

2.2.1. Systemic treatment of subcutaneous xenograft models with anti-ENG therapies alone or in combination with MEKi

7-week old female athymic nude and NSG mice were injected subcutaneously with $1x10^6$ STS26T cells or $10x10^6$ ST88-14/GFP-Luc cells, respectively, suspended in 1:1 serum-free DMEM/Matrigel. Tumors were allowed to form for one week until they were palpable (~100 mm^3 for STS26T xenografts and ~50 mm^3 for ST88-14 xenografts). Then, mice were treated with the anti-human and –mouse ENG mAbs TRC105 and M1043 (TRACON Pharmaceuticals, San Diego, CA, USA) and the MEKi PD-901, in monotherapy or in combination regimens. The control groups received vehicle (0.5% methylcellulose (Sigma, M7140) and 0.2% Tween-80 (Sigma, P1754)) and/or IgG (Jackson InmunoResearch Laboratories, INC). Specific treatment groups are indicated in *Results*. TRC105, M1043 and IgG were diluted in PBS and administered intraperitoneally (i.p.) at a dose of 10mg/kg body weight (BW) twice weekly. PD-901 was dissolved in 0.5% methylcellulose and 0.2% Tween-80 and given by oral gavage (p.o.) at 2mg/kg BW three times a week. Tumor volume was measured one or two times per week and calculated as described above. After three weeks of treatment, mice were sacrificed and ST88-14/GFP-Luc xenografts were analyzed for luciferase activity (see *in vivo and ex vivo imaging analysis* section). In all cases, tumors were dissected and either snap-frozen and stored at -80ºC for molecular biology studies or fixed in 10% formalin for immunohistochemical analysis. Harvested sentinel LNs were paraffin-embedded and stained with H&E in order to evaluate the presence of metastases (see *Molecular and cellular biology-related experiments* and *Immunohistochemical analyses* sections).

2.2.2. Experimental lung metastasis assay

To investigate the efficacy of combined anti-ENG/anti-MEK therapy in MPNST distant metastasis, $1x10^6$ STS26T/GFP-Luc cells, which exhibit lung tropism [282], were resuspended in 200 µl of DMEM and injected via tail vein in 7-week old female athymic nude mice. For this purpose, mice were kept under an infrared heat lamp to allow the vasodilatation of the veins and, then, they were placed in a restraining device. Injection was performed in the lateral veins of the tail.

One week later, non-invasive bioluminescence imaging (BLI) of the STS26T/GFP-Luc-injected mice was performed in order to assess metastasis formation (see *in vivo and ex vivo imaging analysis* section). Mice with established micrometastases were randomly assigned to receive PD-901 therapy either alone (2mg/kg BW p.o. three times a week) or in combination with TRC105 and M1043 (10mg/kg BW i.p. twice-a-week) for a period of three weeks. During this time, control mice were given biweekly i.p. injections of IgG (10mg/kg BW) and thrice-weekly oral administrations of vehicle (0.5% Methylcellulose-0.2% Tween-80). Metastases were monitored weekly by *in vivo* BLI. Mice were sacrificed 28 days after tumor cell injection and lung metastatic burden was measured by *ex vivo* BLI. Lungs were collected for histopathological studies.

2.3. *In vivo* and *ex vivo* imaging analysis

For *in vivo* imaging analysis, animals were anesthetized with isoflurane (3-3.5% for induction and 1.5-2% for maintenance) and injected i.p. with D-luciferin (30 mg/ml in 100 µl PBS) 8 min prior to BIL. Sequential images were captured by a Xenogen IVIS-200 machine (PerkinElmer). For *ex vivo* imaging analysis, D-luciferin was administrated as indicated above and, 8 min later, mice were euthanized. Tumors and organs with metastases (e.g. lungs) were collected and analyzed for luciferase activity using an IVIS Spectrum Imaging System (PerkinElmer). Photons emitted from the specific regions were quantified using the Living Image software 4.7.2. (PerkinElmer).

3. Molecular and cellular biology-related experiments

3.1. *In vitro* luciferase activity measurement

Luciferase activity was measured by the Luciferase Assay System (Promega, E1500) according to the manufacturer's protocol. Briefly, cells were lysed in 1x lysis buffer provided with the kit. After vigorous mixing to ensure complete cell dissociation, the lysates were centrifuged at 12,000 x g for 2 min, and then 20 µl of the supernatant were mixed with 100 µl of Luciferase Assay Reagent. Luminescence was immediately measured in a Modulus single tube multimode reader (Turner Biosystems).

3.2. Protein extraction and quantification

Cells were lysed with radioimmunoprecipitation assay (RIPA) buffer (Sigma, R0278) supplemented with protease and phosphatase inhibitors (Roche). Lysates were vigorously mixed, incubated on ice for 15 min, and then cleared by centrifugation at 14,000 x g for 20 min at 4ºC. Supernatant fractions were collected and used for Western blot.

Protein concentrations were quantified by the bicinchoninic acid (BCA) assay (Pierce™ BCA Protein Assay Kit, Thermo Fisher Scientific) according to the manufacturer's instructions. A standard BSA curve was freshly prepared for each assay in order to assure an accurate determination of unknown sample concentrations. Absorbance at 560 nm was measured by a microplate reader (Modulus™ II Microplate Multimode Reader, Turner BioSystems).

3.3. Western blot analysis

Protein lysates were mixed with 4x Laemmli Sample Buffer (Bio-Rad, 1610747) supplemented with the reducing agent 2-mercaptoetanol (355 mM final concentration, Sigma, M7522), and then boiled at 95ºC for 10 min. Equal amounts of proteins were subjected to sodium dodecyl sulfate–polyacrylamide gel electrophoresis (SDS-PAGE) in 10-12% polyacrylamide gels, and subsequently transferred to a nitrocellulose membrane (GE healthcare life science, 10600003) using a Mini Trans-Blot Cell system (Bio-Rad Laboratories). Transfer was performed at 300 mA during 2 hours at 4ºC. Membranes were blocked with 5% (w/v) BSA or milk in tris-buffered saline with 0.1% Tween-20 (TBS-T) for 1 hour at room temperature (RT) and incubated with the appropriate primary antibody (**Table 3**) overnight at 4ºC. β-actin antibody was used as a loading control. The next day, membranes were rinsed with TBS-T and incubated with horseradish peroxidase (HRP)-linked secondary antibodies (**Table 4**) for 1 hour at RT. Primary and secondary antibodies were diluted in 2.5% BSA or milk in TBS-T. Finally, immunoblots were revealed by the ECL Western Blotting Detection reagent (GE Healthcare) using high sensitivity X-ray films (GE Healthcare). The intensities of the immunoreactive bands were quantified by densitometry using ImageJ software (NIH).

Table 3. Primary antibodies for Western blot used in this PhD

Primary antibody	Company	Cat. Number	Isotype	Dilution
ENG	Abcam	ab169545	Rabbit	1:1000
MEK1/2	Cell Signaling Technology	8727	Rabbit	1:1000
p44/42 MAPK (ERK1/2)	Cell Signaling Technology	9107	Mouse	1:1000
phospho-MEK1/2 (Ser217/221)	Cell Signaling Technology	9154	Rabbit	1:1000
phospho-p44/42 MAPK (ERK1/2)	Cell Signaling Technology	4370	Rabbit	1:2000
phospho-Smad1/5 (Ser463/465)	Cell Signaling Technology	9516	Rabbit	1:800
Smad1	Cell Signaling Technology	6944	Rabbit	1:1000
β-Actin	Sigma	A5441	Mouse	1:10000

Table 4. Secondary antibodies for Western blot used in this PhD

Secondary antibody	Company	Cat. Number	Isotype	Dilution
Anti-mouse IgG-HRP	GE Healthcare	NA931	Sheep	1:5000
Anti-rabbit IgG-HRP	GE Healthcare	NA934	Donkey	1:5000
HRP-AffiniPure Anti-Mouse IgG	Jackson ImmunoResearch	115-035-003	Goat	1:5000
HRP-AffiniPure Anti-Rabbit IgG	Jackson ImmunoResearch	711-035-152	Donkey	1:5000

3.4. Immunofluorescence in fixed cells

Cells were plated on 0.1% gelatin-coated coverslips for 24 hours and then fixed with 4% paraformaldehyde (PFA, Electron Microscopy Sciences) in PBS for 20 min at RT. After washing three times with PBS, fixed cells were permeabilized with 0.1% Triton X-100 (Sigma) in PBS for 10 min at RT. Samples were then rinsed three times with PBS, blocked with 1% BSA and 5% donkey serum (Sigma, D9663) in PBS for 45 min at RT, and incubated with the anti-ENG primary antibody (DAKO, M3527; dilution 1:100 in 1% BSA-PBS) overnight at 4ºC. The next day, cells were washed three times with PBS and incubated with the Alexa Fluor 488 donkey anti-rabbit secondary antibody (Thermo Fisher Scientific, A21206; dilution 1:200 in 1% BSA-PBS) for 45 min at RT. Cell nuclei were counterstained with DAPI and coverslips were mounted using ProLong™ Diamond Antifade Mounting Media (Thermo Fisher Scientific, P36970). Negative controls were obtained by omitting the primary antibody. The fluorescence emission was captured by a confocal TCS SP5-WLL (AOBS-UV) spectral microscope (Leica Mycrosystems, Wetzlar, Germany).

3.5. RNA extraction

Total RNA was extracted from tissues or cells using a combination of the acid guanidinium thiocyanate-phenol-chloroform (AGPC) method and the RNeasy Mini Kit (Qiagen, 74106). RNA isolation was performed with the TRIZOL reagent (Invitrogen), and the collected aqueous phase was passed through the RNeasy mini spin columns, followed by the steps in RNeasy Mini Kit manufacturer's instructions. For tumor samples, frozen tissue was first homogenized with an IKA T10 Basic Ultra Turrax Homogenizer (Cole-Parmer). The concentration and quality of the extracted RNA were determined by a NanoDrop ND-1000 spectrophotometer (Thermo Fisher Scientific) and an Agilent 2100 bioanalyzer (for RNA sequencing (RNA-seq) experiments).

3.6. RNA-seq and bioinformatic analyses

RNA-seq was performed by the CNIO Genomics Unit. 1 µg of total RNA from each sample was used. Average sample RNA Integrity Number (RIN) was 9.65 (ranging from 9.5-9.9), as obtained from an Agilent 2100 Bioanalyzer.
Poly-(A) fraction was purified and randomly fragmented, converted to double stranded cDNA and processed through subsequent enzymatic treatments of end-repair, dA-tailing, and ligation to adapters as in Illumina's "TruSeq Stranded mRNA Sample Preparation Part # 15031047 Rev. D" kit. Adapter-ligated library was completed by PCR with Illumina paired-end primers. The resulting purified cDNA library was applied to an Illumina flow cell for cluster generation and sequenced in a 50 base single-read format using the Illumina HiSeq2500 platform by following manufacturer's protocols.

Poly-(A) tails and adapters were removed with bbduk.sh, following the Lexogen recommendations. Processed reads were analyzed with the nextpresso pipeline [283] as follows. Sequencing quality was checked with FastQC v0.10.1 (ht412tp://www.bioinformatics.babraham.ac.uk/projects/fastqc/). Reads were aligned to the human genome (GRCh37/hg19) with TopHat-2.0.10 [284] using Bowtie 1.0.0 [285] and Samtools 0.1.1.9 [286], allowing three mismatches and 20 multihits. Differential expression was calculated with DESeq2 [287], using the human GRCh37/hg19 transcript annotations from https://ccb.jhu.edu/software/tophat/igenomes.shtml. GSEAPreranked [288] was used to perform gene set enrichment analysis of the described gene signatures on a pre-ranked gene list, setting 1000 gene set permutations. After Kolmogorov-Smirnoff test, only those gene-sets bearing a false discovery rate (FDR) q-value < 0.25 were considered significant.
For the RNA-seq from xenografts treated with anti-ENG therapies or IgG control, an initial filtering was done with Xenome [289] to remove reads coming from mouse. Only human reads and reads common to human and mouse were preserved.

3.7. Quantitative real time PCR (qRT-PCR) analysis

For targeted gene expression analyses, 1 µg of total RNA isolated from cells or frozen tissues was first reverse-transcribed into cDNA using the QuantiTect Reverse Transcription kit (Qiagen, 205313), according to the manufacturer's protocol. Briefly, after a first step of genomic DNA (gDNA) elimination with the gDNA wipeout buffer provided with the kit, reverse transcription was performed at 42ºC for 30 min, followed by heat inactivation of the reverse transcriptase at 95ºC for 3 min.

20 ng of the total cDNA were subjected to a 40-cycle qRT-PCR using TaqMan™ Gene Expression Master Mix (Applied Biosystems, 4369016) and pre-designed TaqMan® probes (Applied Biosystems, **Table 5**) at an annealing temperature of 60ºC. Assays were run in triplicates on a 7500 Fast Real Time PCR System (Applied Biosystems) or a QuantStudio 6 Flex Real-Time PCR System (Applied Biosystems). Gene expression was analyzed using the delta-delta Ct method for relative quantification and all samples were normalized to a housekeeping gene, *HPRT*.

Table 5. TaqMan® probes used in this PhD thesis

Gene	Species	Assay ID
ENG	Human	Hs00923996_m1
FGF1	Human	Hs01092738_m1
FGF2	Human	Hs00266645_m1
HPRT	Human	Hs02800695_m1
ITGA1	Human	Hs00235006_m1
ITGB1	Human	Hs01127536_m1
NFATC4	Human	Hs00190037_m1
PDGFc	Human	Hs00211916_m1
POSTN	Human	Hs01566750_m1
S100A1	Human	Hs00984741_m1
SEMA5A	Human	Hs01549381_m1
THBS1	Human	Hs00962908_m1
THBS2	Human	Hs01568063_m1
VEGFA	Human	Hs00900055_m1
VEGFc	Human	Hs01099203_m1
VEGFR1	Human	Hs01052961_m1

4. Human studies

4.1. Patient and sample collection

All studies involving human samples were performed in accordance to clinical research protocols approved for this purpose by the Ethical Committees from the ISCIII (CEI PI 13_2015v2) and the different implicated hospitals.

Tumor tissue samples were obtained from four independent cohorts of PNST patients at different stages. The paraffin-embedded blocks were provided by the Hospital 12 de Octubre (Madrid, Spain), the Weill Cornell Medical College (New York, USA), the Bambino Gesù Children's Hospital (Rome, Italy) and the Hospital Vall d'Hebron

(Barcelona, Spain). The complete collection comprised benign tumors (DNs and PNs, n=58), pre-malignant lesions (ANNUBPs, n=9) and MPNSTs (n=38). 63.8% of tumors were associated with NF1 and 36.2% were sporadic. The human tissue microarray (TMA) was obtained from the Hospital Virgen del Rocío (Seville, Spain). This array was created from 20 surgical specimens including primary and local recurrent MPNSTs and metastases. MPNSTs were located in the extremities in 75% of cases, the trunk in 13.5% and the head and neck in 11.5%. Metastases were found in the lungs and the thoracic wall. ENG expression was analyzed in all these samples by immunohistochemistry (IHC) and evaluated by independent pathologists, as described below.

Human peripheral blood samples were taken from PNST patients with different stages of disease and healthy subjects at Weill Cornell Medical College (New York, USA), Banco Nacional de ADN Carlos III (Salamanca, Spain), and Istituto Ortopedico Rizzoli (Bologna, Italy). Specifically, these series included 32 healthy control volunteers and 43 PNST patients with benign (PNs, n=32) or malignant (MPNSTs, n=11) tumors, all pathologically and histologically confirmed. All individuals provided informed consent for blood donation on approved institutional protocols.

Whole blood was collected in EDTA tubes, inverted for 8 to 10 times, and centrifuged at 1,100 x g for 10 min at RT using a swing-out bucket rotor. After centrifugation, three different fractions were distinguishable: the upper clear layer was plasma, the intermediate thin white layer called buffy coat was composed of leukocytes and platelets, and the bottom red layer contained concentrated erythrocytes. Then, the plasma fraction was poured into a new collection tube and immediately frozen at -80ºC.

4.2. sEV isolation from patient plasma samples

For sEV purification, plasma samples were thawed at 37ºC and then centrifuged at 3,000 x g for 20 min to remove residual blood cells and debris. The supernatant was collected and further centrifuged at 12,000 x g for 20 min in order to eliminate any possible apoptotic bodies and lEVs. sEVs were subsequently harvested by ultracentrifugation at 100,000 x g for 70min. At this step, the supernatant (EV-depleted plasma) was kept to quantify Sol-ENG concentration (see *ELISA-based analysis of plasma and EV-secreted ENG* section). Finally, the sEV pellet was washed with PBS and collected by another centrifugation at 100,000 x g for 70 min. All centrifugation steps were performed at 10ºC using a Beckman Optima X100 centrifuge with a Beckman 50.4Ti rotor. sEVs were resuspended in 100 µl of PBS and the protein content was measured by the BCA assay (Pierce™ BCA Protein Assay Kit, Thermo Scientific). Particle size and number were determined from an aliquot of 1 µl of plasma sEVs diluted in 1 ml of PBS using Nanosight

Nanoparticle tracking analysis (NTA, NS500 Malvern Panalytical). Nanosight NTA technology is equipped with a violet laser (405 nm) used for particle detection and real-time characterization.

4.3. ELISA-based analysis of soluble and EV-secreted ENG

ENG levels were measured in both sEV-enriched and EV-depleted human plasma fractions by enzyme-linked immunosorbent assay (ELISA) (Human ENG ELISA kit, Abcam, ab100507) according to manufacturer's instructions. For the analysis of sEV-secreted ENG, 5 µg of total sEVs were resuspended in 100 µl of 1x Assay Diluent provided with the kit. For the quantification of Sol-ENG, EV-depleted plasma was diluted 1:100 in 1x Assay Diluent. A standard curve was freshly prepared for each assay. Absorbance was read at 450 nm using a VICTOR 3 1420 Multilabel Counter (Perkin Elmer).

5. Immunohistochemical analyses

5.1. Tissue fixation, processing and staining

Tissue samples were fixed in 10% neutral buffered formalin (4% formaldehyde in solution), paraffin-embedded and cut into 3-µm thick sections, which were mounted in superfrost® plus slides and dried overnight. For different staining methods, slides were deparaffinized in xylene and re-hydrated through a series of graded ethanol until water.
Consecutive tissue sections were stained with H&E. For IHC, an automated immunostaining platform (Ventana Discovery XT, Roche) was used. Antigen retrieval was first performed with high or low pH buffer (CC1m, Roche, or RiboCC, Roche, respectively) depending on the primary antibody and endogenous peroxidase was blocked (peroxide hydrogen at 3%). Then, slides were incubated with the appropriate primary antibody as detailed in **Table 6**. After the primary antibody, slides were incubated with the corresponding secondary antibodies (**Table 7**) and visualization systems (OmniMap anti-Rabbit, Ventana, Roche; BOND Polymer Refine Detection, Leica) when needed conjugated with HRP.
Immunohistochemical reaction was developed using 3, 30-diaminobenzidine tetrahydrochloride (DAB) as a chromogen (Chromomap DAB, Ventana, Roche or DAB solution, Dako) and nuclei were counterstained with Carazzi's hematoxylin. Finally, the slides were dehydrated, cleared and mounted with a permanent mounting medium for microscopic evaluation. Positive control tissue sections known to express the target antigen were included in each staining run.

Table 6. Primary antibodies for IHC used in this PhD

Primary antibody	Company	Cat. Number	Isotype	Dilution
CD31	Abcam	ab28364	Rabbit	1:200
Cleaved Caspase-3 (Asp175)	Cell Signaling Technology	9661	Rabbit	1:400
ENG	DAKO	M3527	Mouse	1:100
Ki-67	DAKO	IR626	Mouse	1:500

Table 7. Secondary antibodies for IHC used in this PhD

Primary antibody	Company	Cat. Number	Isotype	Dilution
Anti-Mouse IgG-Biotinylated	DAKO	E0433	Goat	1:500
Anti-Rabbit IgG-Biotinylated	DAKO	E0432	Goat	1:500

5.2. Quantitative analysis of immunohistochemical staining

Whole slides were acquired with a scanner (Axio Scan Z1, Carl Zeiss, Germany) and images were captured with the ZEN software (Blue edition, Zeiss). Image analysis and quantification were performed using the Image Analysis Module (ZEN, Zeiss). In a first step, five 2-mm^2 rectangular ROIs (regions of interest) were selected in the digital images of each tumor tissue sample. Then, different ROIs from all the slides were chosen for automatic quantification (ZEN 2.6 Image analysis module), using an appropriate script for each antibody. Specific scripts were previously optimized for accurate quantification of the number of positive stained cells/vessels. The output results were exported as excel files with scoring data for each ROI. Finally, all the data were compiled and appropriately analyzed.

ENG-specific staining in human tumor tissues was scored according to the intensity and extent of expression as follows: 0-1, low ENG positivity; 2, moderate ENG positivity; 3, strong ENG positivity. The scoring was blinded by Dr. Eduardo Caleiras Pires (CNIO, Madrid, Spain), Dra. Angela Di Giannatale (Bambino Gesù Children's Hospital, Rome, Italy), Dra. Cleo Romagosa (Hospital Vall d'Hebron, Barcelona, Spain), Dr. Jose Luis Peralto (Hospital 12 de Octubre, Madrid, Spain) and myself. Data were collected only after all analyses were completed.

6. Statistical analyses

Unless otherwise indicated, graphs and statistical analyses were performed using the GraphPad Prism software version 9.1.0. Data are presented as mean ± standard error mean (SEM) and specific biological replicates are stated in the figure legends.
All data sets were first tested for normality using the Anderson-Darling, D'Agostino-Pearson omnibus, Shapiro-Wilk and Kolmogorov-Smirnov tests. When data were normally distributed, unpaired, two-tailed Student's *t* test or one-way ANOVA with post hoc analysis by Tukey's test were used for two-group and multiple-group comparisons, respectively. Unpaired *t* test with Welch's correction or Brown-Forsythe and Welch ANOVA were applied when variances were significantly different. For data with non-normal distributions, the non-parametric Mann-Whitney (2 groups) and Kruskal-Wallis (>2 groups) tests were conducted. Tumor growth curves were analyzed by two-way ANOVA. P-values were indicated in each figure for statistically significant comparisons ($p<0.05$).

7. Figures

All the cartoons shown in figures and schemes were created with Biorender.com (http://Biorender.com) or Microsoft Power Point software.

RESULTS

AIM I. Relevance of ENG in MPNST progression

ENG upregulation has been associated with cancer progression and worse clinical outcome in numerous solid tumors, especially in different sarcoma subtypes [237,238,255]. Nevertheless, there is a lack of information on the potential role of this protein in PNSTs. In order to fill this gap, in this thesis, we first examined the expression of ENG both in tumor tissue and in plasma from patients with different grades of PNST.

1.1. Analysis of ENG expression in different stages of human PNSTs

To address the first aim, we started evaluating ENG expression by IHC in a total of 105 PNSTs at different stages derived from four independent patient cohorts. This collection included benign tumors (DNs and PNs), pre-malignant lesions (ANNUBPs), and MPNSTs. Analysis of ENG staining in both tumor cells and ECs showed that the expression of this protein increased along with the malignant progression of PNSTs (**Figure 5A-B**). Remarkably, we observed a significant upregulation of ENG on these two cell types in MPNSTs compared with ANNUBPs or benign tumors (**Figure 5B**).

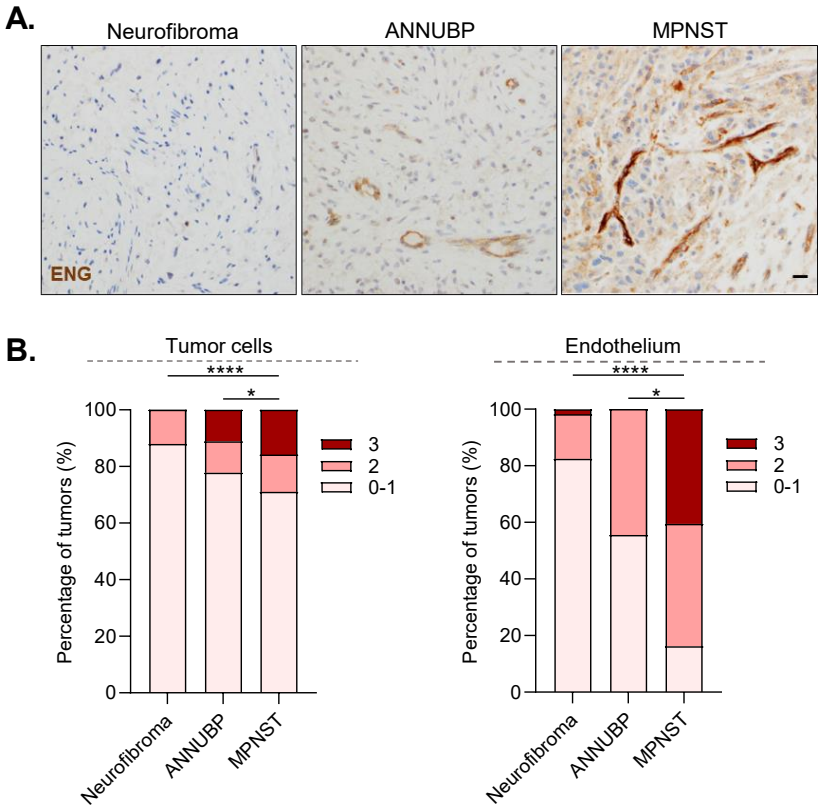

Figure 5. ENG is upregulated in human MPNSTs. A) Immunohistochemical staining for ENG in the indicated PNSTs. Scale bar=100μm, and **B)** their distribution (%) according to ENG expression (score 0-3) in both tumor cells (left panel) and ECs (right panel). Score 0-1, low ENG staining; 2, intermediate ENG staining and 3, high ENG staining. Benign neurofibromas n=58, ANNUBPs n=9, and MPNSTs n=38 from four independent patient cohorts. * P<0.05, **** P<0.0001 by one-way ANOVA.

Next, we examined ENG expression in a human TMA comprising primary and local recurrent MPNSTs, and metastases (from the lung and the thoracic wall). Immunohistochemical analysis revealed that ENG protein levels were elevated in both cancer cells and ECs of recurrent tumors and metastatic lesions (**Figure 6A-B**). Statistical evaluation showed a significant increase in ENG expression in metastatic lesions compared with primary MPNSTs (**Figure 6B**). Overall, these data demonstrate that ENG is significantly overexpressed on both tumor cells and ECs in primary MPNSTs and metastases, suggesting its important role as a novel biomarker in this disease.

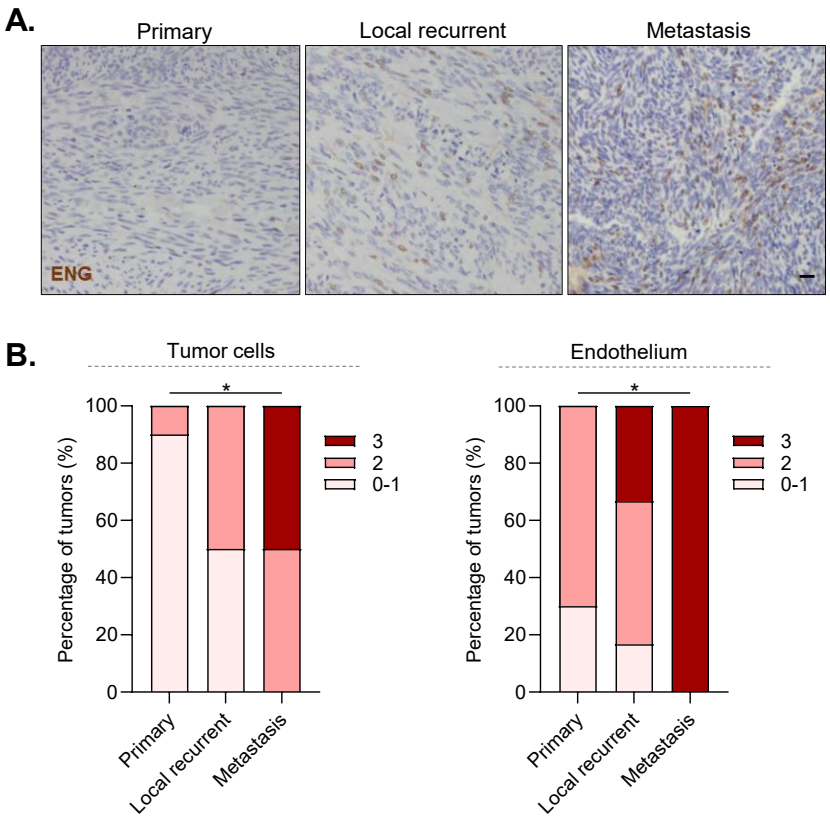

Figure 6. ENG expression correlates with advanced MPNST progression. A) Representative images of ENG IHC staining in a TMA comprising human MPNSTs at different stages. **B)** Quantification of ENG expression (score 0-3) in tumor cells (left panel) and the endothelium (right panel). Primary tumors n=10, local recurrent tumors n=6 and metastases n=2. * P<0.05 by one-way ANOVA.

1.2. Analysis of ENG levels in plasma samples from PNST patients at different disease stages

As mentioned in the introduction, high levels of soluble and EV-secreted ENG have been detected in the plasma from patients with CRC, prostate and breast cancer, correlating with disease progression and/or poor prognosis [264,265,268].

Thus, in order to evaluate the relevance of plasma ENG in PNST progression, we performed an analysis of this protein in the plasma of 44 patients with PNSTs in different degrees of malignancy (benign, PNs, and malignant, MPNSTs) and 23 healthy controls from three independent cohorts. Specifically, we separated plasma soluble proteins from sEVs using standard ultracentrifugation methods and we assessed the ENG protein concentration in both fractions by ELISA (**Figure 7A**). Although we did not find differences in the expression of Sol-ENG between the groups (**Figure 7B**), the levels of ENG in sEVs were significantly increased in MPNST patients compared to patients bearing benign PNs or healthy controls (**Figure 7C**).

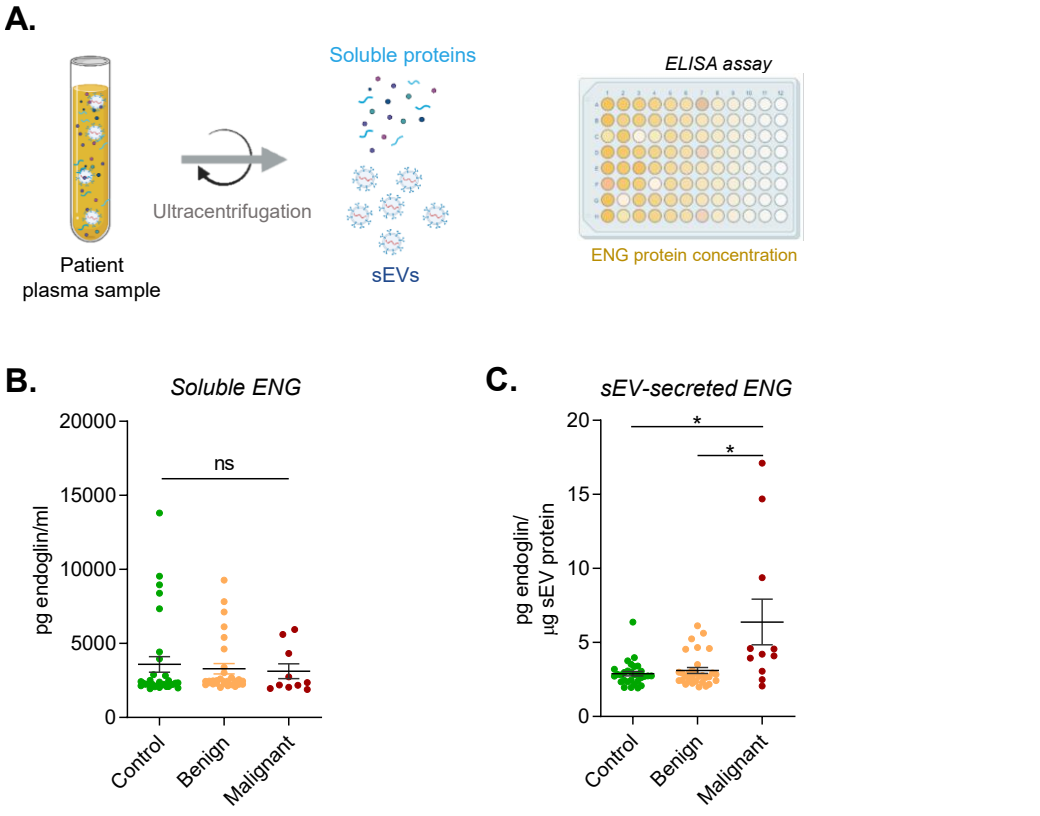

Figure 7. Analysis of ENG expression in plasma from PNST subjects at different stages. A) Experiment set up, circulating sEVs and soluble proteins were isolated from patient plasma samples using differential ultracentrifugation. ENG protein concentration was measured in both fractions by ELISA. **B-C)** Quantification of ENG levels in EV-depleted soluble fraction (B), and circulating sEVs (C) collected from the plasma of healthy controls (n=23) and patients with benign (PNs, n=33) or malignant (MPNSTs, n=11) PNSTs. sEV-secreted ENG levels were normalized to µg of total sEV protein. Mean ± s.e.m.; ns, not significant; * P<0.05 by one-way ANOVA.

Collectively, our results show that ENG is upregulated in both tumor cells and ECs in human MPNST tissue and, its expression correlates with more advanced stages of the disease (i.e. local recurrence and distant metastasis). Our data also demonstrate that ENG levels are increased in plasma-circulating sEVs from patients with MPNSTs. These findings therefore support the importance of ENG as novel biomarker both in tumor tissue and in liquid biopsies for the diagnosis of MPNSTs.

AIM II. Determine the role of ENG in MPNST progression

ENG has been reported to favor the progression and aggressiveness of diverse sarcoma subtypes by promoting malignant phenotypes of tumor cells and contributing to the creation of a favorable TME [238,241-244]. In this respect, our previous data also point to a potential role for ENG in MPNST cells and ECs. Thus, we aimed to define the specific mode of action of our protein in MPNSTs using *in vitro* and *in vivo* complementary studies.

To this end, we first evaluated ENG protein levels in a panel of human MPNST cell lines. All MPNST cells expressed ENG, except for the S462 model that lacked expression of this protein (**Figure 8A**). Moreover, since the MPNST research field has been traditionally hampered by a dearth of successfully established xenograft models [290], we tested the ability of these MPNST cell lines to form tumors in athymic nude mice. Out of all the models tested (STS26T, ST88-14, 90-8, NMS-2, SNF96.2, S462), only STS26T and S462 developed efficiently subcutaneous tumors (data not shown). As STS26T is the only ENG-expressing model that grows consistently as a xenograft, we focused our analysis mostly on this cell line. We silenced *ENG* expression in STS26T cells using lentiviral-driven transduction of shRNAs. We verified by qRT-PCR, Western blot and immunofluorescence that *ENG* levels were reduced by around 80% in *ENG*-depleted cells (shENG) compared to their respective controls (shScramble) (**Figure 8B**).

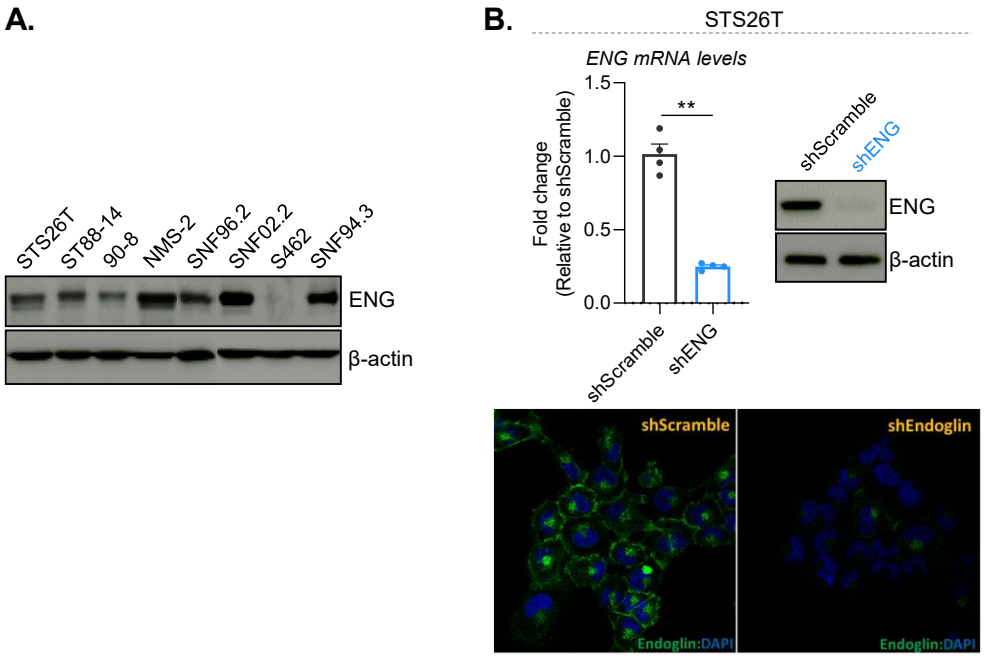

Figure 8. ENG expression in human MPNST cells. A) Immunoblotting showing ENG protein levels in a panel of human MPNST cell lines. **B)** Analysis of ENG expression after shRNA-mediated knockdown of *ENG* in STS26T cells by qRT-PCR, Western blot (upper panels), and immunofluorescence (lower panels). qRT-PCR data were normalized to shScramble. Mean ± s.e.m. of four biological replicates; ** P<0.01 by unpaired t-test.

2.1. Influence of ENG in MPNST cell molecular pathways

2.1.1. ENG-modulated gene expression profiles in MPNST cells

To examine the gene expression changes related to *ENG* silencing in MPNST cells, we performed RNA-seq gene expression profiling after knockdown of *ENG* in STS26T cells compared to shScramble control. Differential expression analysis showed that *ENG* depletion caused notable changes in the transcriptome of STS26T cells, leading to a significant deregulation of 951 genes (**Figure 9A**).

Gene Set Enrichment Analysis (GSEA) was then conducted to interrogate molecular pathways affected by *ENG* downregulation. GSEA revealed a significant suppression of gene signatures associated with oncogenic traits [291], including soluble angiogenic factors (e.g. VEGFA, PDGF, PIGF) and metastasis-related pathways (**Figure 9B**). Accordingly, the downregulation of several pro-angiogenic soluble factors (*VEGFA*, *PDGFc*, *FGF1, FGF2*) and pro-metastatic genes (periostin (*POSTN*), thrombospondin 2 (*THBS2*), semaphorin-5A (*SEMA5A*), integrin subunit beta 1 (*ITGB1*), S100 calcium-binding protein A1 (*S100A1*)) was confirmed at the mRNA level by qRT-PCR in STS26T cells upon *ENG* depletion (**Figure 9C**).

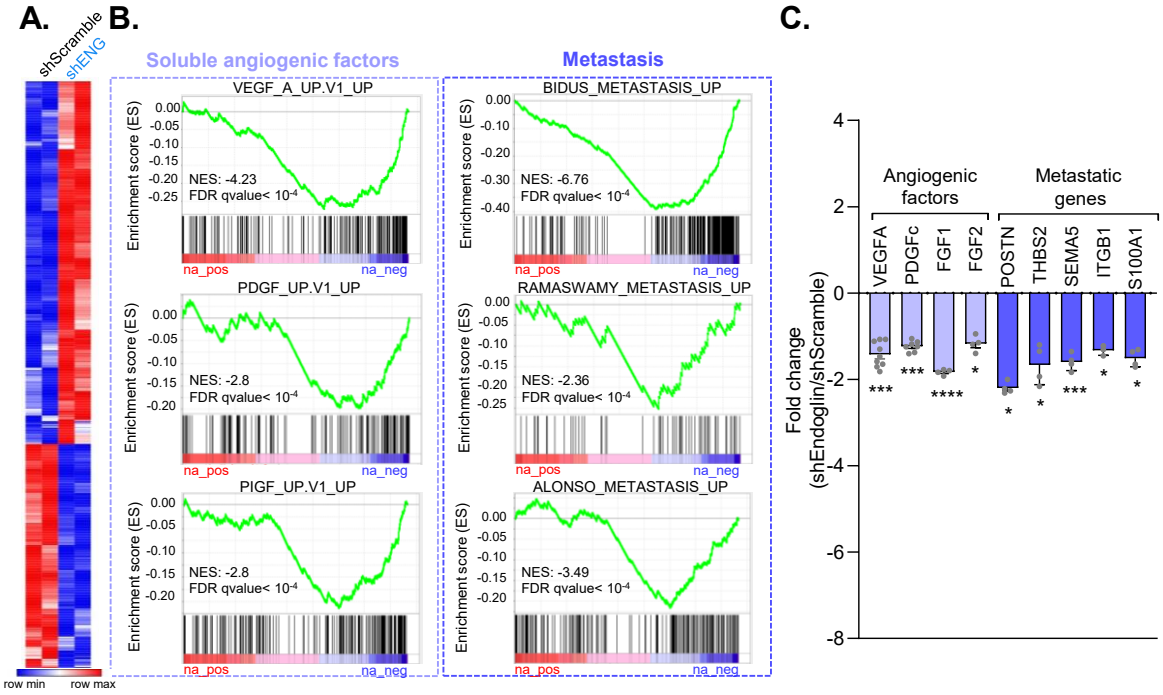

Figure 9. RNAseq reveals significant transcriptome changes in MPNST cells upon *ENG* depletion. A) Heat-map representation of the differentially expressed genes in shENG- versus shScramble-STS26T cells (FDR q-value<0.05). **B)** GSEA plots for the indicated genes signatures available in Molecular Signatures Database (MSigDB) (shENG versus shScramble). **C)** qRT-PCR validation of the selected downregulated genes in STS26T cells upon *ENG* knockdown. Data were normalized to shScramble. Mean ± s.e.m. of at least four biological replicates * P<0.05, *** P<0.001, ****P<0.0001 by unpaired t-test.

In order to validate these results in an additional MPNST model, we knocked down *ENG* in the human NF1-associated MPNST cell line ST88-14. We verified a reduction of around 80% in *ENG* mRNA and protein levels (**Figure 10A**). In accordance with our data in the STS26T model, *ENG* downregulation led to significantly decreased expression of both angiogenic (*VEGFA*, *VEGFc*, *PDGFc*) and metastatic (*THBS1*, *THBS2*, *SEMA5A*, *S100A1*) genes also in ST88-14 cells (**Figure 10B**). Overall, these findings strongly suggest that ENG contributes to the acquisition of pro-angiogenic and -metastatic traits in MPNST cells.

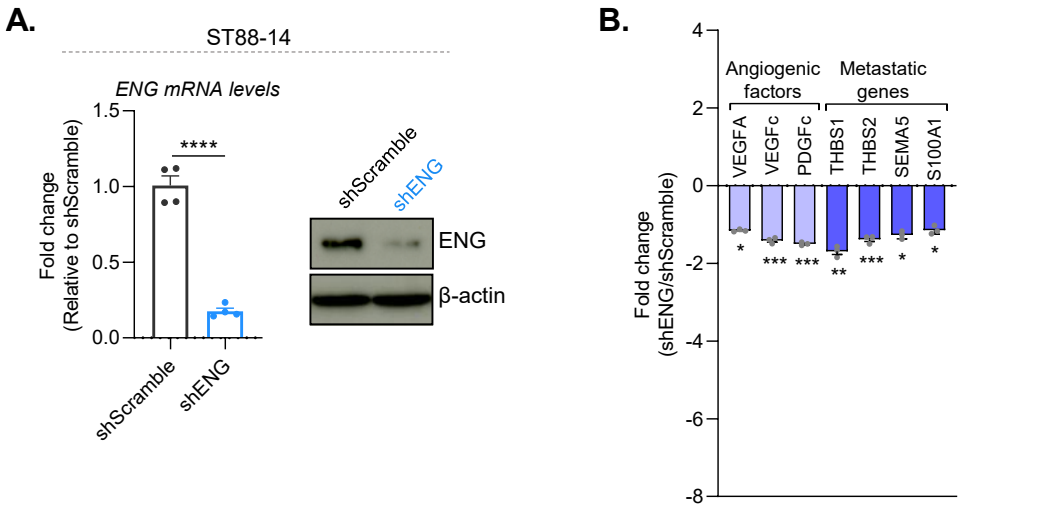

Figure 10. *ENG* downregulation leads to decreased angiogenic and metastatic gene expression in ST88-14 cells. A) Analysis of *ENG* mRNA (left panel) and protein (right panel) expression levels in ST88-14 cells transduced with lentiviral vectors coding for scramble- or ENG-shRNA. **B)** qRT-PCR analysis of the indicated angiogenic and metastatic genes. Data were normalized to shScramble. n=4. Mean ± s.e.m.; * P<0.05, ** P<0.01, *** P<0.001, ****P<0.0001 by unpaired t-test.

2.1.2. Effect of ENG in the activation of candidate signaling pathways in MPNST cells

As previously mentioned, the TGF-β coreceptor ENG is known to promote the ALK1-Smad1/5 signaling pathway [222]. Moreover, ENG can modulate other non-canonical, non-Smads pathways such as the MAPK/ERK signaling cascade [225,227], which plays crucial roles in MPNST malignancy and progression [20,118,121]. Thus, we assessed the impact of *ENG* downregulation on the activation of these signaling pathways in MPNST cells. We observed that knockdown of *ENG* significantly reduced p-Smad1/5 and p-ERK1/2 levels in both STS26T and ST88-14 cells (**Figure 11A-B**). These results indicate that ENG regulates the activation of the ALK1-Smad1/5 and MAPK/ERK signaling pathways in these MPNST cells.

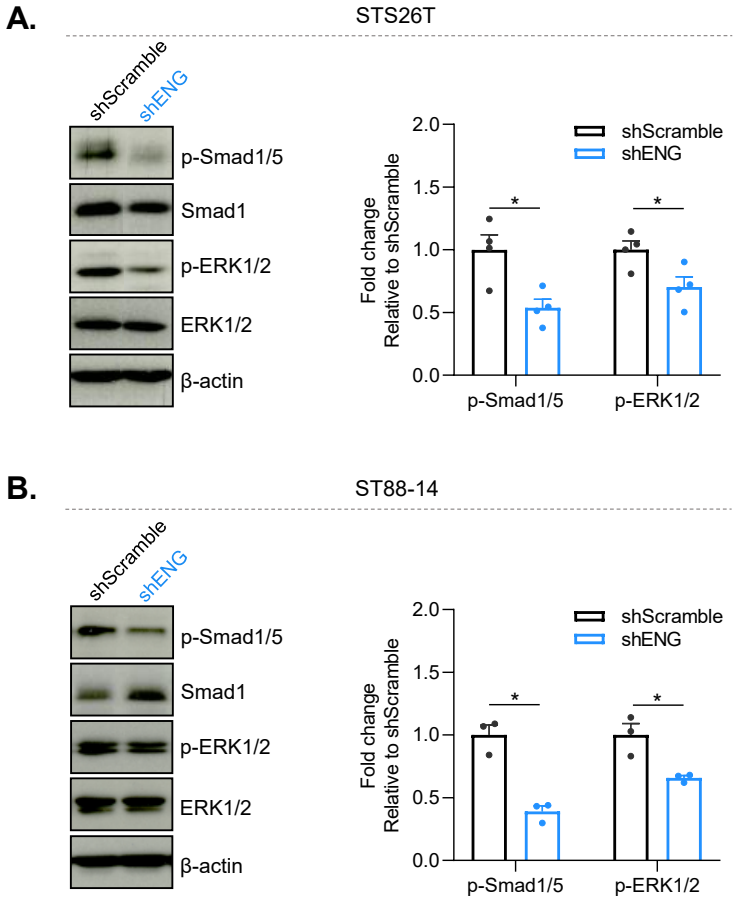

Figure 11. ENG expression modulates the activity of the Smad1/5 and MAPK/ERK signaling pathways in MPNST cells. A-B) Representative Western blot images and quantification of Smad1/5 and ERK1/2 activation in shScramble- and shENG- STS26T (A) and ST88-14 (B) cells. p-Smad1/5 and p-ERK1/2 levels were normalized to total Smad1 and ERK1/2 levels, respectively. Data are presented as the fold change compared to shScramble. Mean ± s.e.m. of at least three biological replicates; * P<0.05 by unpaired t-test.

2.2. Analysis of the role of ENG in MPNST progression *in vivo*

2.2.1. Downregulation of ENG blocks MPNST growth and metastasis

Next, we studied the effect of *ENG* depletion *in vivo*. To this end, we injected *ENG* knockdown (shENG) or control (shScramble) STS26T cells subcutaneously into athymic nude mice and measured tumor growth. Importantly, downregulation of *ENG* was sufficient to significantly reduce MPNST xenograft growth (**Figure 12A**). Moreover, the number and size of sentinel LN metastases were decreased in mice bearing *ENG* knockdown xenografts compared to those with control tumors (**Figure 12B**), suggesting that *ENG*-depleted MPNST cells have diminished metastatic abilities. IHC analysis confirmed a strong reduction of ENG protein levels in *ENG* knockdown tumors at the end of the experiment (**Figure 12C**). These results therefore demonstrate that ENG expression in tumor cells plays an important role in MPNST growth and metastasis.

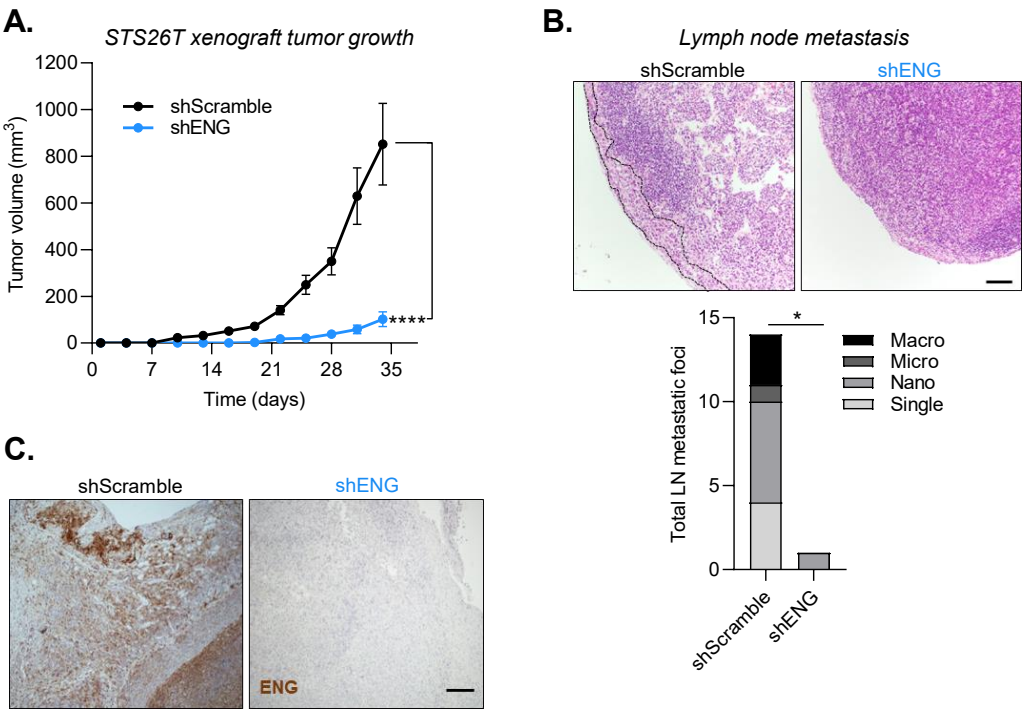

Figure 12. Silencing *ENG* reduces the tumorigenic potential of MPNST cells *in vivo*. A) Analysis of primary tumor growth in shScramble- and shENG-STS26T cells subcutaneously injected into both flanks of athymic nude mice. n=10 mice per group from two independent experiments. Mean ± s.e.m.; **** P<0.0001 by two-way ANOVA. **B)** LN metastasis burden was determined by H&E staining in LN sections at day 32 post-tumor cell injection (end-point). The black points encircle a metastasis. Scale bar=100µm. Quantification of the total number of metastatic foci in the LNs (lower panel). Lesions were binned into five size categories according to the number of tumor cells: single (1-2 cells), nano (3-10 cells), micro (11-30 cells) and macro (greater than 30 cells). n=10 LNs per group; * P<0.05. **C)** IHC for ENG in the xenografts at the human endpoint (day 32). Scale bar=200µm.

2.2.2. Defining the mode of action of ENG in MPNSTs

In order to dissect the mechanisms underlying the role of ENG in MPNST progression *in vivo*, we analyzed the expression of the proliferation and apoptosis markers Ki67 and caspase-3, respectively, in shScramble and shENG STS26T xenografts by IHC. Quantification of active caspase-3 staining showed that *ENG* knockdown does not affect MPNST cell death (**Figure 13A-B**). However, the number of Ki67-positive cells was significantly reduced in *ENG*-depleted xenografts compared to control tumors (**Figure 13A-B**), suggesting that ENG promotes MPNST cell proliferation.

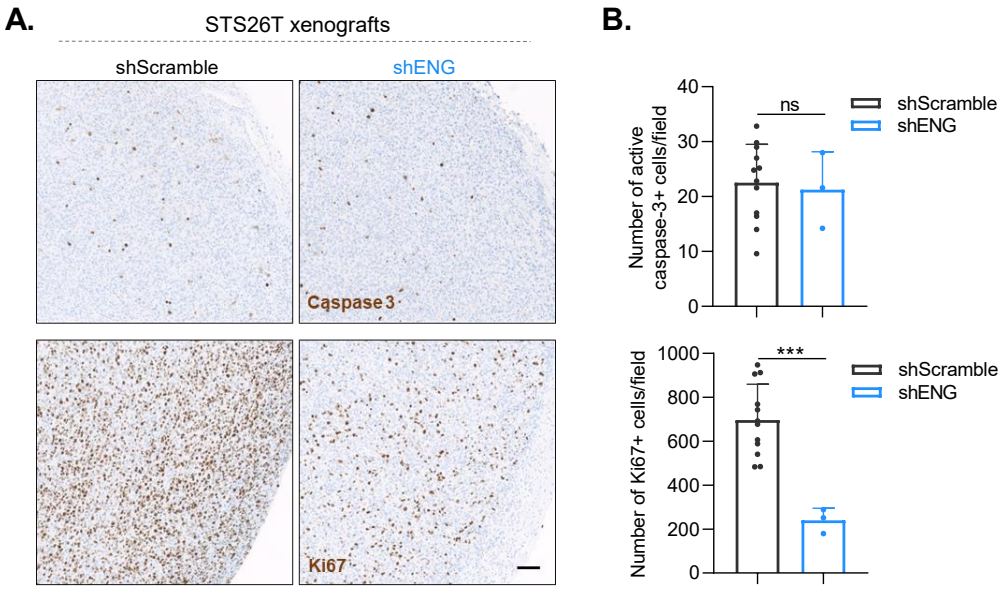

Figure 13. *ENG* depletion reduces tumor cell proliferation in MPNSTs. A) IHC analysis of the apoptotic marker active-caspase 3 (upper panels) and the proliferation marker Ki67 (lower panels) in shScramble- and shENG-STS26T xenografts (Scale bar=100μm), and **B)** quantification of the number of positive stained cells. Dots in the graphs represent the mean number of positive cells per field of each tumor (5 fields/tumor). Mean ± s.e.m.; ns, not significant; *** P<0.001 by unpaired t-test.

Besides being an important mediator of cancer cell behavior, ENG has been widely described to play a crucial role in the modulation of the TME, especially in promoting tumor angiogenesis [236,237,254,255]. In this regard, our previous data showed that *ENG* downregulation in MPNST cells resulted in reduced expression of soluble angiogenic factors. Hence, we next examined the effects of *ENG* knockdown on MPNST vascularization by performing immunohistochemical staining of the EC marker CD31.

Interestingly, *ENG* depletion in tumor cells caused a significant decrease in the number of CD31-positive vessels in STS26T xenografts (**Figure 14A-B**), suggesting that tumor-cell specific ENG indirectly stimulates angiogenesis probably through the up-regulation of proangiogenic factors.

Together, these findings provide a mechanistic explanation for ENG contribution to MPNST progression, giving a strong rationale for testing ENG inhibition in this pathology.

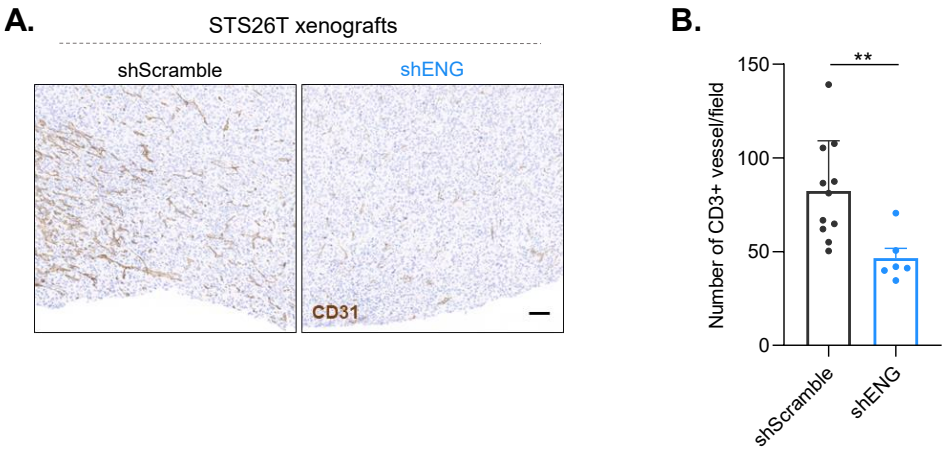

Figure 14. *ENG* knockdown in MPNST cells impairs angiogenesis within the TME. A) Representative images of CD31 immunohistochemical staining in the indicated tumors. Scale bar=100µm. **B)** Quantification of the number of CD31-positive vessels per field. Data correspond to mean ± s.e.m. of at least 6 independent tumors (with a minimum of 5 fields analyzed per tumor); ** P<0.01 by unpaired t-test. .

Overall, the results showed in this section demonstrate that ENG expression in MPNST cells favors the activation of the ALK1/Smad1/5 and MAPK/ERK signaling pathways and the expression of pro-metastatic and pro-angiogenic genes *in vitro*. Moreover, our data support an important role for ENG in MPNST progression *in vivo,* promoting both tumor cell proliferation and angiogenesis.

AIM III. Examine the potential of ENG as a novel therapeutic target in MPNSTs

Therapies targeting ENG have shown promising clinical efficacy in patients with solid tumors, especially with certain STS subtypes [269,275,276]. Since all our previous results demonstrate that ENG is involved in MPNST progression, we next ascertained whether ENG could be exploited as a new therapeutic target in this disease.

3.1. Analysis of the use of anti-ENG therapies for MPNST treatment

3.1.1. TRC105 and M1043 anti-ENG antibodies reduce MPNST progression

As ENG is expressed not only in tumor cells, but also in ECs of human MPNSTs, we aimed to target ENG on both tumor and stromal cells in order to mimic the effects of anti-ENG therapies in the clinical setting.

To this end, we treated nude mice bearing established subcutaneous STS26T xenografts, formed 7 days after tumor cell injection, with either the combination of anti-human (TRC105) and anti-mouse (M1043) ENG mAbs or a rat IgG as control. We monitored tumor growth and assessed sentinel LN metastases at the end of the experiment (**Figure 15A**). We found that the co-treatment with TRC105 and M1043 significantly decreased both primary tumor growth and LN metastatic burden (**Figure 15B-C**).

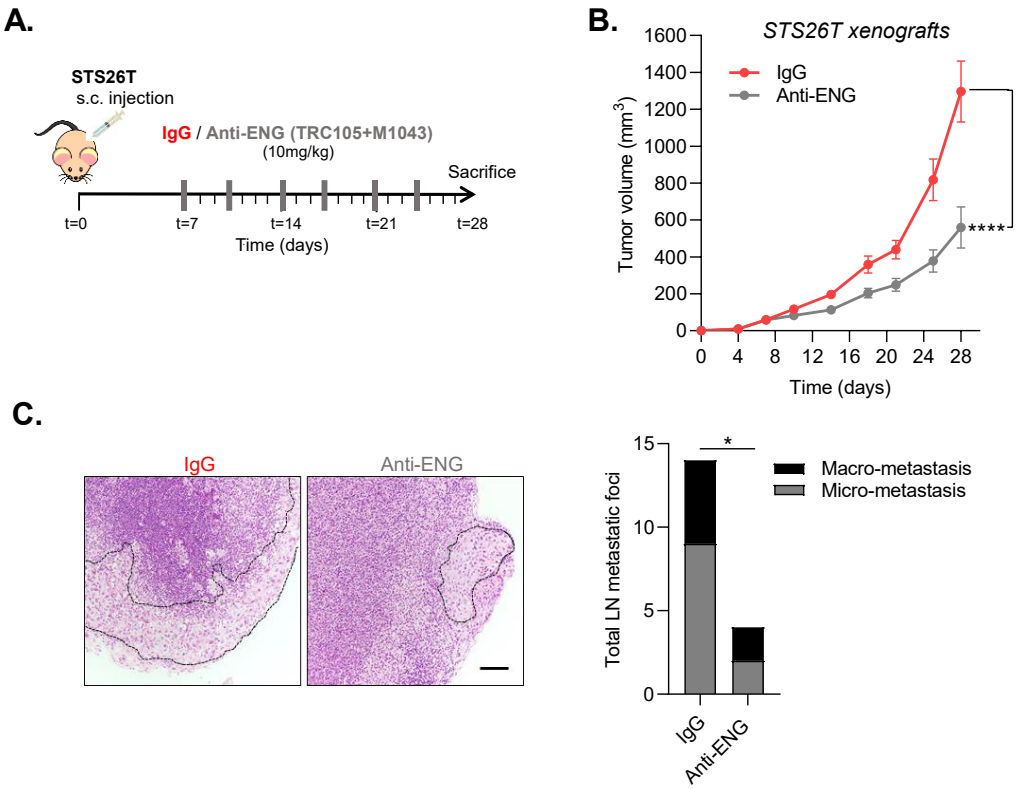

Figure 15. TRC105 and M1043 anti-ENG therapies reduce MPNST progression *in vivo*. A) Experiment set up; 6-8 week-old athymic nude mice were injected subcutaneously (s.c.) into both flanks with $1x10^6$ STS26T cells. One week later, when tumors were palpable (100mm^3 average), mice were treated with the anti-human and -mouse ENG mAbs TRC105 and M1043, respectively, or with a rat IgG as control (10mg/kg, intraperitoneally (i.p.), twice a week) for 3 weeks. Tumor volume was monitored and LN metastases were evaluated at endpoint (day 28). **B)** Growth curves of STS26T xenografts treated with TRC105 and M1043 (anti-ENG) or control IgG. n=5 mice per group (10 tumors/treatment). Mean ± s.e.m.; **** P< 0.0001 by two-way ANOVA. **C)** H&E staining of representative LNs (left panels). Metastases are highlighted by a discontinuous black line. Scale bar=100µm. Quantification of the total number of metastatic foci (right panel). Lesions were divided into micro-metastasis (11-30 cells) and macro-metastasis (greater than 30 cells). n=10 LNs per group; * P<0.05.

Given the importance of validating the pre-clinical efficacy of anti-ENG therapies in additional models of MPNST, we injected immunodeficient NSG mice with ST88-14/GFP-Luc cells subcutaneously and analyzed tumor formation. We found small palpable tumors (~50 mm^3 average) one week after cell injection. Then, mice were treated with either the anti-ENG mAbs TRC105 and M1043 or IgG control for three weeks, whereupon they were sacrificed and tumors were extracted. We observed that anti-ENG treatment significantly reduced tumor growth and led to tumor regression (**Figure 16A-B**).

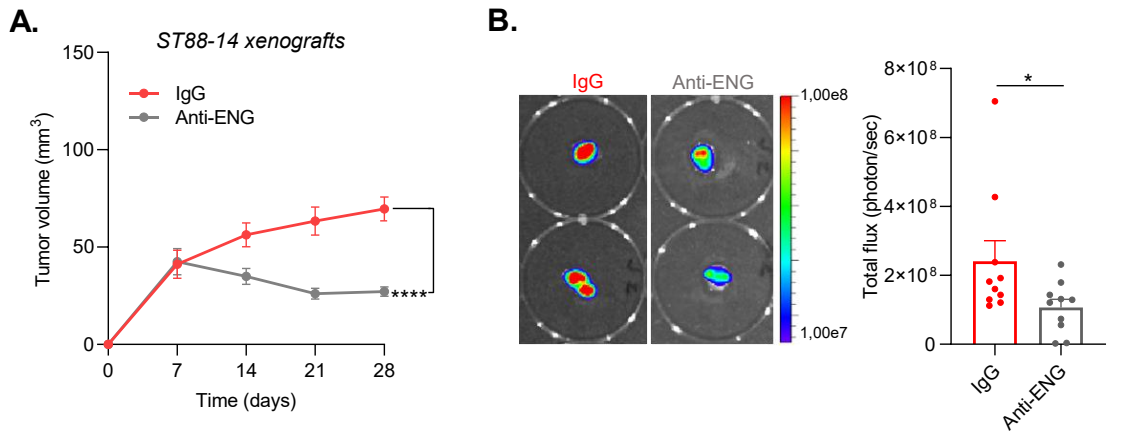

Figure 16. Anti-ENG treatment inhibits the growth of ST88-14 xenografts. A) ST88-14 xenograft tumor growth, assessed by caliper measurements, in mice treated with the anti-ENG mAbs TRC105 and M1043 or control IgG. **B)** Representative bioluminescence images and total flux quantification in control- and anti-ENG-treated tumors at day 28 (end-point). Data correspond to mean ± s.e.m. of 10 tumors per condition; **** P<0.0001 by two-way ANOVA in (A) and * P<0.05 by unpaired t-test in (B).

Together, these results reveal that targeting both tumor and stromal ENG efficiently decreases MPNST tumor growth and metastasis, suggesting that anti-ENG therapies could represent a novel treatment option for this tumor type.

3.1.2. Analysis of the molecular mechanisms mediating the anti-tumor effects of anti-ENG therapies in MPNSTs

To analyze the molecular pathways modulated by ENG targeting, we performed RNA-seq in the STS26T xenografts treated with TRC105 and M1043, and compared their expression profiles with those of IgG-treated control tumors. Differential expression analysis revealed a significant deregulation of 21 human genes in STS26T tumors upon inhibition of both tumor and stromal ENG (**Figure 17A**). Consistent with our previous data *in vitro*, anti-ENG treatment led to a significant suppression of pathways related to angiogenesis and metastasis (e.g. epithelial-mesenchymal transition (EMT)), as demonstrated by GSEA analysis (**Figure 17B**). Accordingly, among the most downregulated genes in anti-ENG-treated tumors, we found several pro-angiogenic (*VEGFR1*, nuclear factor of activated T cells 4 (*NFATC4*), plexin domain containing 1 (*PLXDC1*)) and pro-metastatic (*SEMA5A*, *POSTN*, *THBS2*, integrin subunit alpha 1 (*ITGA1*)) factors, which were validated by qRT-PCR (**Figure 17C**).

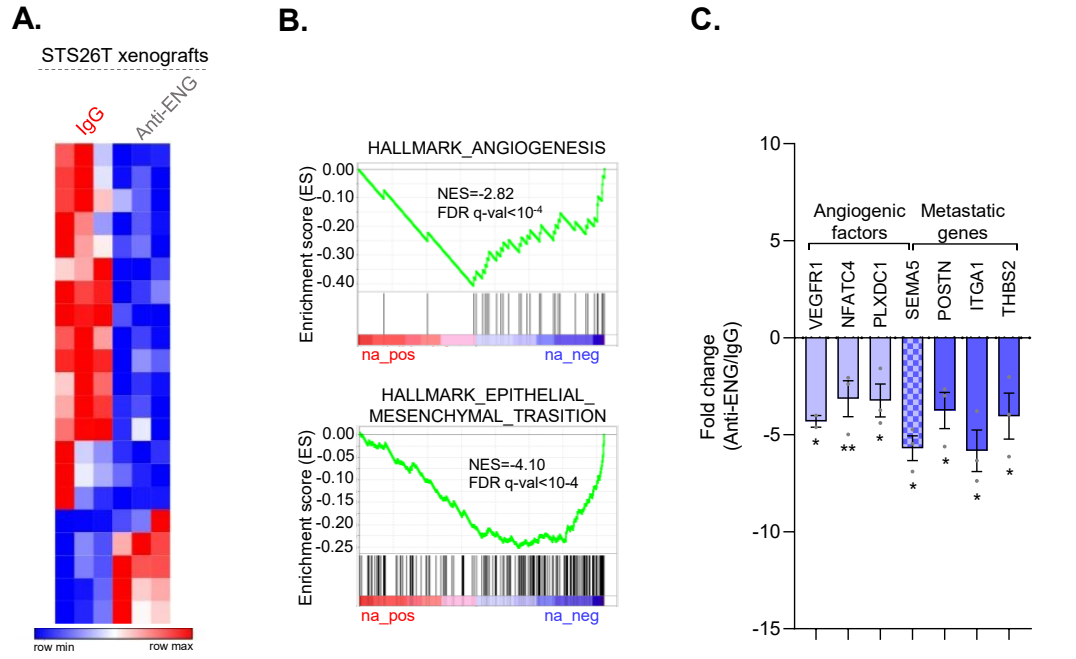

Figure 17. Targeting tumor and stromal ENG reduces angiogenic and metastatic gene expression in MPNST xenografts. A) Heat-map showing the differentially expressed human genes in anti-ENG (TRC105/M1043)-treated STS26T xenografts compared to control IgG-treated tumors. n=3 tumors per group. FDR q-value<0.05. **B)** GSEA plots for selected "hallmark" gene sets (anti-ENG versus IgG). **C)** qRT-PCR analysis of the selected downregulated genes obtained from RNA-seq data. Data were normalized to IgG. Mean ± s.e.m. of three biological replicates; * P< 0.05, ** P< 0.01 by unpaired t-test

Based on these data, we next investigated the functional effect of anti-ENG therapy on tumor angiogenesis. We performed immunohistochemical staining for the EC marker CD31 in the MPNST xenografts treated with TRC105/M1043 or IgG isotype control. ENG inhibition resulted in a significant decrease in the number of CD31-positive vessels in both ST88-14 (**Figure 18A-B**) and STS26T (as shown in **figure 24A-B**) xenografts, indicating that pharmacological targeting of ENG reduces MPNST vascularization.

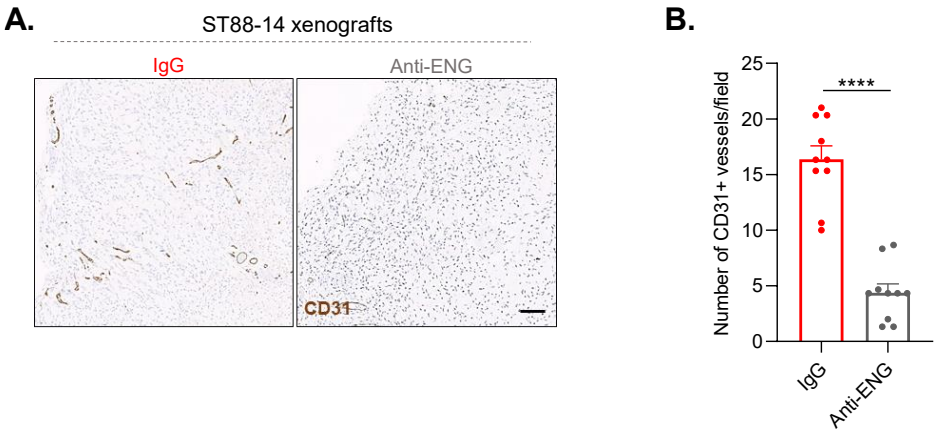

Figure 18. Pharmacological inhibition of ENG impairs MPNST-associated angiogenesis. A) Assessment of tumor vessel density by IHC for CD31 in ST88-14 xenografts treated with the anti-ENG mAbs TRC105 and M1043 or control IgG. Scale bar=100μm. **B)** Quantification of the number of CD31-positive vessels per field. Data correspond to mean ± s.e.m. of 10 independent tumors (with a minimum of 5 fields analyzed per tumor); **** P<0.0001 by unpaired t-test.

Moreover, since our previous results revealed an important role for ENG in promoting tumor cell proliferation in STS26T tumors, we examined the impact of ENG targeting on this biological process. We found that the anti-ENG therapies TRC105 and M1043 significantly reduced tumor cell proliferation in ST88-14 (**Figure 19A-B**) and STS26T (as shown in **figure 23A-B**) xenografts, as denoted by the decrease in the number of Ki67-positive cells.

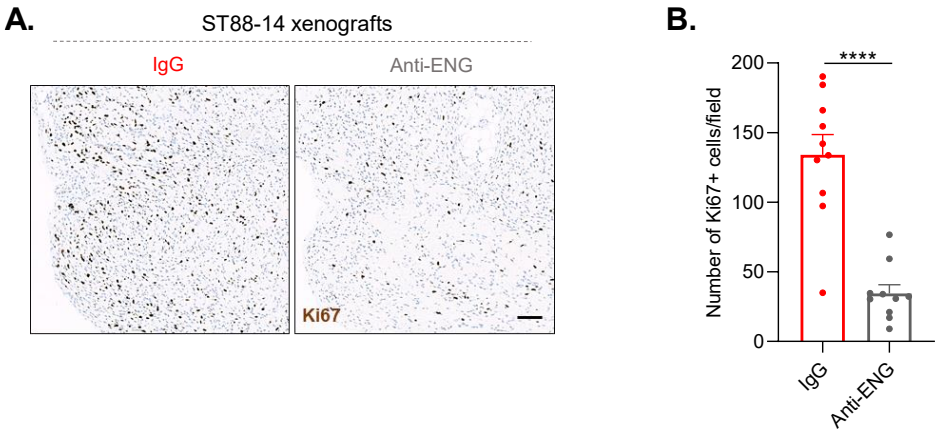

Figure 19. Anti-ENG treatment exerts anti-proliferative effects in ST88-14 tumors. A) Representative images of immunohistochemical Ki67 staining in anti-ENG (TRC105/M1043)- and IgG-treated ST88-14 xenografts. Scale bar=100μm. **B)** Quantification of the number of Ki67-positive cells in tumor sections (5 fields/tumor). Data correspond to mean ± s.e.m. of 10 independent tumors; **** P<0.0001 by unpaired t-test.

In this section, we demonstrate that treatment with TRC105 and M1043, targeting both tumor and stromal ENG, efficiently inhibits MPNST tumor progression by impairing tumor cell proliferation, metastatic ability and angiogenesis in mouse models. Therefore, these findings suggest that anti-ENG therapies could be potentially used as a novel treatment for MPNSTs.

3.2. Exploring the use of anti-ENG therapies in combination with MEKi in MPNSTs

As discussed before, the MAPK/ERK pathway is commonly activated in MPNSTs and it plays a critical role in the development and progression of these tumors [20,117,118]. Indeed, MEKi (e.g. selumetinib) currently represent the most effective targeted therapy for patients with PNs [125,126], and they have demonstrated strong efficacy in preclinical MPNST models, leading to ongoing clinical studies [78]. Hence, we sought to investigate the use of the combination of anti-ENG antibodies with MEKi in MPNSTs.

3.2.1. Combination therapy with anti-ENG and anti-MEK agents inhibits MPNST growth and metastasis

We first examined the efficacy of the combination of anti-ENG and anti–MEK therapies in already established primary MPNSTs. With this objective, STS26T cells were subcutaneously injected into nude mice and tumors were allowed to develop for one week until they were palpable (~100 mm^3 average). Then, mice were treated with the FDA-approved MEKi PD-901 alone, the combination of PD-901 with TRC105/M1043 (combo) or IgG plus vehicle (control) for three weeks, during which tumor volume was monitored. At the end of the experiment, tumors were collected and LN metastases were evaluated (**Figure 20A**). According to previously reported data [121,123], PD-901 treatment resulted in decreased MPNST growth and LN metastatic burden (**Figure 20B-C**). Notably, the combination of PD-901 and TRC105/M1043 synergistically reduced primary tumor growth and almost abolished LN metastases (**Figure 20B-C**). Animal weight loss, which was used as an indirect measurement of general drug toxicity, was not observed during the treatment (**Figure 20D**).

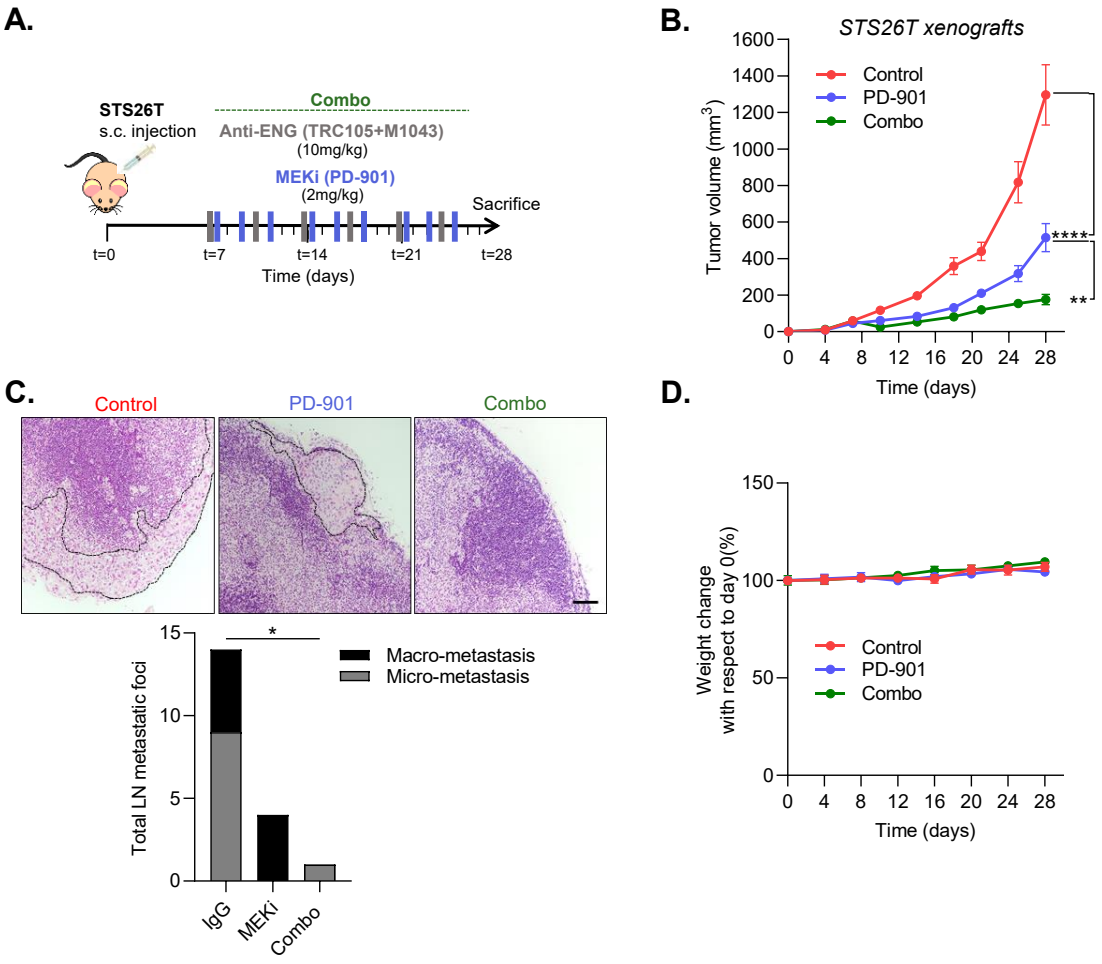

Figure 20. Combination treatment with anti-ENG and anti-MEK therapies strongly inhibits MPNST progression. A) Experiment set up; 1x10^6 STS26T cells were injected subcutaneously (s.c.) into both flanks of athymic nude mice and tumors were allowed to develop for one week (100mm^3 average). Then, mice were randomly distributed into a control group (IgG plus vehicle) and two experimental groups, treated with the MEKi PD-901 (2mg/kg, thrice-weekly) either alone or in combination with the anti-ENG mAbs TRC105 and M1043 (10mg/kg, twice weekly; combo) for three weeks. **B)** STS26T xenograft growth in mice receiving the indicated treatments. n=5 mice per group (10 tumors/condition). Mean ± s.e.m.; ** P<0.01, **** P<0.0001 by two-way ANOVA. **C)** Analysis of LN metastases by H&E staining at day 28 (end-point) (upper panels). Metastases are highlighted by a discontinuous line. Scale bar=100μm. Quantification of the total number of metastatic foci (lower panel). Lesions were divided into micro-metastasis (11-30 cells) and macro-metastasis (greater than 30 cells). n=10 LNs/group; * P<0.05. **D)** Percentage of body weight changes relative to day 0 during the treatment period.

Next, we analyzed the effect of the combination therapy on distant metastasis. To this end, nude mice were injected intravenously with STS26T/GFP-Luc cells, which exhibit metastatic tropism to the lung [282]. One week later, the mice that had developed established metastases were randomly assigned to the control group treated with IgG and vehicle or the therapeutic groups receiving PD-901 either alone or in combination with

TRC105 and M1043 (combo). Metastasis was followed by *In vivo* Imaging System (IVIS) (**Figure 21A**). Although PD-901 alone reduced experimental lung metastasis, only the combination treatment with TRC105/M1043 demonstrated a statistically significant decrease in MPNST metastatic outgrowth and in the lung metastastic burden at end of the experiment when compared to control mice (**Figure 21B-C**).

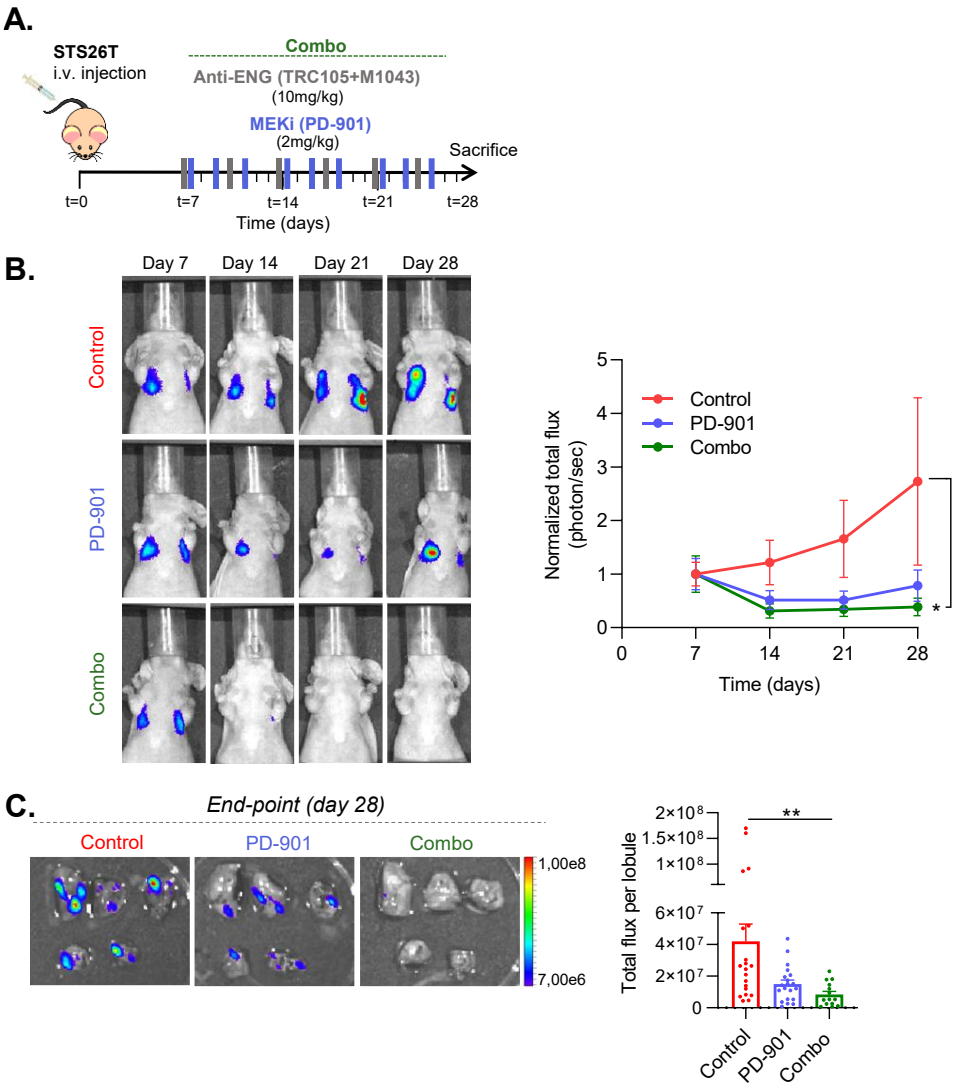

Figure 21. Combined anti-ENG/anti-MEK therapy exhibits enhanced anti-metastatic efficacy in an experimental MPNST lung metastasis model. A) Experiment set up; athymic nude mice were injected intravenously (i.v.) with 1x10^6 STS26T/GFP-Luc cells. Seven days later, mice that had developed established metastases were treated with IgG plus vehicle (control), the MEKi PD-901 alone or the combination of PD-901 with TRC105/M1043 (combo). Metastasis was monitored using IVIS. **B)** Representative images of metastasis follow up (left panels) and quantification (right panel). Data were normalized to the total flux mean from each group at day 7 (start of treatment). **C)** Assessment of lung metastatic burden at day 28 (end-point), with quantification of total photon flux per lung lobe (right panel). n=4 mice per group. Data are mean ± s.e.m.; * P<0.05 by two-way ANOVA in (B) and ** P< 0.01 by one-way ANOVA in (C).

These data therefore show that combined therapy with anti-ENG (TRC105 and M1043) and MEKi (PD-901) is more effective than PD-901 monotherapy in inhibiting both tumor growth and metastasis in a preclinical model of MPNST.

3.2.2. Understanding the mechanisms of action of dual targeting of ENG and MEK

3.2.2.1 Pharmacological inhibition of ENG and MEK cooperatively diminishes Smad1/5 and MAPK/ERK signaling activity in MPNST cells.

In order to explore the molecular mechanisms responsible for the effectiveness of the anti-ENG and anti-MEK combination therapy in MPNSTs, we analyzed its effect on ENG-Smad1/5 and MAPK/ERK pathway activation. STS26T and ST88-14 cells were pre-treated overnight with TRC105 alone, PD-901 alone, the combination of both drugs (combo) or an IgG control. Then, cells were stimulated with BMP-9, the main ENG ligand [270], and VEGF, an important activator of the MAPK/ERK pathway [292,293]. Interestingly, only the TRC105/PD-901 co-treatment significantly reduced ENG expression in both STS26T and ST88-14 cells (**Figure 22A-B**). Accordingly, there was a significant decrease in BMP-9-induced Smad1/5 phosphorylation in combo-treated cells when compared to PD-901-treated or control cells (**Figure 22A-B**). Regarding the MAPK/ERK signaling pathway, although prolonged MEKi treatment (16 hours) increased p-MEK1/2 levels consistent with signaling rebound upon feedback relief [294,295], it led to diminished phosphorylation of ERK, the direct downstream target of MEK (**Figure 22A-B**). In agreement with our previous results from the *ENG* knockdown model, TRC105 alone also produced a significant reduction in p-ERK levels (**Figure 22A-B)**. More importantly, dual targeting of ENG and MEK resulted in synergistic inhibition of ERK phosphorylation in the two MPNST cell lines (**Figure 22A-B**). Overall, these data indicate that ENG targeting cooperates with MEK inhibition to block the activation of the ENG-mediated Smad1/5 and MAPK/ERK signaling pathways in MPNST cells.

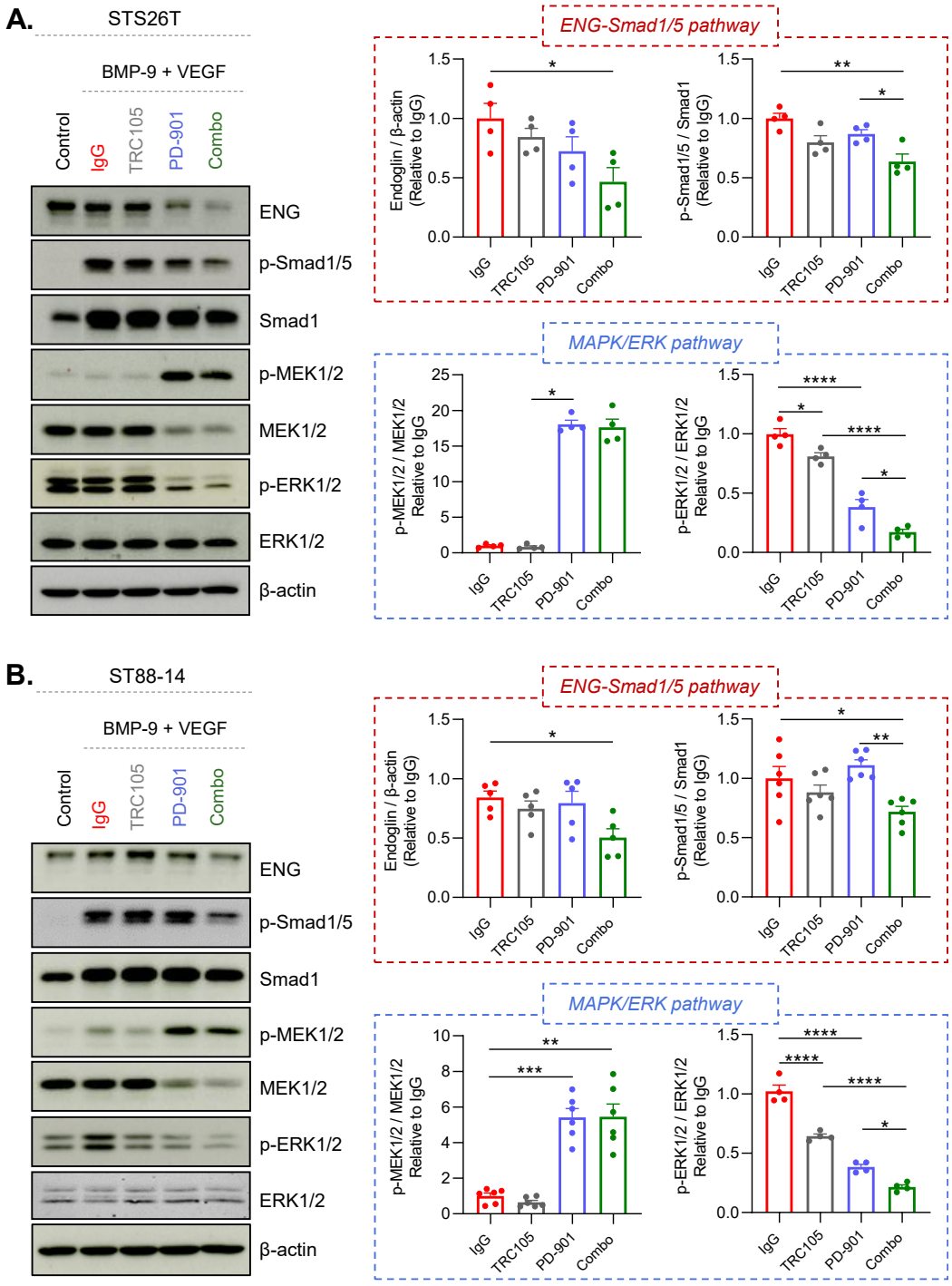

Figure 22. Dual inhibition of ENG and MEK efficiently inhibits Smad1/5 and MAPK/ERK pathway activation in MPNST cells. A-B) Western blot analysis and quantification of ENG expression and Smad1/5, MEK and ERK activation in STS26T (A) and ST88-14 (B) cells pre-treated overnight with the anti-ENG mAb TRC105 alone, the MEKi PD-901 alone, the combination of both drugs (combo) or a IgG control, and then stimulated with BMP-9/VEGF for 1 hour. Cells without neither the pre-treatment nor BMP-9/VEGF stimulation were used as a control. Results were normalized to IgG. Data correspond to mean ± s.e.m. of at least four biological replicates; * P<0.05, ** P<0.01, *** P<0.001, **** P<0.0001 by one-way ANOVA.

3.2.2.2 Combined anti-ENG and anti-MEK therapy suppresses proliferation and angiogenesis in MPNST xenografts.

Smad1/5 and MAPK/ERK signaling pathways have been widely recognized as major contributors to cancer cell proliferation and tumor angiogenesis in several tumor types [222,296-300]. In this respect, our previous data demonstrate an important role for ENG in promoting MPNST cell proliferation and vascularization. Based on these findings, we sought to investigate the effects of the combined blockade of ENG and MEK signaling on these biological processes *in vivo*.

Immunohistochemical analysis of Ki67 showed that both ENG targeting with TRC105 and M1043 and MEK inhibition with PD-901 significantly reduced tumor cell proliferation in STS26T xenografts (**Figure 23A-B**). Importantly, the combination treatment exerted synergistic inhibition on tumor cell proliferation in these tumors (**Figure 23A-B**).

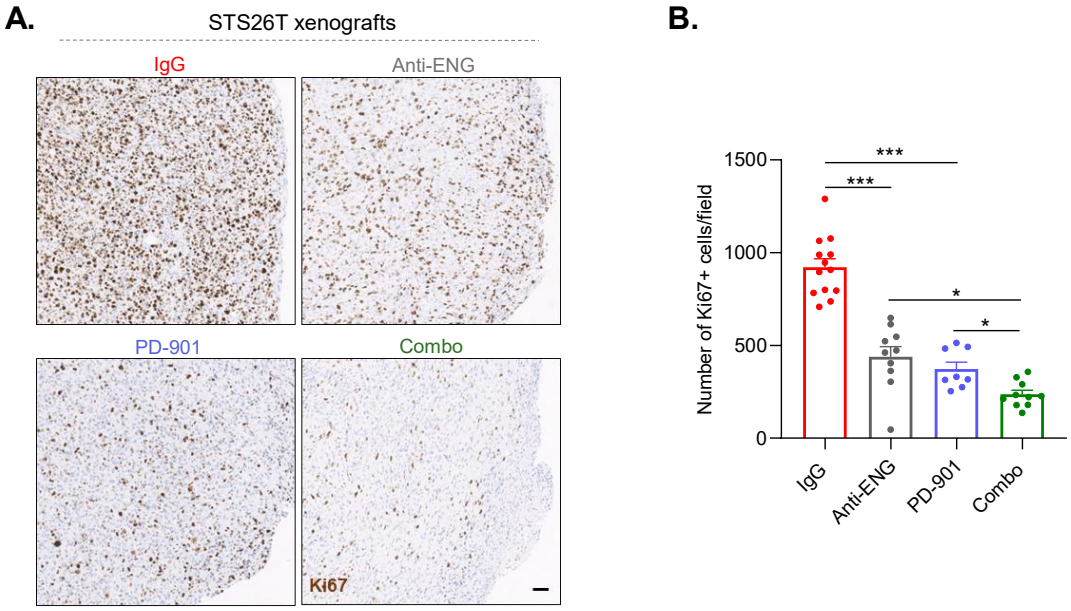

Figure 23. Co-targeting of ENG and MEK synergistically suppresses cancer cell proliferation in MPNST xenografts. A) IHC of Ki67 in STS26T xenografts from mice treated as indicated. Scale bar=100μm. **B)** Quantification of the number of Ki67 positive cells in tumor sections (5 fields/tumor). Dots in the graph represent the mean number of Ki67 positive cells per field of each tumor. Mean ± s.e.m; * P<0.05, *** P<0.001 by one-way ANOVA.

Next, we evaluated tumor vascularization by IHC for CD31. As mentioned before, TRC105/M1043 anti-ENG treatment decreased the number of CD31-positive vessels in STS26T tumors (**Figure 24A-B**). Notably, these anti-angiogenic effects were significantly enhanced upon the combination with PD-901 (**Figure 24A-B**). Together, these results indicate that both MPNST proliferation and angiogenesis are more efficiently inhibited by dual pharmacological targeting of ENG and MEK.

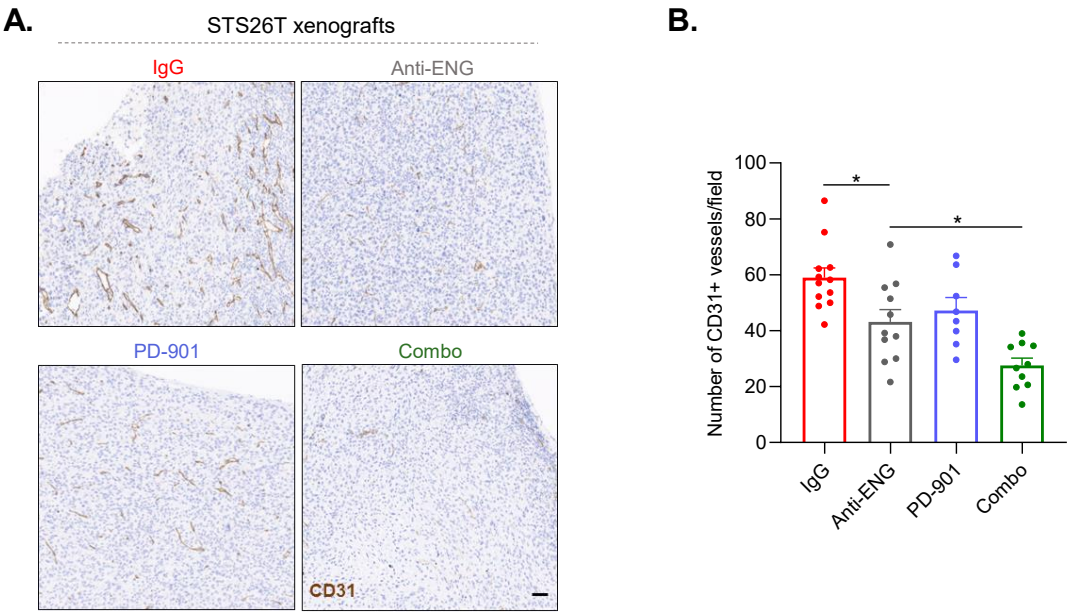

Figure 24. Combined use of anti-ENG and anti-MEK therapies enhances anti-angiogenic effects in MPNST xenografts. A) Representative immunohistochemical staining for CD31 in STS26T tumor sections subjected to the indicated treatments (Scale bar=100μm), with data quantified in **B)**. The number of CD31-positive vessels was counted in 5 fields of each tumor. Dots in the graph represent the mean number of CD31 positive vessels per field. Mean ± s.e.m.; * P<0.05 by one-way ANOVA.

Collectively, the results obtained in this section show that the combination of the ENG-targeting mAbs TRC105 and M1043 with the MEKi PD-901 synergistically decreases MPNST xenograft growth and nearly eliminates metastasis by reducing tumor cell proliferation and angiogenesis. Mechanistically, we demonstrate that this combination acts cooperatively to block the activation of the Smad1/5 and MAPK/ERK signaling pathways in MPNST cells. Overall, our data provide a rationale for combining anti-ENG and anti-MEK agents as a novel therapeutic strategy against MPNSTs.

DISCUSSION

MPNSTs represent a major clinical challenge due to their aggressive behavior, high propensity for recurrence and metastasis and relatively poor response to standard therapies [32,34,62]. In addition, the targeted non-cytotoxic agents that have thus far been tested in clinical trials involving MPNST patients have been mostly unsuccessful [70,78]. Thus, a substantial unmet need remains for new therapeutic strategies in patients with these tumors.

In an attempt to cover this gap, and based on our preliminary data, here we explored the role of ENG in MPNST progression, examining its implication in the pathology, its use as a biomarker and its potential as a therapeutic target for these tumors.

1. ENG, a potential marker of MPNST progression

ENG expression has been mainly detected in the activated endothelium of several human solid tumor specimens, being linked to poor patient outcomes [255]. In fact, numerous studies have reported that the proliferating EC is the primary ENG-expressing cell type in most human epithelial tumors, which harbor only some small subsets of ENG-positive tumor cells [191,238]. However, besides its expression in the endothelium, ENG is also present at very high levels in tumor cells of different human sarcomas, being correlated with malignancy, aggressiveness, high-risk disease or worse survival [242-244,246,247,301]. Consistent with these data, we observed a significant upregulation of ENG on both tumor cells and ECs in human MPNSTs compared to ANNUBPs or benign tumors (e.g. DNs, PNs). A possible explanation for ENG abundance in sarcoma cells, including MPNST cells, may be found in their mesenchymal or neural crest origin, since high ENG expression has been found in both MSCs and neural crest stem cells [195,240,302]. Interestingly, to our knowledge, our study is the first to quantify ENG staining separately in tumor cells and ECs in the same human tumor samples, providing evidence for the use of both tumor and endothelial ENG as a marker of MPNSTs.

Moreover, our results showed that high ENG staining intensity correlated with advanced MPNST stages (local recurrence and distant metastasis), indicating that ENG is upregulated along the course of disease progression. Importantly, we demonstrated for the first time ENG expression in cancer cells of human metastatic tissue specimens, which suggests an intrinsic role for this protein in favoring MPNST metastasis. Some evidence has revealed that the function of tumor cell-specific ENG in metastasis is context-dependent, in some cases promoting metastatic dissemination [303], whereas in other cases it has been associated with metastasis suppression [304,305], as widely

discussed in the section 2. However, to our knowledge, none of these studies analyzed the expression of ENG in human metastases [303-305].

In addition to ENG abundance in tumor cells, we also found a significant upregulation of this protein in the tumor vessels of human MPNST metastatic lesions. In line with our data, some previous studies reported high ENG expression in ECs of human metastases derived from different primary tumors (e.g. melanoma, RCC, CRC, breast, ovarian and lung cancer), which was used as a measure of neovascularization [306,307]. Furthermore, Paauwe and colleagues showed that ENG is expressed on other stromal cell type, namely CAFs, in human metastastic tissues [308]. In particular, they demonstrated that ENG is present in CAFs specifically located at invasive borders of human CRC tumors, as well as in their LN and liver metastases [308]. Notably, this CAF-specific ENG expression significantly correlated with advanced tumor stage and poor metastasis-free survival, suggesting its use as a potential marker of metastastic disease [308].

Unfortunately, solid tumor biopsy presents important limitations for the management of MPNST patients, mainly due to tumor localization and intratumoral heterogeneity, which is especially found in NF1-associated MPNSTs arising from benign PNs [45,309]. Moreover, tissue biopsy is associated with serious complications such as nerve palsy or dissemination of tumor cells [310]. Liquid biopsy that is emerging as a promising, simple, non-invasive method for early cancer detection [311] remains still poorly explored in MPNSTs. Herein, we investigated the potential utility of ENG as a liquid biopsy biomarker for MPNST diagnosis.

To perform these studies, we evaluated the plasma levels of both soluble and EV-shed ENG. Analysis of Sol-ENG showed no differences between patients with PNSTs at different stages (PNs or MPNSTs) or healthy control subjects. However, high plasma Sol-ENG levels have been reported to be correlated with disease progression and metastasis in patients with other cancer types, including CRC, breast cancer and localized prostate cancer [265,312-314]. These inconsistencies could be explained by differences in the mechanisms involved in different tumor types or in the experimental settings, as we quantified the Sol-ENG content in EV-depleted plasma fraction. Nevertheless, the aforementioned studies using whole plasma samples could not verify the origin of circulating ENG since it could be Sol-ENG, EV-secreted ENG or a mix of both forms. Additional discrepancies in this matter were noted by Vidal and colleagues who demonstrated that lower Sol-ENG levels were associated with increased high-grade prostate cancer risk [315]. Furthermore, other authors revealed an anti-angiogenic and anti-tumor role for this circulating form of ENG [262,263]. Therefore, these findings

indicate that the detection of ENG in plasma must be interpreted carefully, since its specific function and diagnostic value can vary depending on the tumor setting and the source of ENG analyzed (soluble or EV-associated).

In contrast to Sol-ENG, in our study, plasma sEV-secreted ENG levels were significantly higher in patients with MPNSTs compared to PN patients or healthy controls. The first experimental evidence of the secretion of ENG in EVs derived from tumor cells was provided in 2011 by Grange and colleagues [267]. Specifically, these authors demonstrated that ENG-expressing EVs released by human renal cancer stem cells were able to trigger angiogenesis and stimulate lung PMN formation and metastasis [267]. Since then, there has been only a study regarding the impact of EV-shed ENG in cancer [268]. In particular, this recent publication has revealed that plasma concentration of ENG-positive EVs was elevated in breast cancer patients and significantly distinguished individuals with this disease from healthy subjects [268]. Based on our data, we propose that an analysis of EV-secreted ENG by liquid biopsy could be useful to detect malignant transformation of PNSTs.

However, it worth pointing out that one of the most important challenges we faced in these human studies was the fact that MPNST is a rare disease and, as a result, the collection of patient samples, especially blood samples, was difficult and limited. Thus, larger paired blood specimens from PN and MPNST patients should be analyzed to validate the capacity of plasma EV-secreted ENG to predict transformation from PNs to MPNSTs. The combined use of this novel potential circulating biomarker with the previously reported cfDNA analysis [58] may represent an attractive non-invasive approach for early MPNST detection and real-time monitoring of the disease or the response to specific treatments. These advances will be essential to reduce morbidity and mortality in MPNST patients who are often diagnosed at advanced stages of the disease [41].

2. Role of ENG in MPNSTs: from its intrinsic function to the modulation of the TME

In light of these results, we next sought to determine the intrinsic molecular mechanisms by which ENG could promote MPNST progression. It is known that ENG modulates malignant phenotypes of cancer cells by regulating the canonical TGF-β/BMP-Smad signaling pathway but also Smad-independent pathways such as the MAPK/ERK signaling cascade [239]. Importantly, upregulation of this pathway is prevalent in all MPNSTs, playing a crucial role in their progression [20,118]. Thus, in this PhD thesis, we investigated the possible impact of ENG on the activation of these signaling pathways in MPNST cells.

In agreement with several studies using different tumor models [222,242,316,317], we found that *ENG* downregulation attenuated Smad1/5 pathway activation in both STS26T and ST88-14 MPNST cell lines. In addition, we observed that knockdown of *ENG* led to reduced basal phosphorylation of ERK1/2 in these MPNST cells. This observation is in line with previous results showing that *ENG* depletion in uterine leiomyosarcoma cells caused a significant decrease in p-ERK1/2 levels, which was proposed to explain the low invasive ability of *ENG*-depleted cells [243]. However, Santibanez and colleagues revealed that ENG expression in transformed keratinocytes inhibited the MAPK/ERK pathway, thus impairing H-RAS-mediated oncogenic transformation [318]. Interestingly, these authors also indicated that ENG directly suppressed ERK1/2 phosphorylation in spindle carcinoma cells [318]. Therefore, these findings suggest that the precise function of ENG in regulating MAPK/ERK signaling depends on the tumor cell type (sarcoma versus carcinoma), which seems to be associated with pro-tumoral or anti-tumoral effects, respectively.

Here, we demonstrated that ENG is required for efficient signaling of both Smad1/5 and MAPK/ERK pathways in MPNST cells. However, in order to gain a deeper understanding of the mechanism involved, it should be taken into account the existence of direct interactions between these signaling pathways [319,320]. For example, activated MEK1 was described to induce phosphorylation of Smad1/5 in different cell types, thus enhancing BMP-dependent responses [321,322]. Accordingly, we observed that MEK inhibition with PD-901 led to a reduction in BMP-9-induced Smad1/5 phosphorylation in both STS26T and ST88-14 cells (data not shown), suggesting a crosstalk between these signaling pathways. Thus, the MAPK/ERK cascade could exacerbate its tumor-promoter action in MPNSTs via activation of the Smad1/5 pathway. In fact, it was previously

reported that pharmacological targeting of the BMP-Smad1/5 signaling cascade cooperated with MEK inhibition to suppress malignant phenotypes of different MPNST cell lines [323]. Our data go beyond these previous findings proposing a role for ENG in favoring the communication between Smad1/5 and MAPK/ERK pathways, which may represent an important mechanism by which this TGF-β coreceptor promotes malignancy of MPNST cells.

Indeed, our *in vivo* experiments revealed that tumor cell-specific ENG is actively involved in promoting MPNST progression. Particularly, we found that *ENG* knockdown resulted in reduced tumor cell proliferation and impaired tumor growth and LN metastasis. In line with our observations, previous studies indicated that genetic silencing of *ENG* expression decreased the metastatic features of different sarcomas cell lines [241-244], and inhibited *in vivo* proliferation and tumorigenesis of Ewing sarcoma cells [242]. Likewise, it was reported that *ENG* depletion led to less aggressive tumor cell behavior and impaired *in vivo* tumorigenicity in melanoma and pancreatic, renal and ovarian cancer [242,324-329]. Interestingly, *ENG* inhibition by shRNA in tumor cells was also described to abrogate metastatic dissemination in mouse models of high-grade serous ovarian cancer [303]. Nevertheless, some publications have shown a tumor suppressor function for ENG in other epithelial tumor cells. Specifically, tumor-cell expression of ENG was associated with tumor growth inhibition in esophageal carcinoma xenograft models [330] and with metastasis suppression in prostate and breast cancer mouse models [304,305]. Similarly, Pérez-Gómez and colleagues demonstrated that loss of ENG expression in squamous carcinoma cells delayed tumor latencies but accelerated the conversion to spindle cell carcinoma via activation of the TGF-β-Smad2/3 signaling pathway [331]. Thus, these authors revealed that ENG acts as a suppressor of malignancy during the late stages of skin carcinogenesis, manifesting the complexity of TGF-β superfamily signaling in cancer [331]. Together, these results suggest that the specific effects of ENG on tumorigenesis and cancer progression vary depending on the type/origin of tumor cells (mesenchymal versus epithelial), which could be associated with differences in ENG expression levels and in the modulation of Smad and non-Smad signaling pathways. In fact, as far as we know, all evidence to date points to a pro-tumoral action of ENG in sarcoma cells [241-247], which is further supported by our data indicating a novel tumor-promoter function of this TGF-β coreceptor in MPNSTs. However, the role of ENG in epithelial cancer cells appears to be context-dependent and, indeed, is a subject of ongoing debate. Therefore, further mechanistic studies are needed to draw firm conclusions on the impact of ENG in carcinomas.

Interestingly, we also observed that downregulation of *ENG* in MPNST cells resulted in a decrease in vessel density in the tumor-adjacent stroma, which could be linked to the reduced expression of pro-angiogenic soluble factors (e.g. VEGF, PDGF, FGF). In this respect, previous work has described that ENG targeting impairs vascularization in different cancer mouse models [258,259,261,263,269,332]. However, these anti-angiogenic effects have been associated with the inhibition of endothelial ENG or the use of an ENG ligand trap, namely the ENG extracellular domain fused to an immunoglobulin Fc domain (ENG-Fc), mimicking Sol-ENG [258,259,261,263,269,332]. Thus, our data represent the first experimental evidence that membrane bound ENG expression in tumor cells can indirectly stimulate angiogenesis within the TME and, therefore, it could be a novel target for ENG-based anti-angiogenic therapy.

Collectively, these data support a dual role for tumor cell-specific ENG in MPNSTs i) affecting tumor cells and promoting their proliferation and metastasis, probably through the activation of the connected Smad1/5 and MAPK/ERK pathways, and ii) favoring the creation of a pro-angiogenic TME via induction of soluble angiogenic factors (**Figure 25**).

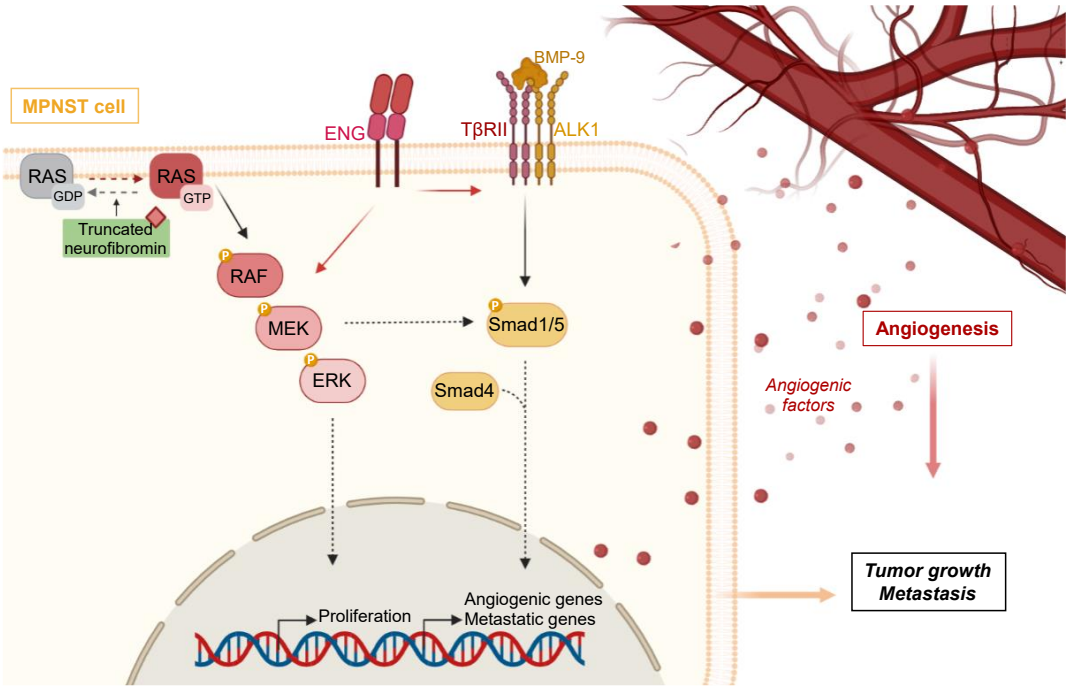

Figure 25. Proposed model of action of ENG in MPNSTs. ENG expression in MPNST cells plays an important role in MPNST growth and metastasis affecting both tumor cells and the TME. i) In MPNST cells, ENG promotes the activation of the canonical BMP-Smad1/5 signaling cascade and the MAPK/ERK signaling pathway, which is commonly upregulated in MPNST cells due to the lack of functional neurofibromin. Activated MEK, in turn, can enhance Smad1/5 phosphorylation, thus exacerbating its tumor-promoter functions. The hyperactivation of these pathways can lead to increased tumor cell proliferation and metastasis- and angiogenesis-related gene expression. ii) In the TME, these soluble pro-angiogenic factors act, in a paracrine manner, in the tumor-associated endothelium by stimulating angiogenesis.

3. Anti-ENG therapies as a novel treatment option in MPNSTs

Based on the above, and taking into consideration that ENG is upregulated in cancer cells but also in ECs in human MPNSTs, we tested a therapeutic strategy to block ENG in both tumor and stromal compartments using the TRC105 and M1043 mAbs, respectively. In fact, this dual inhibition accurately reproduces the effect of anti-ENG therapies in the clinical setting (e.g. TRC105), where it is not possible to discriminate between tumor and stromal ENG.

Notably, our results strongly demonstrate that ENG can be a promising therapeutic target for MPNSTs irrespective of NF1 status, since we found that TRC105 and M1043 inhibited tumor progression in both NF1-associated (ST88-14) and sporadic (STS26T) MPNST xenograft models. This anti-tumor activity of anti-ENG mAbs was associated with reduced *in vivo* proliferation and metastatic ability of MPNST cells and impaired angiogenesis within the TME. These findings are consistent with our results from the *ENG* knockdown model, thus supporting the involvement of ENG in these biological processes in MPNSTs. In this context, it is important to highlight that the combined targeting of tumor and stromal ENG upon co-treatment with TRC105 and M1043 resulted in enhanced anti-angiogenic effects as compared to the specific inhibition of ENG in cancer cells with the use of TRC105 alone (data not shown). Therefore, these observations suggest that endothelial and tumor ENG play a complementary role in promoting MPNST-associated angiogenesis, either directly or indirectly.

In line with our data, several previous studies showed that anti-ENG mAbs efficiently suppress primary tumor growth and block metastatic spread in different mouse tumor models, including subcutaneous, orthotopic and experimental metastasis models [269]. This preclinical efficacy was assigned to the targeting of ENG on cancer cells, tumor vasculature and/or other cell types within the TME such as CAFs and immune cells (e.g. Tregs or tumor-associated macrophages (TAMs)) [269]. In this respect, it should be mentioned that we used athymic nude and NSG mice that lack mature T cells but have innate immune cells such as macrophages [333,334]. In fact, although macrophage-mediated responses are delayed in NSG mice because of mutations in the protein kinase, DNA-activated, catalytic subunit (*Prkdc*) and interleukin 2 receptor subunit gamma (*Il2rg*) genes, they continue to be functional [335,336]. Thus, we cannot rule out the possibility that the therapeutic effects of anti-ENG therapy in our MPNST xenograft models are also due to ENG inhibition in CAFs or immune cells (e.g. TAMs). Additional studies using cell-type specific *ENG* knockout or overexpressing mouse models should be performed in

order to unveil the precise contribution of ENG on these individual cell types in MPNSTs. Of note, the fact that ENG is expressed by tumor cells and several non-tumorigenic cell types within the TME enhances the potential of TRC105 to be used as a promising multi-target directed cancer therapy.

Increasing evidence indicates that, besides blocking BMP-9 binding to ENG, TRC105 acts via immune-dependent mechanisms [269,337]. Indeed, this anti-ENG mAb showed stronger inhibitory effects on tumor growth in immunocompetent bagg albino (BALB/c) mice compared with severe combined immunodeficiency (SCID) mice [338]. Accordingly, TRC105-related anti-tumor action was considerably reduced in xenograft mouse models when $CD4^+$- and, especially, $CD8^+$-T cells were depleted, demonstrating that the T cell compartment, principally the $CD8^+$ T cell compartment, plays an important role in the therapeutic response [339]. Therefore, these findings suggest that the potent preclinical efficacy of TRC105 in MPNSTs can be further improved by the use of mouse models with a fully intact immune system.

In this context, it is worth to note that *ENG* knockdown exerted higher anti-tumor activity than anti-ENG mAbs in our STS26T xenograft models, suggesting that shRNA-mediated silencing of *ENG* in tumor cells could be a more effective therapeutic strategy than pharmacological inhibition of this protein. Nevertheless, these findings must be interpreted carefully, since, as mentioned above, the precise therapeutic effect of TRC105 should be tested in immunocompetent mouse models. Of note, clinical translation of *ENG* gene therapy would present great challenges (e.g. specific delivery in tumor cells, immune response, off-target effects) and, indeed, has not yet been examined, whereas TRC105 has undergone extensive clinical evaluation [237,269].

In fact, in phase I-III trials, TRC105 alone or in combination therapy has shown a favorable safety profile and promising efficacy in patients with different solid tumor types, especially with some advanced STS subtypes [269,275,276]. However, to date, this ENG-targeting antibody has not been investigated in MPNSTs, which lack effective targeted-therapies [70,78]. Here, our preclinical data support a novel use of TRC105 for the treatment of these aggressive tumors.

4. Combining anti-ENG and anti-MEK agents to enhance therapeutic efficacy in MPNSTs

To date, single-agent therapies have failed to demonstrate efficacy in the treatment of MPNST patients, probably due to the tremendous intra- and inter-tumor heterogeneity and the development of drug resistance by diverse mechanisms [70,78]. Hence, we focused our efforts on evaluating the combination of anti-ENG antibodies with therapies currently used in the clinic against PNSTs.

MEK inhibition is emerging as a promising therapeutic approach for the treatment of PNSTs, which commonly harbor hyperactivation of the MAPK/ERK signaling pathway [127,128]. In fact, in a Phase II trial, the MEKi selumetinib demonstrated strong efficacy in children with inoperable PNs, leading to confirmed partial responses (PRs) in 70% of patients, lasting at least 1 year in 56% [125]. Thus, this drug has become the first ever FDA-approved therapy for these patients [125]. In MPNSTs, monotherapy with PD-901, a MEKi currently in clinical cancer trials, hindered tumor growth in several NF1-associated and sporadic MPNST GEMM and xenograft models [78]. Notably, in a case report, recurrent and metastatic MPNST showed complete response to the MEKi trametinib used as a single-agent [340]. However, *in vivo* evidence has indicated robust yet transient anti-tumor effects of MEK inhibition alone in MPNSTs, suggesting that MEKi could achieve more long-lasting responses and prove more useful in combination with other agents [78,121].

Our results revealed that the combination of the anti-ENG mAbs TRC105 and M1043 with PD-901 exerts better therapeutic efficacy than MEKi monotherapy, resulting in sustained inhibition of primary tumor growth and LN metastasis in the STS26T subcutaneous xenograft model. Notably, this combination treatment almost completely abrogated lung metastases in an experimental metastasis model of MPNST. Therefore, these data support the combined use of anti-ENG and anti-MEK therapies as a novel improved strategy to fight MPNSTs.

An important challenge we faced in this PhD thesis was the relative dearth of available MPNST mouse models [290]. In general, the MPNST research field has been hampered by great difficulties in achieving engraftment of human cell lines in immunodeficient mice [184,290]. Indeed, among the wide variety of MPNST cell lines tested *in vivo* in this thesis, STS26T was the only ENG-expressing model that efficiently formed tumors in athymic nude mice. ST88-14 xenografts developed in NSG mice were considerably smaller and they practically disappeared after anti-ENG treatment alone, which supports the use of

ENG-targeting agents in MPNST management. However, precisely for this reason, we could not evaluate the effect of the combination therapy in this model. A major advantage of these xenografts over the existing GEMMs is that they accurately recapitulate the molecular features of human MPNSTs [290], enabling the assessment of the value of biological therapies with human tropism such as TRC105. Nevertheless, as mentioned before, some components of the immune system (e.g. T cells) are missing in these models, since they are generated in immunocompromised mice [333,334]. Based on our data, it would be interesting to test the dual pharmacological inhibition of ENG and MEK in additional models of MPNST. Of note, substantial efforts are being made to generate new MPNST models, including GEMMs, and subcutaneous and orthotopic cell line- and patient-derived xenografts [290,341].

Mechanistically, we found that ENG targeting cooperated with MEK inhibition to effectively block the activation of the ENG-Smad1/5 and MAPK/ERK signaling pathways in MPNST cells. Our data also showed that the combination of anti-ENG mAbs and MEKi synergistically impaired tumor cell proliferation and angiogenesis *in vivo*. These results support the crosstalk between ENG-Smad1/5 and MAPK/ERK pathways in MPNSTs, which appears to be involved in tumor progression through effects on: i) tumor cells (promotion of proliferation), and ii) the TME (stimulation of angiogenesis) (see **figure 25**).

Remarkably, we demonstrated that the combined anti-ENG and anti-MEK therapy inhibited the growth of both primary tumors and established metastases, which suggests that the treatment could be equally effective for localized or metastatic disease. These findings have important translational implications, since intervention timing and disease staging have been reported as possible causes of failure of clinical trials involving MPNST patients [45,175]. Thus, it would be interesting to investigate the use of this novel drug combination in the clinical management of MPNSTs.

At the moment, the combination of anti-ENG and anti-MEK therapies is not being tested in clinical studies. However, several phase I-II trials have demonstrated the feasibility, safety and preliminary efficacy of combining anti-angiogenic agents (e.g. sorafenib or pazopanib) with MEKi in patients with different solid malignancies, including HCC, melanoma, STS, CRC, and head and neck, breast and thyroid cancer [342-347]. More specifically, in a phase Ib/II study involving patients with advanced or metastatic STS, the combination of pazopanib and the MEKi trametinib was well-tolerated and led to encouraging responses with a DCR of 56% [348]. Nevertheless, it is important to take into account this trial has an important limitation since it included STS in general without selecting specific subtypes with hyperactive MAPK/ERK signaling, which are more sensitive to MEK inhibition [348].

Patients with MPNSTs, therefore, could be ideal candidates for future clinical trials testing these types of combinations.

Importantly, TRC105 is emerging as a more promising strategy than the aforementioned classic anti-angiogenic drugs for the treatment of patients with diverse advanced tumors, such as some STS subtypes, and prostate, bladder, liver, renal, breast and ovarian cancer, among others [236,237,269]. Indeed, the clinical effects of TRC105 have been attributed to the inhibition of angiogenesis [349] but also to a significant reduction in the number of Tregs and B regulatory cells (Bregs) [272,273], which was associated with better OS in urothelial carcinoma patients [272]. Some evidence has suggested that, besides targeting the TME, TRC105 can directly act on ENG-expressing cancer cells of human tumors, possibly impairing their proliferation and metastasis [271,272,349,350], which is consistent with our preclinical data. In particular, analysis of plasma biomarkers in cancer patients receiving TRC105 showed a significant decrease in the levels of TGF-β1, which is known to be a strong inducer of tumor cell proliferation and metastasis [349,350]. Of note, TRC105 treatment markedly reduced the number of circulating tumor cells (CTCs) in urothelial carcinoma patients [272] and the size of pre-existing metastases in prostate and uterine cancer patients [271]. These findings therefore reveal that the multi-target effects of TRC105 contribute to its favorable efficacy in cancer patients [269].

Overall, these data, together with the *in vivo* efficacy results obtained in this PhD thesis, provide support for the clinical investigation of the combination of TRC105 with a MEKi (e.g. PD-901) as a novel therapy for MPNSTs.

In **figure 26**, we summarize the main preclinical effects of the combination of anti-ENG mAbs and MEKi in MPNSTs.

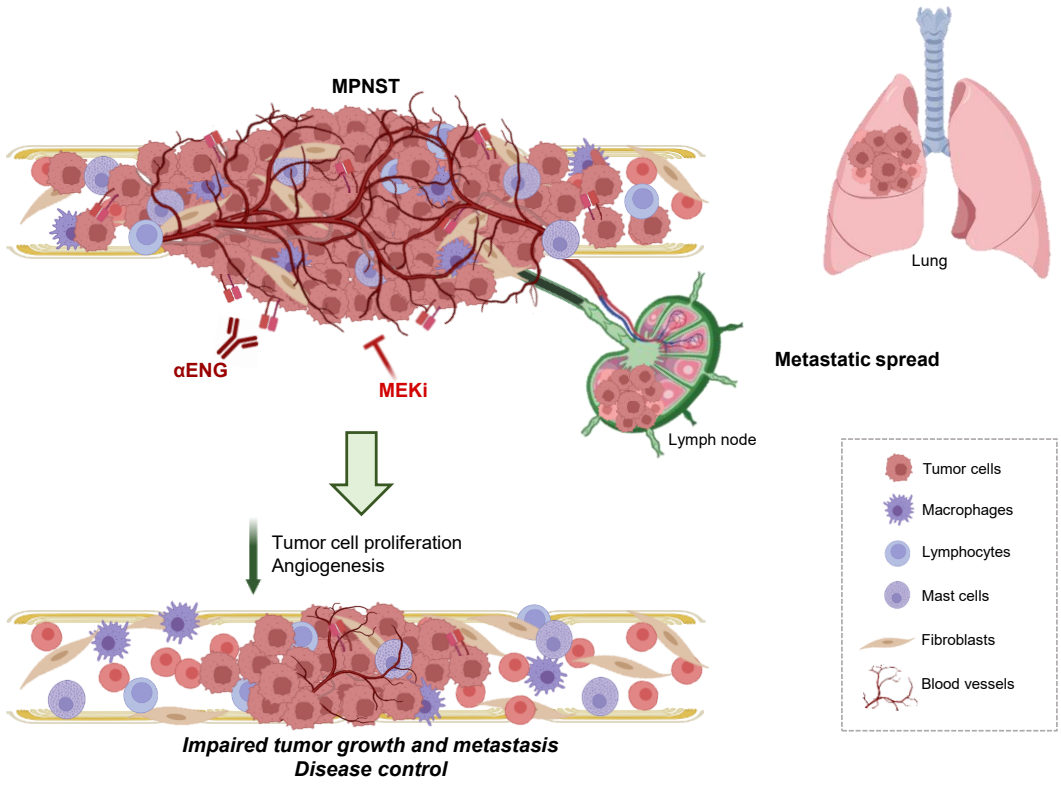

Figure 26. Therapeutic impact of anti-ENG and anti-MEK combination therapy in MPNSTs. Anti-ENG mAbs (TRC105/M1043) cooperate with MEK inhibition to reduce cancer cell proliferation and angiogenesis in MPNSTs, resulting in impaired tumor growth and metastasis and, therefore, disease control.

CONCLUSIONS

1. ENG is upregulated in both tumor cells and ECs in human MPNSTs and, its overexpression correlates with advanced stages of the disease (i.e. local recurrence and distant metastasis).

2. ENG levels are significantly increased in plasma-circulating sEVs from patients with MPNSTs compared with patients bearing benign PNs or healthy controls.

3. ENG regulates the activation of the Smad1/5 and MAPK/ERK signaling pathways and the expression of pro-metastatic and pro-angiogenic genes in the STS26T and ST88-14 human MPNST cell lines.

4. Depletion of *ENG* by RNA interfetence in STS26T cells markedly reduces primary tumor growth and LN metastasis *in vivo*. *ENG*-depleted tumors exhibit diminished expression of the proliferation and angiogenesis markers Ki67 and CD31, respectively.

5. Co-treatment with TRC105 and M1043 anti-ENG antibodies significantly decreases tumor growth in STS26T and ST88-14 xenograft models. The therapy leads to a reduction in pro-angiogenic and pro-metastatic gene expression, tumor cell proliferation and angiogenesis in these tumors.

6. The combination of TRC105/M1043 and the MEKi PD-901 synergistically inhibits tumor growth, and almost abolishes spontaneous and experimental metastasis in STS26T xenograft models.

7. Mechanistically, ENG targeting cooperates with MEK inhibition to block the activation of the ENG-Smad1/5 and MAPK/ERK signaling pathways in STS26T and ST88-14 cells. The combination therapy strongly reduces tumor cell proliferation and angiogenesis in STS26T primary tumors.

CONCLUSIONES

1. La expresión de ENG está aumentada tanto en células tumorales como en células endoteliales en muestras humanas de tumores malignos de la vaina del nervio periférico (MPNSTs, por sus siglas en inglés) y, correlaciona con estadios avanzados de la enfermedad (i.e. recurrencia local y metástasis distal).

2. Los niveles de ENG están significativamente incrementados en vesículas extracelulares pequeñas circulantes en plasma de pacientes con MPNSTs en comparación con pacientes con neurofibromas plexiformes o controles sanos.

3. ENG regula la activación de las rutas de señalización Smad1/5 y MAPK/ERK y la expresión de genes pro-metastásicos y pro-angiogénicos en las líneas celulares de MPNST humano STS26T y ST88-14.

4. El silenciamiento de *ENG* mediante ARN de interferencia en las células STS26T reduce el crecimiento tumoral y la metástasis a nódulo linfático *in vivo*. Los tumores procedentes de células en las que se ha deplecionado *ENG* tienen menor expresión de los marcadores de proliferación y angiogénesis Ki67 y CD31, respectivamente.

5. El tratamiento con las terapias anti-ENG TRC105 y M1043 disminuye de manera significativa el crecimiento tumoral en xenoinjertos derivados de las células STS26T y ST88-14. La terapia reduce la expresión de genes pro-angiogénicos y pro-metastásicos, la proliferación de las células tumorales y la angiogénesis en estos tumores.

6. La combinación de TRC105/M1043 con el inhibidor de MEK PD-901 inhibe de manera sinérgica el crecimiento tumoral y, elimina casi por completo las metástasis espontáneas y experimentales en modelos de xenoinjerto derivados de células STS26T.

7. Desde un punto de vista mecanístico, la inhibición de ENG y de MEK bloquea de forma cooperativa la activación de las vías de señalización Smad1/5 y MAPK/ERK en las células STS26T y ST88-14. La terapia combinada reduce considerablemente la proliferación de las células tumorales y la angiogénesis en tumores primarios procedentes de células STS26T.

REFERENCES

1. Grunewald, T.G.; Alonso, M.; Avnet, S.; Banito, A.; Burdach, S.; Cidre-Aranaz, F.; Di Pompo, G.; Distel, M.; Dorado-Garcia, H.; Garcia-Castro, J., et al. Sarcoma treatment in the era of molecular medicine. *EMBO Mol Med* **2020**, *12*, e11131, doi:10.15252/emmm.201911131.
2. Dufresne, A.; Brahmi, M.; Karanian, M.; Blay, J.Y. Using biology to guide the treatment of sarcomas and aggressive connective-tissue tumours. *Nat Rev Clin Oncol* **2018**, *15*, 443-458, doi:10.1038/s41571-018-0012-4.
3. Damerell, V.; Pepper, M.S.; Prince, S. Molecular mechanisms underpinning sarcomas and implications for current and future therapy. *Signal Transduct Target Ther* **2021**, *6*, 246, doi:10.1038/s41392-021-00647-8.
4. Hoang, N.T.; Acevedo, L.A.; Mann, M.J.; Tolani, B. A review of soft-tissue sarcomas: translation of biological advances into treatment measures. *Cancer Manag Res* **2018**, *10*, 1089-1114, doi:10.2147/CMAR.S159641.
5. Linch, M.; Miah, A.B.; Thway, K.; Judson, I.R.; Benson, C. Systemic treatment of soft-tissue sarcoma-gold standard and novel therapies. *Nat Rev Clin Oncol* **2014**, *11*, 187-202, doi:10.1038/nrclinonc.2014.26.
6. James, A.W.; Shurell, E.; Singh, A.; Dry, S.M.; Eilber, F.C. Malignant Peripheral Nerve Sheath Tumor. *Surg Oncol Clin N Am* **2016**, *25*, 789-802, doi:10.1016/j.soc.2016.05.009.
7. Farid, M.; Demicco, E.G.; Garcia, R.; Ahn, L.; Merola, P.R.; Cioffi, A.; Maki, R.G. Malignant peripheral nerve sheath tumors. *Oncologist* **2014**, *19*, 193-201, doi:10.1634/theoncologist.2013-0328.
8. Jessen, K.R.; Mirsky, R.; Lloyd, A.C. Schwann Cells: Development and Role in Nerve Repair. *Cold Spring Harb Perspect Biol* **2015**, *7*, a020487, doi:10.1101/cshperspect.a020487.
9. Whalley, K. Glia: Schwann cells provide life support for axons. *Nat Rev Neurosci* **2014**, *15*, 698-699, doi:10.1038/nrn3840.
10. Goldstein, B. Anatomy of the peripheral nervous system. *Phys Med Rehabil Clin N Am* **2001**, *12*, 207-236.
11. Catala, M.; Kubis, N. Gross anatomy and development of the peripheral nervous system. *Handb Clin Neurol* **2013**, *115*, 29-41, doi:10.1016/B978-0-444-52902-2.00003-5.
12. Rodriguez, F.J.; Folpe, A.L.; Giannini, C.; Perry, A. Pathology of peripheral nerve sheath tumors: diagnostic overview and update on selected diagnostic problems. *Acta Neuropathol* **2012**, *123*, 295-319, doi:10.1007/s00401-012-0954-z.

13. Stucky, C.C.; Johnson, K.N.; Gray, R.J.; Pockaj, B.A.; Ocal, I.T.; Rose, P.S.; Wasif, N. Malignant peripheral nerve sheath tumors (MPNST): the Mayo Clinic experience. *Ann Surg Oncol* **2012**, *19*, 878-885, doi:10.1245/s10434-011-1978-7.
14. Kragha, K.O. Malignant Peripheral Nerve Sheath Tumor: MRI and CT Findings. *Case Rep Radiol* **2015**, *2015*, 241259, doi:10.1155/2015/241259.
15. Widemann, B.C. Current status of sporadic and neurofibromatosis type 1-associated malignant peripheral nerve sheath tumors. *Curr Oncol Rep* **2009**, *11*, 322-328, doi:10.1007/s11912-009-0045-z.
16. Carli, M.; Ferrari, A.; Mattke, A.; Zanetti, I.; Casanova, M.; Bisogno, G.; Cecchetto, G.; Alaggio, R.; De Sio, L.; Koscielniak, E., et al. Pediatric malignant peripheral nerve sheath tumor: the Italian and German soft tissue sarcoma cooperative group. *J Clin Oncol* **2005**, *23*, 8422-8430, doi:10.1200/JCO.2005.01.4886.
17. Bates, J.E.; Peterson, C.R.; Dhakal, S.; Giampoli, E.J.; Constine, L.S. Malignant peripheral nerve sheath tumors (MPNST): a SEER analysis of incidence across the age spectrum and therapeutic interventions in the pediatric population. *Pediatr Blood Cancer* **2014**, *61*, 1955-1960, doi:10.1002/pbc.25149.
18. Korfhage, J.; Lombard, D.B. Malignant Peripheral Nerve Sheath Tumors: From Epigenome to Bedside. *Mol Cancer Res* **2019**, *17*, 1417-1428, doi:10.1158/1541-7786.MCR-19-0147.
19. Longo, J.F.; Weber, S.M.; Turner-Ivey, B.P.; Carroll, S.L. Recent Advances in the Diagnosis and Pathogenesis of Neurofibromatosis Type 1 (NF1)-associated Peripheral Nervous System Neoplasms. *Adv Anat Pathol* **2018**, *25*, 353-368, doi:10.1097/PAP.0000000000000197.
20. Zou, C.; Smith, K.D.; Liu, J.; Lahat, G.; Myers, S.; Wang, W.L.; Zhang, W.; McCutcheon, I.E.; Slopis, J.M.; Lazar, A.J., et al. Clinical, pathological, and molecular variables predictive of malignant peripheral nerve sheath tumor outcome. *Ann Surg* **2009**, *249*, 1014-1022, doi:10.1097/SLA.0b013e3181a77e9a.
21. Gutmann, D.H.; Ferner, R.E.; Listernick, R.H.; Korf, B.R.; Wolters, P.L.; Johnson, K.J. Neurofibromatosis type 1. *Nat Rev Dis Primers* **2017**, *3*, 17004, doi:10.1038/nrdp.2017.4.
22. Rad, E.; Tee, A.R. Neurofibromatosis type 1: Fundamental insights into cell signalling and cancer. *Semin Cell Dev Biol* **2016**, *52*, 39-46, doi:10.1016/j.semcdb.2016.02.007.
23. Carroll, S.L. Molecular mechanisms promoting the pathogenesis of Schwann cell neoplasms. *Acta Neuropathol* **2012**, *123*, 321-348, doi:10.1007/s00401-011-0928-6.

24. Reilly, K.M.; Kim, A.; Blakely, J.; Ferner, R.E.; Gutmann, D.H.; Legius, E.; Miettinen, M.M.; Randall, R.L.; Ratner, N.; Jumbe, N.L., et al. Neurofibromatosis Type 1-Associated MPNST State of the Science: Outlining a Research Agenda for the Future. *J Natl Cancer Inst* **2017**, *109*, doi:10.1093/jnci/djx124.
25. Staser, K.; Yang, F.C.; Clapp, D.W. Pathogenesis of plexiform neurofibroma: tumor-stromal/hematopoietic interactions in tumor progression. *Annu Rev Pathol* **2012**, *7*, 469-495, doi:10.1146/annurev-pathol-011811-132441.
26. Staedtke, V.; Bai, R.Y.; Blakeley, J.O. Cancer of the Peripheral Nerve in Neurofibromatosis Type 1. *Neurotherapeutics* **2017**, *14*, 298-306, doi:10.1007/s13311-017-0518-y.
27. Miettinen, M.M.; Antonescu, C.R.; Fletcher, C.D.M.; Kim, A.; Lazar, A.J.; Quezado, M.M.; Reilly, K.M.; Stemmer-Rachamimov, A.; Stewart, D.R.; Viskochil, D., et al. Histopathologic evaluation of atypical neurofibromatous tumors and their transformation into malignant peripheral nerve sheath tumor in patients with neurofibromatosis 1-a consensus overview. *Hum Pathol* **2017**, *67*, 1-10, doi:10.1016/j.humpath.2017.05.010.
28. Beert, E.; Brems, H.; Daniels, B.; De Wever, I.; Van Calenbergh, F.; Schoenaers, J.; Debiec-Rychter, M.; Gevaert, O.; De Raedt, T.; Van Den Bruel, A., et al. Atypical neurofibromas in neurofibromatosis type 1 are premalignant tumors. *Genes Chromosomes Cancer* **2011**, *50*, 1021-1032, doi:10.1002/gcc.20921.
29. Evans, D.G.; Baser, M.E.; McGaughran, J.; Sharif, S.; Howard, E.; Moran, A. Malignant peripheral nerve sheath tumours in neurofibromatosis 1. *J Med Genet* **2002**, *39*, 311-314, doi:10.1136/jmg.39.5.311.
30. Meyer, A. Review and update in the diagnosis of peripheral nerve sheath tumors. *Curr Opin Neurol* **2020**, *33*, 575-586, doi:10.1097/WCO.0000000000000857.
31. Stemmer-Rachamimov, A.O.; Louis, D.N.; Nielsen, G.P.; Antonescu, C.R.; Borowsky, A.D.; Bronson, R.T.; Burns, D.K.; Cervera, P.; McLaughlin, M.E.; Reifenberger, G., et al. Comparative pathology of nerve sheath tumors in mouse models and humans. *Cancer Res* **2004**, *64*, 3718-3724, doi:10.1158/0008-5472.CAN-03-4079.
32. Durbin, A.D.; Ki, D.H.; He, S.; Look, A.T. Malignant Peripheral Nerve Sheath Tumors. *Adv Exp Med Biol* **2016**, *916*, 495-530, doi:10.1007/978-3-319-30654-4_22.
33. Valentin, T.; Le Cesne, A.; Ray-Coquard, I.; Italiano, A.; Decanter, G.; Bompas, E.; Isambert, N.; Thariat, J.; Linassier, C.; Bertucci, F., et al. Management and prognosis of malignant peripheral nerve sheath tumors: The experience of the

French Sarcoma Group (GSF-GETO). *Eur J Cancer* **2016**, *56*, 77-84, doi:10.1016/j.ejca.2015.12.015.

34. Watson, K.L.; Al Sannaa, G.A.; Kivlin, C.M.; Ingram, D.R.; Landers, S.M.; Roland, C.L.; Cormier, J.N.; Hunt, K.K.; Feig, B.W.; Ashleigh Guadagnolo, B., et al. Patterns of recurrence and survival in sporadic, neurofibromatosis Type 1-associated, and radiation-associated malignant peripheral nerve sheath tumors. *J Neurosurg* **2017**, *126*, 319-329, doi:10.3171/2015.12.JNS152443.
35. Kolberg, M.; Holand, M.; Agesen, T.H.; Brekke, H.R.; Liestol, K.; Hall, K.S.; Mertens, F.; Picci, P.; Smeland, S.; Lothe, R.A. Survival meta-analyses for >1800 malignant peripheral nerve sheath tumor patients with and without neurofibromatosis type 1. *Neuro Oncol* **2013**, *15*, 135-147, doi:10.1093/neuonc/nos287.
36. LaFemina, J.; Qin, L.X.; Moraco, N.H.; Antonescu, C.R.; Fields, R.C.; Crago, A.M.; Brennan, M.F.; Singer, S. Oncologic outcomes of sporadic, neurofibromatosis-associated, and radiation-induced malignant peripheral nerve sheath tumors. *Ann Surg Oncol* **2013**, *20*, 66-72, doi:10.1245/s10434-012-2573-2.
37. Yan, P.; Huang, R.; Hu, P.; Liu, F.; Zhu, X.; Hu, P.; Yin, H.; Zhang, J.; Meng, T.; Huang, Z. Nomograms for predicting the overall and cause-specific survival in patients with malignant peripheral nerve sheath tumor: a population-based study. *J Neurooncol* **2019**, *143*, 495-503, doi:10.1007/s11060-019-03181-4.
38. Cai, Z.; Tang, X.; Liang, H.; Yang, R.; Yan, T.; Guo, W. Prognosis and risk factors for malignant peripheral nerve sheath tumor: a systematic review and meta-analysis. *World J Surg Oncol* **2020**, *18*, 257, doi:10.1186/s12957-020-02036-x.
39. Fan, Q.; Yang, J.; Wang, G. Clinical and molecular prognostic predictors of malignant peripheral nerve sheath tumor. *Clin Transl Oncol* **2014**, *16*, 191-199, doi:10.1007/s12094-013-1061-x.
40. Ducatman, B.S.; Scheithauer, B.W.; Piepgras, D.G.; Reiman, H.M.; Ilstrup, D.M. Malignant peripheral nerve sheath tumors. A clinicopathologic study of 120 cases. *Cancer* **1986**, *57*, 2006-2021, doi:10.1002/1097-0142(19860515)57:10<2006::aid-cncr2820571022>3.0.co;2-6.
41. Prudner, B.C.; Ball, T.; Rathore, R.; Hirbe, A.C. Diagnosis and management of malignant peripheral nerve sheath tumors: Current practice and future perspectives. *Neurooncol Adv* **2020**, *2*, i40-i49, doi:10.1093/noajnl/vdz047.
42. Belakhoua, S.M.; Rodriguez, F.J. Diagnostic Pathology of Tumors of Peripheral Nerve. *Neurosurgery* **2021**, *88*, 443-456, doi:10.1093/neuros/nyab021.
43. Pekmezci, M.; Reuss, D.E.; Hirbe, A.C.; Dahiya, S.; Gutmann, D.H.; von Deimling, A.; Horvai, A.E.; Perry, A. Morphologic and immunohistochemical features of

malignant peripheral nerve sheath tumors and cellular schwannomas. *Mod Pathol* **2015**, *28*, 187-200, doi:10.1038/modpathol.2014.109.

44. Higham, C.S.; Dombi, E.; Rogiers, A.; Bhaumik, S.; Pans, S.; Connor, S.E.J.; Miettinen, M.; Sciot, R.; Tirabosco, R.; Brems, H., et al. The characteristics of 76 atypical neurofibromas as precursors to neurofibromatosis 1 associated malignant peripheral nerve sheath tumors. *Neuro Oncol* **2018**, *20*, 818-825, doi:10.1093/neuonc/noy013.
45. Kim, A.; Stewart, D.R.; Reilly, K.M.; Viskochil, D.; Miettinen, M.M.; Widemann, B.C. Malignant Peripheral Nerve Sheath Tumors State of the Science: Leveraging Clinical and Biological Insights into Effective Therapies. *Sarcoma* **2017**, *2017*, 7429697, doi:10.1155/2017/7429697.
46. Bernthal, N.M.; Putnam, A.; Jones, K.B.; Viskochil, D.; Randall, R.L. The effect of surgical margins on outcomes for low grade MPNSTs and atypical neurofibroma. *J Surg Oncol* **2014**, *110*, 813-816, doi:10.1002/jso.23736.
47. Zhang, J.; Li, Y.; Zhao, Y.; Qiao, J. CT and MRI of superficial solid tumors. *Quant Imaging Med Surg* **2018**, *8*, 232-251, doi:10.21037/qims.2018.03.03.
48. Warbey, V.S.; Ferner, R.E.; Dunn, J.T.; Calonje, E.; O'Doherty, M.J. [18F]FDG PET/CT in the diagnosis of malignant peripheral nerve sheath tumours in neurofibromatosis type-1. *Eur J Nucl Med Mol Imaging* **2009**, *36*, 751-757, doi:10.1007/s00259-008-1038-0.
49. Ferner, R.E.; Golding, J.F.; Smith, M.; Calonje, E.; Jan, W.; Sanjayanathan, V.; O'Doherty, M. [18F]2-fluoro-2-deoxy-D-glucose positron emission tomography (FDG PET) as a diagnostic tool for neurofibromatosis 1 (NF1) associated malignant peripheral nerve sheath tumours (MPNSTs): a long-term clinical study. *Ann Oncol* **2008**, *19*, 390-394, doi:10.1093/annonc/mdm450.
50. Wilson, M.P.; Katlariwala, P.; Low, G.; Murad, M.H.; McInnes, M.D.F.; Jacques, L.; Jack, A.S. Diagnostic Accuracy of MRI for the Detection of Malignant Peripheral Nerve Sheath Tumors: A Systematic Review and Meta-Analysis. *AJR Am J Roentgenol* **2021**, *217*, 31-39, doi:10.2214/AJR.20.23403.
51. Katal, S.; Gholamrezanezhad, A.; Kessler, M.; Olyaei, M.; Jadvar, H. PET in the Diagnostic Management of Soft Tissue Sarcomas of Musculoskeletal Origin. *PET Clin* **2018**, *13*, 609-621, doi:10.1016/j.cpet.2018.05.011.
52. Guo, A.; Liu, A.; Wei, L.; Song, X. Malignant peripheral nerve sheath tumors: differentiation patterns and immunohistochemical features - a mini-review and our new findings. *J Cancer* **2012**, *3*, 303-309, doi:10.7150/jca.4179.
53. Lee, W.; Teckie, S.; Wiesner, T.; Ran, L.; Prieto Granada, C.N.; Lin, M.; Zhu, S.; Cao, Z.; Liang, Y.; Sboner, A., et al. PRC2 is recurrently inactivated through EED

or SUZ12 loss in malignant peripheral nerve sheath tumors. *Nat Genet* **2014**, *46*, 1227-1232, doi:10.1038/ng.3095.

54. Kirmizis, A.; Bartley, S.M.; Kuzmichev, A.; Margueron, R.; Reinberg, D.; Green, R.; Farnham, P.J. Silencing of human polycomb target genes is associated with methylation of histone H3 Lys 27. *Genes Dev* **2004**, *18*, 1592-1605, doi:10.1101/gad.1200204.
55. Meyer, A.; Billings, S.D. What's new in nerve sheath tumors. *Virchows Arch* **2020**, *476*, 65-80, doi:10.1007/s00428-019-02671-0.
56. Makise, N.; Sekimizu, M.; Konishi, E.; Motoi, T.; Kubo, T.; Ikoma, H.; Watanabe, S.I.; Okuma, T.; Hiraoka, N.; Fukayama, M., et al. H3K27me3 deficiency defines a subset of dedifferentiated chondrosarcomas with characteristic clinicopathological features. *Mod Pathol* **2019**, *32*, 435-445, doi:10.1038/s41379-018-0140-5.
57. Makise, N.; Sekimizu, M.; Kubo, T.; Wakai, S.; Hiraoka, N.; Komiyama, M.; Fukayama, M.; Kawai, A.; Ichikawa, H.; Yoshida, A. Clarifying the Distinction Between Malignant Peripheral Nerve Sheath Tumor and Dedifferentiated Liposarcoma: A Critical Reappraisal of the Diagnostic Utility of MDM2 and H3K27me3 Status. *Am J Surg Pathol* **2018**, *42*, 656-664, doi:10.1097/PAS.0000000000001014.
58. Szymanski, J.J.; Sundby, R.T.; Jones, P.A.; Srihari, D.; Earland, N.; Harris, P.K.; Feng, W.; Qaium, F.; Lei, H.; Roberts, D., et al. Cell-free DNA ultra-low-pass whole genome sequencing to distinguish malignant peripheral nerve sheath tumor (MPNST) from its benign precursor lesion: A cross-sectional study. *PLoS Med* **2021**, *18*, e1003734, doi:10.1371/journal.pmed.1003734.
59. Park, S.J.; Sawitzki, B.; Kluwe, L.; Mautner, V.F.; Holtkamp, N.; Kurtz, A. Serum biomarkers for neurofibromatosis type 1 and early detection of malignant peripheral nerve-sheath tumors. *BMC Med* **2013**, *11*, 109, doi:10.1186/1741-7015-11-109.
60. Hummel, T.R.; Jessen, W.J.; Miller, S.J.; Kluwe, L.; Mautner, V.F.; Wallace, M.R.; Lazaro, C.; Page, G.P.; Worley, P.F.; Aronow, B.J., et al. Gene expression analysis identifies potential biomarkers of neurofibromatosis type 1 including adrenomedullin. *Clin Cancer Res* **2010**, *16*, 5048-5057, doi:10.1158/1078-0432.CCR-10-0613.
61. Scaife, C.L.; Pisters, P.W. Combined-modality treatment of localized soft tissue sarcomas of the extremities. *Surg Oncol Clin N Am* **2003**, *12*, 355-368, doi:10.1016/s1055-3207(03)00003-6.

62. Bradford, D.; Kim, A. Current treatment options for malignant peripheral nerve sheath tumors. *Curr Treat Options Oncol* **2015**, *16*, 328, doi:10.1007/s11864-015-0328-6.
63. Tora, M.S.; Xenos, D.; Texakalidis, P.; Boulis, N.M. Treatment of neurofibromatosis 1-associated malignant peripheral nerve sheath tumors: a systematic review. *Neurosurg Rev* **2020**, *43*, 1039-1046, doi:10.1007/s10143-019-01135-y.
64. Kahn, J.; Gillespie, A.; Tsokos, M.; Ondos, J.; Dombi, E.; Camphausen, K.; Widemann, B.C.; Kaushal, A. Radiation therapy in management of sporadic and neurofibromatosis type 1-associated malignant peripheral nerve sheath tumors. *Front Oncol* **2014**, *4*, 324, doi:10.3389/fonc.2014.00324.
65. Ferner, R.E.; Gutmann, D.H. International consensus statement on malignant peripheral nerve sheath tumors in neurofibromatosis. *Cancer Res* **2002**, *62*, 1573-1577.
66. Yang, J.C.; Chang, A.E.; Baker, A.R.; Sindelar, W.F.; Danforth, D.N.; Topalian, S.L.; DeLaney, T.; Glatstein, E.; Steinberg, S.M.; Merino, M.J., et al. Randomized prospective study of the benefit of adjuvant radiation therapy in the treatment of soft tissue sarcomas of the extremity. *J Clin Oncol* **1998**, *16*, 197-203, doi:10.1200/JCO.1998.16.1.197.
67. Khanna, L.; Prasad, S.R.; Yedururi, S.; Parameswaran, A.M.; Marcal, L.P.; Sandrasegaran, K.; Tirumani, S.H.; Menias, C.O.; Katabathina, V.S. Second Malignancies after Radiation Therapy: Update on Pathogenesis and Cross-sectional Imaging Findings. *Radiographics* **2021**, *41*, 876-894, doi:10.1148/rg.2021200171.
68. Yamanaka, R.; Hayano, A. Radiation-Induced Malignant Peripheral Nerve Sheath Tumors: A Systematic Review. *World Neurosurg* **2017**, *105*, 961-970 e968, doi:10.1016/j.wneu.2017.06.010.
69. Sharif, S.; Ferner, R.; Birch, J.M.; Gillespie, J.E.; Gattamaneni, H.R.; Baser, M.E.; Evans, D.G. Second primary tumors in neurofibromatosis 1 patients treated for optic glioma: substantial risks after radiotherapy. *J Clin Oncol* **2006**, *24*, 2570-2575, doi:10.1200/JCO.2005.03.8349.
70. Hassan, A.; Pestana, R.C.; Parkes, A. Systemic Options for Malignant Peripheral Nerve Sheath Tumors. *Curr Treat Options Oncol* **2021**, *22*, 33, doi:10.1007/s11864-021-00830-7.
71. Wong, W.W.; Hirose, T.; Scheithauer, B.W.; Schild, S.E.; Gunderson, L.L. Malignant peripheral nerve sheath tumor: analysis of treatment outcome. *Int J Radiat Oncol Biol Phys* **1998**, *42*, 351-360, doi:10.1016/s0360-3016(98)00223-5.

72. Gronchi, A.; Ferrari, S.; Quagliuolo, V.; Broto, J.M.; Pousa, A.L.; Grignani, G.; Basso, U.; Blay, J.Y.; Tendero, O.; Beveridge, R.D., et al. Histotype-tailored neoadjuvant chemotherapy versus standard chemotherapy in patients with high-risk soft-tissue sarcomas (ISG-STS 1001): an international, open-label, randomised, controlled, phase 3, multicentre trial. *Lancet Oncol* **2017**, *18*, 812-822, doi:10.1016/S1470-2045(17)30334-0.

73. Kroep, J.R.; Ouali, M.; Gelderblom, H.; Le Cesne, A.; Dekker, T.J.A.; Van Glabbeke, M.; Hogendoorn, P.C.W.; Hohenberger, P. First-line chemotherapy for malignant peripheral nerve sheath tumor (MPNST) versus other histological soft tissue sarcoma subtypes and as a prognostic factor for MPNST: an EORTC soft tissue and bone sarcoma group study. *Ann Oncol* **2011**, *22*, 207-214, doi:10.1093/annonc/mdq338.

74. Shurell-Linehan, E.; DiPardo, B.J.; Elliott, I.A.; Graham, D.S.; Eckardt, M.A.; Dry, S.M.; Nelson, S.D.; Singh, A.S.; Kalbasi, A.; Federman, N., et al. Pathologic Response to Neoadjuvant Therapy is Associated With Improved Long-term Survival in High-risk Primary Localized Malignant Peripheral Nerve Sheath Tumors. *Am J Clin Oncol* **2019**, *42*, 426-431, doi:10.1097/COC.0000000000000536.

75. Higham, C.S.; Steinberg, S.M.; Dombi, E.; Perry, A.; Helman, L.J.; Schuetze, S.M.; Ludwig, J.A.; Staddon, A.; Milhem, M.M.; Rushing, D., et al. SARC006: Phase II Trial of Chemotherapy in Sporadic and Neurofibromatosis Type 1 Associated Chemotherapy-Naive Malignant Peripheral Nerve Sheath Tumors. *Sarcoma* **2017**, *2017*, 8685638, doi:10.1155/2017/8685638.

76. Zehou, O.; Fabre, E.; Zelek, L.; Sbidian, E.; Ortonne, N.; Banu, E.; Wolkenstein, P.; Valeyrie-Allanore, L. Chemotherapy for the treatment of malignant peripheral nerve sheath tumors in neurofibromatosis 1: a 10-year institutional review. *Orphanet J Rare Dis* **2013**, *8*, 127, doi:10.1186/1750-1172-8-127.

77. Anghileri, M.; Miceli, R.; Fiore, M.; Mariani, L.; Ferrari, A.; Mussi, C.; Lozza, L.; Collini, P.; Olmi, P.; Casali, P.G., et al. Malignant peripheral nerve sheath tumors: prognostic factors and survival in a series of patients treated at a single institution. *Cancer* **2006**, *107*, 1065-1074, doi:10.1002/cncr.22098.

78. Martin, E.; Lamba, N.; Flucke, U.E.; Verhoef, C.; Coert, J.H.; Versleijen-Jonkers, Y.M.H.; Desar, I.M.E. Non-cytotoxic systemic treatment in malignant peripheral nerve sheath tumors (MPNST): A systematic review from bench to bedside. *Crit Rev Oncol Hematol* **2019**, *138*, 223-232, doi:10.1016/j.critrevonc.2019.04.007.

79. Albritton, K.H.; Rankin, C.; Coffin, C.M.; Ratner, N.; Budd, G.T.; Schuetze, S.M.; Randall, R.L.; Declue, J.E.; Borden, E.C. Phase II study of erlotinib in metastatic or

unresectable malignant peripheral nerve sheath tumors (MPNST). *Journal of Clinical Oncology* **2006**, *24*, 9518-9518, doi:10.1200/jco.2006.24.18_suppl.9518.

80. Maki, R.G.; D'Adamo, D.R.; Keohan, M.L.; Saulle, M.; Schuetze, S.M.; Undevia, S.D.; Livingston, M.B.; Cooney, M.M.; Hensley, M.L.; Mita, M.M., et al. Phase II study of sorafenib in patients with metastatic or recurrent sarcomas. *J Clin Oncol* **2009**, *27*, 3133-3140, doi:10.1200/JCO.2008.20.4495.
81. Schuetze, S.M.; Wathen, J.K.; Lucas, D.R.; Choy, E.; Samuels, B.L.; Staddon, A.P.; Ganjoo, K.N.; von Mehren, M.; Chow, W.A.; Loeb, D.M., et al. SARC009: Phase 2 study of dasatinib in patients with previously treated, high-grade, advanced sarcoma. *Cancer* **2016**, *122*, 868-874, doi:10.1002/cncr.29858.
82. Dickson, M.A.; Mahoney, M.R.; Tap, W.D.; D'Angelo, S.P.; Keohan, M.L.; Van Tine, B.A.; Agulnik, M.; Horvath, L.E.; Nair, J.S.; Schwartz, G.K. Phase II study of MLN8237 (Alisertib) in advanced/metastatic sarcoma. *Ann Oncol* **2016**, *27*, 1855-1860, doi:10.1093/annonc/mdw281.
83. Chugh, R.; Wathen, J.K.; Maki, R.G.; Benjamin, R.S.; Patel, S.R.; Meyers, P.A.; Priebat, D.A.; Reinke, D.K.; Thomas, D.G.; Keohan, M.L., et al. Phase II multicenter trial of imatinib in 10 histologic subtypes of sarcoma using a bayesian hierarchical statistical model. *J Clin Oncol* **2009**, *27*, 3148-3153, doi:10.1200/JCO.2008.20.5054.
84. Widemann, B.C.; Lu, Y.; Reinke, D.; Okuno, S.H.; Meyer, C.F.; Cote, G.M.; Chugh, R.; Milhem, M.M.; Hirbe, A.C.; Kim, A., et al. Targeting Sporadic and Neurofibromatosis Type 1 (NF1) Related Refractory Malignant Peripheral Nerve Sheath Tumors (MPNST) in a Phase II Study of Everolimus in Combination with Bevacizumab (SARC016). *Sarcoma* **2019**, *2019*, 7656747, doi:10.1155/2019/7656747.
85. Kim, A.; Lu, Y.; Okuno, S.H.; Reinke, D.; Maertens, O.; Perentesis, J.; Basu, M.; Wolters, P.L.; De Raedt, T.; Chawla, S., et al. Targeting Refractory Sarcomas and Malignant Peripheral Nerve Sheath Tumors in a Phase I/II Study of Sirolimus in Combination with Ganetespib (SARC023). *Sarcoma* **2020**, *2020*, 5784876, doi:10.1155/2020/5784876.
86. Nishida, Y.; Urakawa, H.; Nakayama, R.; Kobayashi, E.; Ozaki, T.; Ae, K.; Matsumoto, Y.; Tsuchiya, H.; Goto, T.; Hiraga, H., et al. Phase II clinical trial of pazopanib for patients with unresectable or metastatic malignant peripheral nerve sheath tumors. *Int J Cancer* **2021**, *148*, 140-149, doi:10.1002/ijc.33201.
87. Carroll, S.L. The Challenge of Cancer Genomics in Rare Nervous System Neoplasms: Malignant Peripheral Nerve Sheath Tumors as a Paradigm for Cross-

Species Comparative Oncogenomics. *Am J Pathol* **2016**, *186*, 464-477, doi:10.1016/j.ajpath.2015.10.023.

88. Bridge, R.S., Jr.; Bridge, J.A.; Neff, J.R.; Naumann, S.; Althof, P.; Bruch, L.A. Recurrent chromosomal imbalances and structurally abnormal breakpoints within complex karyotypes of malignant peripheral nerve sheath tumour and malignant triton tumour: a cytogenetic and molecular cytogenetic study. *J Clin Pathol* **2004**, *57*, 1172-1178, doi:10.1136/jcp.2004.019026.
89. Schmidt, H.; Taubert, H.; Meye, A.; Wurl, P.; Bache, M.; Bartel, F.; Holzhausen, H.J.; Hinze, R. Gains in chromosomes 7, 8q, 15q and 17q are characteristic changes in malignant but not in benign peripheral nerve sheath tumors from patients with Recklinghausen's disease. *Cancer Lett* **2000**, *155*, 181-190, doi:10.1016/s0304-3835(00)00426-2.
90. Mechtersheimer, G.; Otano-Joos, M.; Ohl, S.; Benner, A.; Lehnert, T.; Willeke, F.; Moller, P.; Otto, H.F.; Lichter, P.; Joos, S. Analysis of chromosomal imbalances in sporadic and NF1-associated peripheral nerve sheath tumors by comparative genomic hybridization. *Genes Chromosomes Cancer* **1999**, *25*, 362-369.
91. Pemov, A.; Li, H.; Presley, W.; Wallace, M.R.; Miller, D.T. Genetics of human malignant peripheral nerve sheath tumors. *Neurooncol Adv* **2020**, *2*, i50-i61, doi:10.1093/noajnl/vdz049.
92. Lemberg, K.M.; Wang, J.; Pratilas, C.A. From Genes to -Omics: The Evolving Molecular Landscape of Malignant Peripheral Nerve Sheath Tumor. *Genes (Basel)* **2020**, *11*, doi:10.3390/genes11060691.
93. Brohl, A.S.; Kahen, E.; Yoder, S.J.; Teer, J.K.; Reed, D.R. The genomic landscape of malignant peripheral nerve sheath tumors: diverse drivers of Ras pathway activation. *Sci Rep* **2017**, *7*, 14992, doi:10.1038/s41598-017-15183-1.
94. Bottillo, I.; Ahlquist, T.; Brekke, H.; Danielsen, S.A.; van den Berg, E.; Mertens, F.; Lothe, R.A.; Dallapiccola, B. Germline and somatic NF1 mutations in sporadic and NF1-associated malignant peripheral nerve sheath tumours. *J Pathol* **2009**, *217*, 693-701, doi:10.1002/path.2494.
95. Watson, M.A.; Perry, A.; Tihan, T.; Prayson, R.A.; Guha, A.; Bridge, J.; Ferner, R.; Gutmann, D.H. Gene expression profiling reveals unique molecular subtypes of Neurofibromatosis Type I-associated and sporadic malignant peripheral nerve sheath tumors. *Brain Pathol* **2004**, *14*, 297-303, doi:10.1111/j.1750-3639.2004.tb00067.x.
96. Zhang, M.; Wang, Y.; Jones, S.; Sausen, M.; McMahon, K.; Sharma, R.; Wang, Q.; Belzberg, A.J.; Chaichana, K.; Gallia, G.L., et al. Somatic mutations of SUZ12 in

malignant peripheral nerve sheath tumors. *Nat Genet* **2014**, *46*, 1170-1172, doi:10.1038/ng.3116.

97. Binobaid, L.; Masternak, M.M. Molecular targets for NF1-associated malignant peripheral nerve sheath tumor. *Rep Pract Oncol Radiother* **2020**, *25*, 556-561, doi:10.1016/j.rpor.2020.04.010.
98. Upadhyaya, M.; Kluwe, L.; Spurlock, G.; Monem, B.; Majounie, E.; Mantripragada, K.; Ruggieri, M.; Chuzhanova, N.; Evans, D.G.; Ferner, R., et al. Germline and somatic NF1 gene mutation spectrum in NF1-associated malignant peripheral nerve sheath tumors (MPNSTs). *Hum Mutat* **2008**, *29*, 74-82, doi:10.1002/humu.20601.
99. Jett, K.; Friedman, J.M. Clinical and genetic aspects of neurofibromatosis 1. *Genet Med* **2010**, *12*, 1-11, doi:10.1097/GIM.0b013e3181bf15e3.
100. Yap, Y.S.; McPherson, J.R.; Ong, C.K.; Rozen, S.G.; Teh, B.T.; Lee, A.S.; Callen, D.F. The NF1 gene revisited - from bench to bedside. *Oncotarget* **2014**, *5*, 5873-5892, doi:10.18632/oncotarget.2194.
101. Bergoug, M.; Doudeau, M.; Godin, F.; Mosrin, C.; Vallee, B.; Benedetti, H. Neurofibromin Structure, Functions and Regulation. *Cells* **2020**, *9*, doi:10.3390/cells9112365.
102. Cichowski, K.; Jacks, T. NF1 tumor suppressor gene function: narrowing the GAP. *Cell* **2001**, *104*, 593-604, doi:10.1016/s0092-8674(01)00245-8.
103. Simanshu, D.K.; Nissley, D.V.; McCormick, F. RAS Proteins and Their Regulators in Human Disease. *Cell* **2017**, *170*, 17-33, doi:10.1016/j.cell.2017.06.009.
104. Basu, T.N.; Gutmann, D.H.; Fletcher, J.A.; Glover, T.W.; Collins, F.S.; Downward, J. Aberrant regulation of ras proteins in malignant tumour cells from type 1 neurofibromatosis patients. *Nature* **1992**, *356*, 713-715, doi:10.1038/356713a0.
105. Hirbe, A.C.; Dahiya, S.; Miller, C.A.; Li, T.; Fulton, R.S.; Zhang, X.; McDonald, S.; DeSchryver, K.; Duncavage, E.J.; Walrath, J., et al. Whole Exome Sequencing Reveals the Order of Genetic Changes during Malignant Transformation and Metastasis in a Single Patient with NF1-plexiform Neurofibroma. *Clin Cancer Res* **2015**, *21*, 4201-4211, doi:10.1158/1078-0432.CCR-14-3049.
106. Endo, M.; Kobayashi, C.; Setsu, N.; Takahashi, Y.; Kohashi, K.; Yamamoto, H.; Tamiya, S.; Matsuda, S.; Iwamoto, Y.; Tsuneyoshi, M., et al. Prognostic significance of p14ARF, p15INK4b, and p16INK4a inactivation in malignant peripheral nerve sheath tumors. *Clin Cancer Res* **2011**, *17*, 3771-3782, doi:10.1158/1078-0432.CCR-10-2393.
107. Nielsen, G.P.; Stemmer-Rachamimov, A.O.; Ino, Y.; Moller, M.B.; Rosenberg, A.E.; Louis, D.N. Malignant transformation of neurofibromas in neurofibromatosis 1

is associated with CDKN2A/p16 inactivation. *Am J Pathol* **1999**, *155*, 1879-1884, doi:10.1016/S0002-9440(10)65507-1.

108. Kourea, H.P.; Orlow, I.; Scheithauer, B.W.; Cordon-Cardo, C.; Woodruff, J.M. Deletions of the INK4A gene occur in malignant peripheral nerve sheath tumors but not in neurofibromas. *Am J Pathol* **1999**, *155*, 1855-1860, doi:10.1016/S0002-9440(10)65504-6.
109. De Raedt, T.; Beert, E.; Pasmant, E.; Luscan, A.; Brems, H.; Ortonne, N.; Helin, K.; Hornick, J.L.; Mautner, V.; Kehrer-Sawatzki, H., et al. PRC2 loss amplifies Ras-driven transcription and confers sensitivity to BRD4-based therapies. *Nature* **2014**, *514*, 247-251, doi:10.1038/nature13561.
110. Verdijk, R.M.; den Bakker, M.A.; Dubbink, H.J.; Hop, W.C.; Dinjens, W.N.; Kros, J.M. TP53 mutation analysis of malignant peripheral nerve sheath tumors. *J Neuropathol Exp Neurol* **2010**, *69*, 16-26, doi:10.1097/NEN.0b013e3181c55d55.
111. Holtkamp, N.; Atallah, I.; Okuducu, A.F.; Mucha, J.; Hartmann, C.; Mautner, V.F.; Friedrich, R.E.; Mawrin, C.; von Deimling, A. MMP-13 and p53 in the progression of malignant peripheral nerve sheath tumors. *Neoplasia* **2007**, *9*, 671-677, doi:10.1593/neo.07304.
112. Birindelli, S.; Perrone, F.; Oggionni, M.; Lavarino, C.; Pasini, B.; Vergani, B.; Ranzani, G.N.; Pierotti, M.A.; Pilotti, S. Rb and TP53 pathway alterations in sporadic and NF1-related malignant peripheral nerve sheath tumors. *Lab Invest* **2001**, *81*, 833-844, doi:10.1038/labinvest.3780293.
113. Bradtmoller, M.; Hartmann, C.; Zietsch, J.; Jaschke, S.; Mautner, V.F.; Kurtz, A.; Park, S.J.; Baier, M.; Harder, A.; Reuss, D., et al. Impaired Pten expression in human malignant peripheral nerve sheath tumours. *PLoS One* **2012**, *7*, e47595, doi:10.1371/journal.pone.0047595.
114. Gregorian, C.; Nakashima, J.; Dry, S.M.; Nghiemphu, P.L.; Smith, K.B.; Ao, Y.; Dang, J.; Lawson, G.; Mellinghoff, I.K.; Mischel, P.S., et al. PTEN dosage is essential for neurofibroma development and malignant transformation. *Proc Natl Acad Sci U S A* **2009**, *106*, 19479-19484, doi:10.1073/pnas.0910398106.
115. Mawrin, C.; Kirches, E.; Boltze, C.; Dietzmann, K.; Roessner, A.; Schneider-Stock, R. Immunohistochemical and molecular analysis of p53, RB, and PTEN in malignant peripheral nerve sheath tumors. *Virchows Arch* **2002**, *440*, 610-615, doi:10.1007/s00428-001-0550-4.
116. Holtkamp, N.; Malzer, E.; Zietsch, J.; Okuducu, A.F.; Mucha, J.; Mawrin, C.; Mautner, V.F.; Schildhaus, H.U.; von Deimling, A. EGFR and erbB2 in malignant peripheral nerve sheath tumors and implications for targeted therapy. *Neuro Oncol* **2008**, *10*, 946-957, doi:10.1215/15228517-2008-053.

117. Mohamad, T.; Plante, C.; Brosseau, J.P. Toward Understanding the Mechanisms of Malignant Peripheral Nerve Sheath Tumor Development. *Int J Mol Sci* **2021**, *22*, doi:10.3390/ijms22168620.

118. Endo, M.; Yamamoto, H.; Setsu, N.; Kohashi, K.; Takahashi, Y.; Ishii, T.; Iida, K.; Matsumoto, Y.; Hakozaki, M.; Aoki, M., et al. Prognostic significance of AKT/mTOR and MAPK pathways and antitumor effect of mTOR inhibitor in NF1-related and sporadic malignant peripheral nerve sheath tumors. *Clin Cancer Res* **2013**, *19*, 450-461, doi:10.1158/1078-0432.CCR-12-1067.

119. Liu, P.; Wang, Y.; Li, X. Targeting the untargetable KRAS in cancer therapy. *Acta Pharm Sin B* **2019**, *9*, 871-879, doi:10.1016/j.apsb.2019.03.002.

120. Ryan, M.B.; Corcoran, R.B. Therapeutic strategies to target RAS-mutant cancers. *Nat Rev Clin Oncol* **2018**, *15*, 709-720, doi:10.1038/s41571-018-0105-0.

121. Jessen, W.J.; Miller, S.J.; Jousma, E.; Wu, J.; Rizvi, T.A.; Brundage, M.E.; Eaves, D.; Widemann, B.; Kim, M.O.; Dombi, E., et al. MEK inhibition exhibits efficacy in human and mouse neurofibromatosis tumors. *J Clin Invest* **2013**, *123*, 340-347, doi:10.1172/JCI60578.

122. Dodd, R.D.; Mito, J.K.; Eward, W.C.; Chitalia, R.; Sachdeva, M.; Ma, Y.; Barretina, J.; Dodd, L.; Kirsch, D.G. NF1 deletion generates multiple subtypes of soft-tissue sarcoma that respond to MEK inhibition. *Mol Cancer Ther* **2013**, *12*, 1906-1917, doi:10.1158/1535-7163.MCT-13-0189.

123. Kendall, J.J.; Chaney, K.E.; Patel, A.V.; Rizvi, T.A.; Largaespada, D.A.; Ratner, N. CK2 blockade causes MPNST cell apoptosis and promotes degradation of beta-catenin. *Oncotarget* **2016**, *7*, 53191-53203, doi:10.18632/oncotarget.10668.

124. Ramkissoon, A.; Chaney, K.E.; Milewski, D.; Williams, K.B.; Williams, R.L.; Choi, K.; Miller, A.; Kalin, T.V.; Pressey, J.G.; Szabo, S., et al. Targeted Inhibition of the Dual Specificity Phosphatases DUSP1 and DUSP6 Suppress MPNST Growth via JNK. *Clin Cancer Res* **2019**, *25*, 4117-4127, doi:10.1158/1078-0432.CCR-18-3224.

125. Gross, A.M.; Wolters, P.L.; Dombi, E.; Baldwin, A.; Whitcomb, P.; Fisher, M.J.; Weiss, B.; Kim, A.; Bornhorst, M.; Shah, A.C., et al. Selumetinib in Children with Inoperable Plexiform Neurofibromas. *N Engl J Med* **2020**, *382*, 1430-1442, doi:10.1056/NEJMoa1912735.

126. Dombi, E.; Baldwin, A.; Marcus, L.J.; Fisher, M.J.; Weiss, B.; Kim, A.; Whitcomb, P.; Martin, S.; Aschbacher-Smith, L.E.; Rizvi, T.A., et al. Activity of Selumetinib in Neurofibromatosis Type 1-Related Plexiform Neurofibromas. *N Engl J Med* **2016**, *375*, 2550-2560, doi:10.1056/NEJMoa1605943.

127. Selumetinib Shrinks Tumors in Neurofibromatosis. *Cancer Discov* **2020**, *10*, OF10, doi:10.1158/2159-8290.CD-NB2020-025.
128. Killock, D. Selumetinib benefits children with inoperable plexiform neurofibromas. *Nat Rev Clin Oncol* **2020**, *17*, 273, doi:10.1038/s41571-020-0361-7.
129. Kahen, E.J.; Brohl, A.; Yu, D.; Welch, D.; Cubitt, C.L.; Lee, J.K.; Chen, Y.; Yoder, S.J.; Teer, J.K.; Zhang, Y.O., et al. Neurofibromin level directs RAS pathway signaling and mediates sensitivity to targeted agents in malignant peripheral nerve sheath tumors. *Oncotarget* **2018**, *9*, 22571-22585, doi:10.18632/oncotarget.25181.
130. Grit, J.L.; Pridgeon, M.G.; Essenburg, C.J.; Wolfrum, E.; Madaj, Z.B.; Turner, L.; Wulfkuhle, J.; Petricoin, E.F., 3rd; Graveel, C.R.; Steensma, M.R. Kinome Profiling of NF1-Related MPNSTs in Response to Kinase Inhibition and Doxorubicin Reveals Therapeutic Vulnerabilities. *Genes (Basel)* **2020**, *11*, doi:10.3390/genes11030331.
131. Peacock, J.D.; Pridgeon, M.G.; Tovar, E.A.; Essenburg, C.J.; Bowman, M.; Madaj, Z.; Koeman, J.; Boguslawski, E.A.; Grit, J.; Dodd, R.D., et al. Genomic Status of MET Potentiates Sensitivity to MET and MEK Inhibition in NF1-Related Malignant Peripheral Nerve Sheath Tumors. *Cancer Res* **2018**, *78*, 3672-3687, doi:10.1158/0008-5472.CAN-17-3167.
132. Semenova, G.; Stepanova, D.S.; Dubyk, C.; Handorf, E.; Deyev, S.M.; Lazar, A.J.; Chernoff, J. Targeting group I p21-activated kinases to control malignant peripheral nerve sheath tumor growth and metastasis. *Oncogene* **2017**, *36*, 5421-5431, doi:10.1038/onc.2017.143.
133. Sweeney, E.E.; Burga, R.A.; Li, C.; Zhu, Y.; Fernandes, R. Photothermal therapy improves the efficacy of a MEK inhibitor in neurofibromatosis type 1-associated malignant peripheral nerve sheath tumors. *Sci Rep* **2016**, *6*, 37035, doi:10.1038/srep37035.
134. Lock, R.; Ingraham, R.; Maertens, O.; Miller, A.L.; Weledji, N.; Legius, E.; Konicek, B.M.; Yan, S.C.; Graff, J.R.; Cichowski, K. Cotargeting MNK and MEK kinases induces the regression of NF1-mutant cancers. *J Clin Invest* **2016**, *126*, 2181-2190, doi:10.1172/JCI85183.
135. Malone, C.F.; Fromm, J.A.; Maertens, O.; DeRaedt, T.; Ingraham, R.; Cichowski, K. Defining key signaling nodes and therapeutic biomarkers in NF1-mutant cancers. *Cancer Discov* **2014**, *4*, 1062-1073, doi:10.1158/2159-8290.CD-14-0159.
136. Watson, A.L.; Anderson, L.K.; Greeley, A.D.; Keng, V.W.; Rahrmann, E.P.; Halfond, A.L.; Powell, N.M.; Collins, M.H.; Rizvi, T.; Moertel, C.L., et al. Co-targeting the MAPK and PI3K/AKT/mTOR pathways in two genetically engineered

mouse models of schwann cell tumors reduces tumor grade and multiplicity. *Oncotarget* **2014**, *5*, 1502-1514, doi:10.18632/oncotarget.1609.

137. Quail, D.F.; Joyce, J.A. Microenvironmental regulation of tumor progression and metastasis. *Nat Med* **2013**, *19*, 1423-1437, doi:10.1038/nm.3394.
138. Casey, S.C.; Amedei, A.; Aquilano, K.; Azmi, A.S.; Benencia, F.; Bhakta, D.; Bilsland, A.E.; Boosani, C.S.; Chen, S.; Ciriolo, M.R., et al. Cancer prevention and therapy through the modulation of the tumor microenvironment. *Semin Cancer Biol* **2015**, *35 Suppl*, S199-S223, doi:10.1016/j.semcancer.2015.02.007.
139. Jin, M.Z.; Jin, W.L. The updated landscape of tumor microenvironment and drug repurposing. *Signal Transduct Target Ther* **2020**, *5*, 166, doi:10.1038/s41392-020-00280-x.
140. Hinshaw, D.C.; Shevde, L.A. The Tumor Microenvironment Innately Modulates Cancer Progression. *Cancer Res* **2019**, *79*, 4557-4566, doi:10.1158/0008-5472.CAN-18-3962.
141. Zhang, S.; Yang, X.; Wang, L.; Zhang, C. Interplay between inflammatory tumor microenvironment and cancer stem cells. *Oncol Lett* **2018**, *16*, 679-686, doi:10.3892/ol.2018.8716.
142. Paget, S. The distribution of secondary growths in cancer of the breast. 1889. *Cancer Metastasis Rev* **1989**, *8*, 98-101.
143. Kaplan, R.N.; Riba, R.D.; Zacharoulis, S.; Bramley, A.H.; Vincent, L.; Costa, C.; MacDonald, D.D.; Jin, D.K.; Shido, K.; Kerns, S.A., et al. VEGFR1-positive haematopoietic bone marrow progenitors initiate the pre-metastatic niche. *Nature* **2005**, *438*, 820-827, doi:10.1038/nature04186.
144. Peinado, H.; Zhang, H.; Matei, I.R.; Costa-Silva, B.; Hoshino, A.; Rodrigues, G.; Psaila, B.; Kaplan, R.N.; Bromberg, J.F.; Kang, Y., et al. Pre-metastatic niches: organ-specific homes for metastases. *Nat Rev Cancer* **2017**, *17*, 302-317, doi:10.1038/nrc.2017.6.
145. Chin, A.R.; Wang, S.E. Cancer Tills the Premetastatic Field: Mechanistic Basis and Clinical Implications. *Clin Cancer Res* **2016**, *22*, 3725-3733, doi:10.1158/1078-0432.CCR-16-0028.
146. Psaila, B.; Lyden, D. The metastatic niche: adapting the foreign soil. *Nat Rev Cancer* **2009**, *9*, 285-293, doi:10.1038/nrc2621.
147. Peinado, H.; Lavotshkin, S.; Lyden, D. The secreted factors responsible for pre-metastatic niche formation: old sayings and new thoughts. *Semin Cancer Biol* **2011**, *21*, 139-146, doi:10.1016/j.semcancer.2011.01.002.

148. Becker, A.; Thakur, B.K.; Weiss, J.M.; Kim, H.S.; Peinado, H.; Lyden, D. Extracellular Vesicles in Cancer: Cell-to-Cell Mediators of Metastasis. *Cancer Cell* **2016**, *30*, 836-848, doi:10.1016/j.ccell.2016.10.009.
149. Colombo, M.; Raposo, G.; Thery, C. Biogenesis, secretion, and intercellular interactions of exosomes and other extracellular vesicles. *Annu Rev Cell Dev Biol* **2014**, *30*, 255-289, doi:10.1146/annurev-cellbio-101512-122326.
150. Witwer, K.W.; Thery, C. Extracellular vesicles or exosomes? On primacy, precision, and popularity influencing a choice of nomenclature. *J Extracell Vesicles* **2019**, *8*, 1648167, doi:10.1080/20013078.2019.1648167.
151. Jaiswal, R.; Sedger, L.M. Intercellular Vesicular Transfer by Exosomes, Microparticles and Oncosomes - Implications for Cancer Biology and Treatments. *Front Oncol* **2019**, *9*, 125, doi:10.3389/fonc.2019.00125.
152. Zhang, H.; Freitas, D.; Kim, H.S.; Fabijanic, K.; Li, Z.; Chen, H.; Mark, M.T.; Molina, H.; Martin, A.B.; Bojmar, L., et al. Identification of distinct nanoparticles and subsets of extracellular vesicles by asymmetric flow field-flow fractionation. *Nat Cell Biol* **2018**, *20*, 332-343, doi:10.1038/s41556-018-0040-4.
153. Thery, C.; Zitvogel, L.; Amigorena, S. Exosomes: composition, biogenesis and function. *Nat Rev Immunol* **2002**, *2*, 569-579, doi:10.1038/nri855.
154. Camussi, G.; Deregibus, M.C.; Bruno, S.; Cantaluppi, V.; Biancone, L. Exosomes/microvesicles as a mechanism of cell-to-cell communication. *Kidney Int* **2010**, *78*, 838-848, doi:10.1038/ki.2010.278.
155. Ciardiello, C.; Cavallini, L.; Spinelli, C.; Yang, J.; Reis-Sobreiro, M.; de Candia, P.; Minciacchi, V.R.; Di Vizio, D. Focus on Extracellular Vesicles: New Frontiers of Cell-to-Cell Communication in Cancer. *Int J Mol Sci* **2016**, *17*, 175, doi:10.3390/ijms17020175.
156. Nogues, L.; Benito-Martin, A.; Hergueta-Redondo, M.; Peinado, H. The influence of tumour-derived extracellular vesicles on local and distal metastatic dissemination. *Mol Aspects Med* **2018**, *60*, 15-26, doi:10.1016/j.mam.2017.11.012.
157. Peinado, H.; Aleckovic, M.; Lavotshkin, S.; Matei, I.; Costa-Silva, B.; Moreno-Bueno, G.; Hergueta-Redondo, M.; Williams, C.; Garcia-Santos, G.; Ghajar, C., et al. Melanoma exosomes educate bone marrow progenitor cells toward a pro-metastatic phenotype through MET. *Nat Med* **2012**, *18*, 883-891, doi:10.1038/nm.2753.
158. Hoshino, A.; Costa-Silva, B.; Shen, T.L.; Rodrigues, G.; Hashimoto, A.; Tesic Mark, M.; Molina, H.; Kohsaka, S.; Di Giannatale, A.; Ceder, S., et al. Tumour exosome integrins determine organotropic metastasis. *Nature* **2015**, *527*, 329-335, doi:10.1038/nature15756.

159. Maas, S.L.N.; Breakefield, X.O.; Weaver, A.M. Extracellular Vesicles: Unique Intercellular Delivery Vehicles. *Trends Cell Biol* **2017**, *27*, 172-188, doi:10.1016/j.tcb.2016.11.003.

160. Zhao, Z.; Fan, J.; Hsu, Y.S.; Lyon, C.J.; Ning, B.; Hu, T.Y. Extracellular vesicles as cancer liquid biopsies: from discovery, validation, to clinical application. *Lab Chip* **2019**, *19*, 1114-1140, doi:10.1039/c8lc01123k.

161. Zhou, B.; Xu, K.; Zheng, X.; Chen, T.; Wang, J.; Song, Y.; Shao, Y.; Zheng, S. Application of exosomes as liquid biopsy in clinical diagnosis. *Signal Transduct Target Ther* **2020**, *5*, 144, doi:10.1038/s41392-020-00258-9.

162. Torrano, V.; Royo, F.; Peinado, H.; Loizaga-Iriarte, A.; Unda, M.; Falcon-Perez, J.M.; Carracedo, A. Vesicle-MaNiA: extracellular vesicles in liquid biopsy and cancer. *Curr Opin Pharmacol* **2016**, *29*, 47-53, doi:10.1016/j.coph.2016.06.003.

163. Yu, W.; Hurley, J.; Roberts, D.; Chakrabortty, S.K.; Enderle, D.; Noerholm, M.; Breakefield, X.O.; Skog, J.K. Exosome-based liquid biopsies in cancer: opportunities and challenges. *Ann Oncol* **2021**, *32*, 466-477, doi:10.1016/j.annonc.2021.01.074.

164. Stratton, J.A.; Assinck, P.; Sinha, S.; Kumar, R.; Moulson, A.; Patrick, N.; Raharjo, E.; Chan, J.A.; Midha, R.; Tetzlaff, W., et al. Factors Within the Endoneurial Microenvironment Act to Suppress Tumorigenesis of MPNST. *Front Cell Neurosci* **2018**, *12*, 356, doi:10.3389/fncel.2018.00356.

165. Scherer, A.; Stephens, V.R.; McGivney, G.R.; Gutierrez, W.R.; Laverty, E.A.; Knepper-Adrian, V.; Dodd, R.D. Distinct Tumor Microenvironments Are a Defining Feature of Strain-Specific CRISPR/Cas9-Induced MPNSTs. *Genes (Basel)* **2020**, *11*, doi:10.3390/genes11050583.

166. Thomson, C.S.; Pundavela, J.; Perrino, M.R.; Coover, R.A.; Choi, K.; Chaney, K.E.; Rizvi, T.A.; Largaespada, D.A.; Ratner, N. WNT5A inhibition alters the malignant peripheral nerve sheath tumor microenvironment and enhances tumor growth. *Oncogene* **2021**, *40*, 4229-4241, doi:10.1038/s41388-021-01773-x.

167. Dodd, R.D.; Lee, C.L.; Overton, T.; Huang, W.; Eward, W.C.; Luo, L.; Ma, Y.; Ingram, D.R.; Torres, K.E.; Cardona, D.M., et al. NF1(+/-) Hematopoietic Cells Accelerate Malignant Peripheral Nerve Sheath Tumor Development without Altering Chemotherapy Response. *Cancer Res* **2017**, *77*, 4486-4497, doi:10.1158/0008-5472.CAN-16-2643.

168. Errico, A.; Stocco, A.; Riccardi, V.M.; Gambalunga, A.; Bassetto, F.; Grigatti, M.; Ferlosio, A.; Tadini, G.; Garozzo, D.; Ferraresi, S., et al. Neurofibromin Deficiency and Extracellular Matrix Cooperate to Increase Transforming Potential through

FAK-Dependent Signaling. *Cancers (Basel)* **2021**, *13*, doi:10.3390/cancers13102329.

169. Yang, F.C.; Ingram, D.A.; Chen, S.; Hingtgen, C.M.; Ratner, N.; Monk, K.R.; Clegg, T.; White, H.; Mead, L.; Wenning, M.J., et al. Neurofibromin-deficient Schwann cells secrete a potent migratory stimulus for Nf1+/- mast cells. *J Clin Invest* **2003**, *112*, 1851-1861, doi:10.1172/JCI19195.
170. Fletcher, J.S.; Pundavela, J.; Ratner, N. After Nf1 loss in Schwann cells, inflammation drives neurofibroma formation. *Neurooncol Adv* **2020**, *2*, i23-i32, doi:10.1093/noajnl/vdz045.
171. Choi, K.; Komurov, K.; Fletcher, J.S.; Jousma, E.; Cancelas, J.A.; Wu, J.; Ratner, N. An inflammatory gene signature distinguishes neurofibroma Schwann cells and macrophages from cells in the normal peripheral nervous system. *Sci Rep* **2017**, *7*, 43315, doi:10.1038/srep43315.
172. Prada, C.E.; Jousma, E.; Rizvi, T.A.; Wu, J.; Dunn, R.S.; Mayes, D.A.; Cancelas, J.A.; Dombi, E.; Kim, M.O.; West, B.L., et al. Neurofibroma-associated macrophages play roles in tumor growth and response to pharmacological inhibition. *Acta Neuropathol* **2013**, *125*, 159-168, doi:10.1007/s00401-012-1056-7.
173. Shurell, E.; Singh, A.S.; Crompton, J.G.; Jensen, S.; Li, Y.; Dry, S.; Nelson, S.; Chmielowski, B.; Bernthal, N.; Federman, N., et al. Characterizing the immune microenvironment of malignant peripheral nerve sheath tumor by PD-L1 expression and presence of CD8+ tumor infiltrating lymphocytes. *Oncotarget* **2016**, *7*, 64300-64308, doi:10.18632/oncotarget.11734.
174. Katz, D.; Lazar, A.; Lev, D. Malignant peripheral nerve sheath tumour (MPNST): the clinical implications of cellular signalling pathways. *Expert Rev Mol Med* **2009**, *11*, e30, doi:10.1017/S1462399409001227.
175. Marjanska, A.; Galazka, P.; Wysocki, M.; Styczynski, J. New Frontiers in Therapy of Peripheral Nerve Sheath Tumors in Patients With Neurofibromatosis Type 1: Latest Evidence and Clinical Implications. *Anticancer Res* **2020**, *40*, 1817-1831, doi:10.21873/anticanres.14136.
176. Friedrich, R.E.; Beer, C.; Glatzel, M.; Hagel, C. Vascular endothelial growth factor, basic fibroblast growth factor and epithelial growth factor receptor in peripheral nerve sheath tumors of neurofibromatosis type 1. *Anticancer Res* **2015**, *35*, 137-144.
177. Wasa, J.; Nishida, Y.; Suzuki, Y.; Tsukushi, S.; Shido, Y.; Hosono, K.; Shimoyama, Y.; Nakamura, S.; Ishiguro, N. Differential expression of angiogenic factors in peripheral nerve sheath tumors. *Clin Exp Metastasis* **2008**, *25*, 819-825, doi:10.1007/s10585-008-9197-8.

178. Friedrich, R.E.; Naber, U.; Glatzel, M.; Hagel, C. Vessel and Mast Cell Densities in Sporadic and Syndrome-associated Peripheral Nerve Sheath Tumors. *Anticancer Res* **2015**, *35*, 4713-4722.

179. Vasconcelos, R.A.T.; Guimaraes Coscarelli, P.; Vieira, T.M.; Noguera, W.S.; Rapozo, D.C.M.; Acioly, M.A. Prognostic significance of mast cell and microvascular densities in malignant peripheral nerve sheath tumor with and without neurofibromatosis type 1. *Cancer Med* **2019**, *8*, 972-981, doi:10.1002/cam4.1977.

180. Gesundheit, B.; Parkin, P.; Greenberg, M.; Baruchel, S.; Senger, C.; Kapelushnik, J.; Smith, C.; Klement, G.L. The role of angiogenesis in the transformation of plexiform neurofibroma into malignant peripheral nerve sheath tumors in children with neurofibromatosis type 1. *J Pediatr Hematol Oncol* **2010**, *32*, 548-553, doi:10.1097/MPH.0b013e3181e887c7.

181. Perrone, F.; Da Riva, L.; Orsenigo, M.; Losa, M.; Jocolle, G.; Millefanti, C.; Pastore, E.; Gronchi, A.; Pierotti, M.A.; Pilotti, S. PDGFRA, PDGFRB, EGFR, and downstream signaling activation in malignant peripheral nerve sheath tumor. *Neuro Oncol* **2009**, *11*, 725-736, doi:10.1215/15228517-2009-003.

182. Holtkamp, N.; Okuducu, A.F.; Mucha, J.; Afanasieva, A.; Hartmann, C.; Atallah, I.; Estevez-Schwarz, L.; Mawrin, C.; Friedrich, R.E.; Mautner, V.F., et al. Mutation and expression of PDGFRA and KIT in malignant peripheral nerve sheath tumors, and its implications for imatinib sensitivity. *Carcinogenesis* **2006**, *27*, 664-671, doi:10.1093/carcin/bgi273.

183. Torres, K.E.; Zhu, Q.S.; Bill, K.; Lopez, G.; Ghadimi, M.P.; Xie, X.; Young, E.D.; Liu, J.; Nguyen, T.; Bolshakov, S., et al. Activated MET is a molecular prognosticator and potential therapeutic target for malignant peripheral nerve sheath tumors. *Clin Cancer Res* **2011**, *17*, 3943-3955, doi:10.1158/1078-0432.CCR-11-0193.

184. Mahller, Y.Y.; Vaikunth, S.S.; Currier, M.A.; Miller, S.J.; Ripberger, M.C.; Hsu, Y.H.; Mehrian-Shai, R.; Collins, M.H.; Crombleholme, T.M.; Ratner, N., et al. Oncolytic HSV and erlotinib inhibit tumor growth and angiogenesis in a novel malignant peripheral nerve sheath tumor xenograft model. *Mol Ther* **2007**, *15*, 279-286, doi:10.1038/sj.mt.6300038.

185. Liu, T.C.; Zhang, T.; Fukuhara, H.; Kuroda, T.; Todo, T.; Canron, X.; Bikfalvi, A.; Martuza, R.L.; Kurtz, A.; Rabkin, S.D. Dominant-negative fibroblast growth factor receptor expression enhances antitumoral potency of oncolytic herpes simplex virus in neural tumors. *Clin Cancer Res* **2006**, *12*, 6791-6799, doi:10.1158/1078-0432.CCR-06-0263.

186. Longo, J.F.; Brosius, S.N.; Black, L.; Worley, S.H.; Wilson, R.C.; Roth, K.A.; Carroll, S.L. ErbB4 promotes malignant peripheral nerve sheath tumor pathogenesis via Ras-independent mechanisms. *Cell Commun Signal* **2019**, *17*, 74, doi:10.1186/s12964-019-0388-5.
187. Kawachi, Y.; Maruyama, H.; Ishitsuka, Y.; Fujisawa, Y.; Furuta, J.; Nakamura, Y.; Ichikawa, E.; Furumura, M.; Otsuka, F. NF1 gene silencing induces upregulation of vascular endothelial growth factor expression in both Schwann and non-Schwann cells. *Exp Dermatol* **2013**, *22*, 262-265, doi:10.1111/exd.12115.
188. Thomas, S.L.; De Vries, G.H. Angiogenic expression profile of normal and neurofibromin-deficient human Schwann cells. *Neurochem Res* **2007**, *32*, 1129-1141, doi:10.1007/s11064-007-9279-z.
189. Sheela, S.; Riccardi, V.M.; Ratner, N. Angiogenic and invasive properties of neurofibroma Schwann cells. *J Cell Biol* **1990**, *111*, 645-653, doi:10.1083/jcb.111.2.645.
190. Rad, E.; Dodd, K.; Thomas, L.; Upadhyaya, M.; Tee, A. STAT3 and HIF1alpha Signaling Drives Oncogenic Cellular Phenotypes in Malignant Peripheral Nerve Sheath Tumors. *Mol Cancer Res* **2015**, *13*, 1149-1160, doi:10.1158/1541-7786.MCR-14-0182.
191. Paauwe, M.; ten Dijke, P.; Hawinkels, L.J. Endoglin for tumor imaging and targeted cancer therapy. *Expert Opin Ther Targets* **2013**, *17*, 421-435, doi:10.1517/14728222.2013.758716.
192. Cheifetz, S.; Bellon, T.; Cales, C.; Vera, S.; Bernabeu, C.; Massague, J.; Letarte, M. Endoglin is a component of the transforming growth factor-beta receptor system in human endothelial cells. *J Biol Chem* **1992**, *267*, 19027-19030.
193. Wikstrom, P.; Lissbrant, I.F.; Stattin, P.; Egevad, L.; Bergh, A. Endoglin (CD105) is expressed on immature blood vessels and is a marker for survival in prostate cancer. *Prostate* **2002**, *51*, 268-275, doi:10.1002/pros.10083.
194. Barry, F.P.; Boynton, R.E.; Haynesworth, S.; Murphy, J.M.; Zaia, J. The monoclonal antibody SH-2, raised against human mesenchymal stem cells, recognizes an epitope on endoglin (CD105). *Biochem Biophys Res Commun* **1999**, *265*, 134-139, doi:10.1006/bbrc.1999.1620.
195. Mancini, M.L.; Verdi, J.M.; Conley, B.A.; Nicola, T.; Spicer, D.B.; Oxburgh, L.H.; Vary, C.P. Endoglin is required for myogenic differentiation potential of neural crest stem cells. *Dev Biol* **2007**, *308*, 520-533, doi:10.1016/j.ydbio.2007.06.009.
196. St-Jacques, S.; Cymerman, U.; Pece, N.; Letarte, M. Molecular characterization and in situ localization of murine endoglin reveal that it is a transforming growth

factor-beta binding protein of endothelial and stromal cells. *Endocrinology* **1994**, *134*, 2645-2657, doi:10.1210/endo.134.6.8194490.

197. Pierelli, L.; Bonanno, G.; Rutella, S.; Marone, M.; Scambia, G.; Leone, G. CD105 (endoglin) expression on hematopoietic stem/progenitor cells. *Leuk Lymphoma* **2001**, *42*, 1195-1206, doi:10.3109/10428190109097744.
198. Rodriguez-Barbero, A.; Obreo, J.; Eleno, N.; Rodriguez-Pena, A.; Duwel, A.; Jerkic, M.; Sanchez-Rodriguez, A.; Bernabeu, C.; Lopez-Novoa, J.M. Endoglin expression in human and rat mesangial cells and its upregulation by TGF-beta1. *Biochem Biophys Res Commun* **2001**, *282*, 142-147, doi:10.1006/bbrc.2001.4526.
199. Parker, W.L.; Goldring, M.B.; Philip, A. Endoglin is expressed on human chondrocytes and forms a heteromeric complex with betaglycan in a ligand and type II TGFbeta receptor independent manner. *J Bone Miner Res* **2003**, *18*, 289-302, doi:10.1359/jbmr.2003.18.2.289.
200. Quintanilla, M.; Ramirez, J.R.; Perez-Gomez, E.; Romero, D.; Velasco, B.; Letarte, M.; Lopez-Novoa, J.M.; Bernabeu, C. Expression of the TGF-beta coreceptor endoglin in epidermal keratinocytes and its dual role in multistage mouse skin carcinogenesis. *Oncogene* **2003**, *22*, 5976-5985, doi:10.1038/sj.onc.1206841.
201. Ishibashi, O.; Ikegame, M.; Takizawa, F.; Yoshizawa, T.; Moksed, M.A.; Iizawa, F.; Mera, H.; Matsuda, A.; Kawashima, H. Endoglin is involved in BMP-2-induced osteogenic differentiation of periodontal ligament cells through a pathway independent of Smad-1/5/8 phosphorylation. *J Cell Physiol* **2010**, *222*, 465-473, doi:10.1002/jcp.21968.
202. Meurer, S.K.; Tihaa, L.; Lahme, B.; Gressner, A.M.; Weiskirchen, R. Identification of endoglin in rat hepatic stellate cells: new insights into transforming growth factor beta receptor signaling. *J Biol Chem* **2005**, *280*, 3078-3087, doi:10.1074/jbc.M405411200.
203. Meurer, S.K.; Weiskirchen, R. Endoglin: An 'Accessory' Receptor Regulating Blood Cell Development and Inflammation. *Int J Mol Sci* **2020**, *21*, doi:10.3390/ijms21239247.
204. Trentin Brum, S.; Demasi, A.P.; Fantelli Stelini, R.; Cintra, M.L.; Cavalcanti de Araujo, V.; Borges Soares, A. Endoglin is Highly Expressed in Human Mast Cells. *Appl Immunohistochem Mol Morphol* **2019**, *27*, 613-617, doi:10.1097/PAI.0000000000000668.
205. Schmidt-Weber, C.B.; Letarte, M.; Kunzmann, S.; Ruckert, B.; Bernabeu, C.; Blaser, K. TGF-{beta} signaling of human T cells is modulated by the ancillary TGF-{beta} receptor endoglin. *Int Immunol* **2005**, *17*, 921-930, doi:10.1093/intimm/dxh272.

206. Lastres, P.; Bellon, T.; Cabanas, C.; Sanchez-Madrid, F.; Acevedo, A.; Gougos, A.; Letarte, M.; Bernabeu, C. Regulated expression on human macrophages of endoglin, an Arg-Gly-Asp-containing surface antigen. *Eur J Immunol* **1992**, *22*, 393-397, doi:10.1002/eji.1830220216.

207. Gougos, A.; Letarte, M. Identification of a human endothelial cell antigen with monoclonal antibody 44G4 produced against a pre-B leukemic cell line. *J Immunol* **1988**, *141*, 1925-1933.

208. Gougos, A.; Letarte, M. Primary structure of endoglin, an RGD-containing glycoprotein of human endothelial cells. *J Biol Chem* **1990**, *265*, 8361-8364.

209. Bellon, T.; Corbi, A.; Lastres, P.; Cales, C.; Cebrian, M.; Vera, S.; Cheifetz, S.; Massague, J.; Letarte, M.; Bernabeu, C. Identification and expression of two forms of the human transforming growth factor-beta-binding protein endoglin with distinct cytoplasmic regions. *Eur J Immunol* **1993**, *23*, 2340-2345, doi:10.1002/eji.1830230943.

210. Velasco, S.; Alvarez-Munoz, P.; Pericacho, M.; Dijke, P.T.; Bernabeu, C.; Lopez-Novoa, J.M.; Rodriguez-Barbero, A. L- and S-endoglin differentially modulate TGFbeta1 signaling mediated by ALK1 and ALK5 in L6E9 myoblasts. *J Cell Sci* **2008**, *121*, 913-919, doi:10.1242/jcs.023283.

211. Aristorena, M.; Blanco, F.J.; de Las Casas-Engel, M.; Ojeda-Fernandez, L.; Gallardo-Vara, E.; Corbi, A.; Botella, L.M.; Bernabeu, C. Expression of endoglin isoforms in the myeloid lineage and their role during aging and macrophage polarization. *J Cell Sci* **2014**, *127*, 2723-2735, doi:10.1242/jcs.143644.

212. Blanco, F.J.; Grande, M.T.; Langa, C.; Oujo, B.; Velasco, S.; Rodriguez-Barbero, A.; Perez-Gomez, E.; Quintanilla, M.; Lopez-Novoa, J.M.; Bernabeu, C. S-endoglin expression is induced in senescent endothelial cells and contributes to vascular pathology. *Circ Res* **2008**, *103*, 1383-1392, doi:10.1161/CIRCRESAHA.108.176552.

213. Gordon, K.J.; Blobe, G.C. Role of transforming growth factor-beta superfamily signaling pathways in human disease. *Biochim Biophys Acta* **2008**, *1782*, 197-228, doi:10.1016/j.bbadis.2008.01.006.

214. Schmierer, B.; Hill, C.S. TGFbeta-SMAD signal transduction: molecular specificity and functional flexibility. *Nat Rev Mol Cell Biol* **2007**, *8*, 970-982, doi:10.1038/nrm2297.

215. Shi, Y.; Massague, J. Mechanisms of TGF-beta signaling from cell membrane to the nucleus. *Cell* **2003**, *113*, 685-700, doi:10.1016/s0092-8674(03)00432-x.

216. Koleva, R.I.; Conley, B.A.; Romero, D.; Riley, K.S.; Marto, J.A.; Lux, A.; Vary, C.P. Endoglin structure and function: Determinants of endoglin phosphorylation by

transforming growth factor-beta receptors. *J Biol Chem* **2006**, *281*, 25110-25123, doi:10.1074/jbc.M601288200.

217. Guerrero-Esteo, M.; Sanchez-Elsner, T.; Letamendia, A.; Bernabeu, C. Extracellular and cytoplasmic domains of endoglin interact with the transforming growth factor-beta receptors I and II. *J Biol Chem* **2002**, *277*, 29197-29209, doi:10.1074/jbc.M111991200.
218. Barbara, N.P.; Wrana, J.L.; Letarte, M. Endoglin is an accessory protein that interacts with the signaling receptor complex of multiple members of the transforming growth factor-beta superfamily. *J Biol Chem* **1999**, *274*, 584-594, doi:10.1074/jbc.274.2.584.
219. Alt, A.; Miguel-Romero, L.; Donderis, J.; Aristorena, M.; Blanco, F.J.; Round, A.; Rubio, V.; Bernabeu, C.; Marina, A. Structural and functional insights into endoglin ligand recognition and binding. *PLoS One* **2012**, *7*, e29948, doi:10.1371/journal.pone.0029948.
220. Saito, T.; Bokhove, M.; Croci, R.; Zamora-Caballero, S.; Han, L.; Letarte, M.; de Sanctis, D.; Jovine, L. Structural Basis of the Human Endoglin-BMP9 Interaction: Insights into BMP Signaling and HHT1. *Cell Rep* **2017**, *19*, 1917-1928, doi:10.1016/j.celrep.2017.05.011.
221. Yamashita, H.; Ichijo, H.; Grimsby, S.; Moren, A.; ten Dijke, P.; Miyazono, K. Endoglin forms a heteromeric complex with the signaling receptors for transforming growth factor-beta. *J Biol Chem* **1994**, *269*, 1995-2001.
222. Lebrin, F.; Goumans, M.J.; Jonker, L.; Carvalho, R.L.; Valdimarsdottir, G.; Thorikay, M.; Mummery, C.; Arthur, H.M.; ten Dijke, P. Endoglin promotes endothelial cell proliferation and TGF-beta/ALK1 signal transduction. *EMBO J* **2004**, *23*, 4018-4028, doi:10.1038/sj.emboj.7600386.
223. Goumans, M.J.; Valdimarsdottir, G.; Itoh, S.; Rosendahl, A.; Sideras, P.; ten Dijke, P. Balancing the activation state of the endothelium via two distinct TGF-beta type I receptors. *EMBO J* **2002**, *21*, 1743-1753, doi:10.1093/emboj/21.7.1743.
224. Goumans, M.J.; Lebrin, F.; Valdimarsdottir, G. Controlling the angiogenic switch: a balance between two distinct TGF-b receptor signaling pathways. *Trends Cardiovasc Med* **2003**, *13*, 301-307, doi:10.1016/s1050-1738(03)00142-7.
225. Vander Ark, A.; Cao, J.; Li, X. TGF-beta receptors: In and beyond TGF-beta signaling. *Cell Signal* **2018**, *52*, 112-120, doi:10.1016/j.cellsig.2018.09.002.
226. Lee, N.Y.; Golzio, C.; Gatza, C.E.; Sharma, A.; Katsanis, N.; Blobe, G.C. Endoglin regulates PI3-kinase/Akt trafficking and signaling to alter endothelial capillary stability during angiogenesis. *Mol Biol Cell* **2012**, *23*, 2412-2423, doi:10.1091/mbc.E11-12-0993.

227. Lee, N.Y.; Blobe, G.C. The interaction of endoglin with beta-arrestin2 regulates transforming growth factor-beta-mediated ERK activation and migration in endothelial cells. *J Biol Chem* **2007**, *282*, 21507-21517, doi:10.1074/jbc.M700176200.
228. Bautch, V.L. Endoglin moves and shapes endothelial cells. *Nat Cell Biol* **2017**, *19*, 593-595, doi:10.1038/ncb3543.
229. Jin, Y.; Muhl, L.; Burmakin, M.; Wang, Y.; Duchez, A.C.; Betsholtz, C.; Arthur, H.M.; Jakobsson, L. Endoglin prevents vascular malformation by regulating flow-induced cell migration and specification through VEGFR2 signalling. *Nat Cell Biol* **2017**, *19*, 639-652, doi:10.1038/ncb3534.
230. ten Dijke, P.; Goumans, M.J.; Pardali, E. Endoglin in angiogenesis and vascular diseases. *Angiogenesis* **2008**, *11*, 79-89, doi:10.1007/s10456-008-9101-9.
231. Kumar, P.; Wang, J.M.; Bernabeu, C. CD 105 and angiogenesis. *J Pathol* **1996**, *178*, 363-366, doi:10.1002/(SICI)1096-9896(199604)178:4<363::AID-PATH491>3.0.CO;2-8.
232. Arthur, H.M.; Ure, J.; Smith, A.J.; Renforth, G.; Wilson, D.I.; Torsney, E.; Charlton, R.; Parums, D.V.; Jowett, T.; Marchuk, D.A., et al. Endoglin, an ancillary TGFbeta receptor, is required for extraembryonic angiogenesis and plays a key role in heart development. *Dev Biol* **2000**, *217*, 42-53, doi:10.1006/dbio.1999.9534.
233. Li, D.Y.; Sorensen, L.K.; Brooke, B.S.; Urness, L.D.; Davis, E.C.; Taylor, D.G.; Boak, B.B.; Wendel, D.P. Defective angiogenesis in mice lacking endoglin. *Science* **1999**, *284*, 1534-1537, doi:10.1126/science.284.5419.1534.
234. Pece-Barbara, N.; Cymerman, U.; Vera, S.; Marchuk, D.A.; Letarte, M. Expression analysis of four endoglin missense mutations suggests that haploinsufficiency is the predominant mechanism for hereditary hemorrhagic telangiectasia type 1. *Hum Mol Genet* **1999**, *8*, 2171-2181, doi:10.1093/hmg/8.12.2171.
235. McAllister, K.A.; Grogg, K.M.; Johnson, D.W.; Gallione, C.J.; Baldwin, M.A.; Jackson, C.E.; Helmbold, E.A.; Markel, D.S.; McKinnon, W.C.; Murrell, J., et al. Endoglin, a TGF-beta binding protein of endothelial cells, is the gene for hereditary haemorrhagic telangiectasia type 1. *Nat Genet* **1994**, *8*, 345-351, doi:10.1038/ng1294-345.
236. Schoonderwoerd, M.J.A.; Goumans, M.T.H.; Hawinkels, L. Endoglin: Beyond the Endothelium. *Biomolecules* **2020**, *10*, doi:10.3390/biom10020289.
237. Gonzalez Munoz, T.; Amaral, A.T.; Puerto-Camacho, P.; Peinado, H.; de Alava, E. Endoglin in the Spotlight to Treat Cancer. *Int J Mol Sci* **2021**, *22*, doi:10.3390/ijms22063186.

238. Rosen, L.S.; Gordon, M.S.; Robert, F.; Matei, D.E. Endoglin for targeted cancer treatment. *Curr Oncol Rep* **2014**, *16*, 365, doi:10.1007/s11912-013-0365-x.

239. Perez-Gomez, E.; Del Castillo, G.; Juan Francisco, S.; Lopez-Novoa, J.M.; Bernabeu, C.; Quintanilla, M. The role of the TGF-beta coreceptor endoglin in cancer. *ScientificWorldJournal* **2010**, *10*, 2367-2384, doi:10.1100/tsw.2010.230.

240. Dominici, M.; Le Blanc, K.; Mueller, I.; Slaper-Cortenbach, I.; Marini, F.; Krause, D.; Deans, R.; Keating, A.; Prockop, D.; Horwitz, E. Minimal criteria for defining multipotent mesenchymal stromal cells. The International Society for Cellular Therapy position statement. *Cytotherapy* **2006**, *8*, 315-317, doi:10.1080/14653240600855905.

241. Postiglione, L.; Di Domenico, G.; Caraglia, M.; Marra, M.; Giuberti, G.; Del Vecchio, L.; Montagnani, S.; Macri, M.; Bruno, E.M.; Abbruzzese, A., et al. Differential expression and cytoplasm/membrane distribution of endoglin (CD105) in human tumour cell lines: Implications in the modulation of cell proliferation. *Int J Oncol* **2005**, *26*, 1193-1201, doi:10.3892/ijo.26.5.1193.

242. Pardali, E.; van der Schaft, D.W.; Wiercinska, E.; Gorter, A.; Hogendoorn, P.C.; Griffioen, A.W.; ten Dijke, P. Critical role of endoglin in tumor cell plasticity of Ewing sarcoma and melanoma. *Oncogene* **2011**, *30*, 334-345, doi:10.1038/onc.2010.418.

243. Mitsui, H.; Shibata, K.; Mano, Y.; Suzuki, S.; Umezu, T.; Mizuno, M.; Yamamoto, E.; Kajiyama, H.; Kotani, T.; Senga, T., et al. The expression and characterization of endoglin in uterine leiomyosarcoma. *Clin Exp Metastasis* **2013**, *30*, 731-740, doi:10.1007/s10585-013-9574-9.

244. Sakamoto, R.; Kajihara, I.; Miyauchi, H.; Maeda-Otsuka, S.; Yamada-Kanazawa, S.; Sawamura, S.; Kanemaru, H.; Makino, K.; Aoi, J.; Makino, T., et al. Inhibition of Endoglin Exerts Antitumor Effects through the Regulation of Non-Smad TGF-beta Signaling in Angiosarcoma. *J Invest Dermatol* **2020**, *140*, 2060-2072 e2066, doi:10.1016/j.jid.2020.01.031.

245. Aziz, M.N.M.; Rahim, N.F.C.; Hussin, Y.; Yeap, S.K.; Masarudin, M.J.; Mohamad, N.E.; Akhtar, M.N.; Osman, M.A.; Cheah, Y.K.; Alitheen, N.B. Anti-Metastatic and Anti-Angiogenic Effects of Curcumin Analog DK1 on Human Osteosarcoma Cells In Vitro. *Pharmaceuticals (Basel)* **2021**, *14*, doi:10.3390/ph14060532.

246. Boeuf, S.; Bovee, J.V.; Lehner, B.; van den Akker, B.; van Ruler, M.; Cleton-Jansen, A.M.; Richter, W. BMP and TGFbeta pathways in human central chondrosarcoma: enhanced endoglin and Smad 1 signaling in high grade tumors. *BMC Cancer* **2012**, *12*, 488, doi:10.1186/1471-2407-12-488.

247. Gromova, P.; Rubin, B.P.; Thys, A.; Cullus, P.; Erneux, C.; Vanderwinden, J.M. ENDOGLIN/CD105 is expressed in KIT positive cells in the gut and in gastrointestinal stromal tumours. *J Cell Mol Med* **2012**, *16*, 306-317, doi:10.1111/j.1582-4934.2011.01315.x.

248. Tansi, F.L.; Ruger, R.; Kollmeier, A.M.; Rabenhold, M.; Steiniger, F.; Kontermann, R.E.; Teichgraeber, U.K.; Fahr, A.; Hilger, I. Endoglin based in vivo near-infrared fluorescence imaging of tumor models in mice using activatable liposomes. *Biochim Biophys Acta Gen Subj* **2018**, *1862*, 1389-1400, doi:10.1016/j.bbagen.2018.03.012.

249. Ciernik, I.F.; Krayenbuhl Ciernik, B.H.; Cockerell, C.J.; Minna, J.D.; Gazdar, A.F.; Carbone, D.P. Expression of transforming growth factor beta and transforming growth factor beta receptors on AIDS-associated Kaposi's sarcoma. *Clin Cancer Res* **1995**, *1*, 1119-1124.

250. Morozov, A.; Downey, R.J.; Healey, J.; Moreira, A.L.; Lou, E.; Franceschino, A.; Dogan, Y.; Leung, R.; Edgar, M.; LaQuaglia, M., et al. Benign mesenchymal stromal cells in human sarcomas. *Clin Cancer Res* **2010**, *16*, 5630-5640, doi:10.1158/1078-0432.CCR-09-2886.

251. Royer-Pokora, B.; Busch, M.; Beier, M.; Duhme, C.; de Torres, C.; Mora, J.; Brandt, A.; Royer, H.D. Wilms tumor cells with WT1 mutations have characteristic features of mesenchymal stem cells and express molecular markers of paraxial mesoderm. *Hum Mol Genet* **2010**, *19*, 1651-1668, doi:10.1093/hmg/ddq042.

252. Colletti, M.; Galardi, A.; Miele, E.; Di Paolo, V.; Russo, I.; De Stefanis, C.; De Vito, R.; Rinelli, M.; Ciolfi, A.; De Angelis, B., et al. Establishment and Characterization of a Cell Line (S-RMS1) Derived from an Infantile Spindle Cell Rhabdomyosarcoma with SRF-NCOA2 Fusion Transcript. *Int J Mol Sci* **2021**, *22*, doi:10.3390/ijms22115484.

253. Ollauri-Ibanez, C.; Ayuso-Inigo, B.; Pericacho, M. Hot and Cold Tumors: Is Endoglin (CD105) a Potential Target for Vessel Normalization? *Cancers (Basel)* **2021**, *13*, doi:10.3390/cancers13071552.

254. Seon, B.K.; Haba, A.; Matsuno, F.; Takahashi, N.; Tsujie, M.; She, X.; Harada, N.; Uneda, S.; Tsujie, T.; Toi, H., et al. Endoglin-targeted cancer therapy. *Curr Drug Deliv* **2011**, *8*, 135-143, doi:10.2174/156720111793663570.

255. Nassiri, F.; Cusimano, M.D.; Scheithauer, B.W.; Rotondo, F.; Fazio, A.; Yousef, G.M.; Syro, L.V.; Kovacs, K.; Lloyd, R.V. Endoglin (CD105): a review of its role in angiogenesis and tumor diagnosis, progression and therapy. *Anticancer Res* **2011**, *31*, 2283-2290.

256. Ollauri-Ibanez, C.; Nunez-Gomez, E.; Egido-Turrion, C.; Silva-Sousa, L.; Diaz-Rodriguez, E.; Rodriguez-Barbero, A.; Lopez-Novoa, J.M.; Pericacho, M. Continuous endoglin (CD105) overexpression disrupts angiogenesis and facilitates tumor cell metastasis. *Angiogenesis* **2020**, *23*, 231-247, doi:10.1007/s10456-019-09703-y.

257. Xu, Y.; Wang, D.; Zhao, L.M.; Zhao, X.L.; Shen, J.J.; Xie, Y.; Cao, L.L.; Chen, Z.B.; Luo, Y.M.; Bao, B.H., et al. Endoglin is necessary for angiogenesis in human ovarian carcinoma-derived primary endothelial cells. *Cancer Biol Ther* **2013**, *14*, 937-948, doi:10.4161/cbt.25940.

258. Dolinsek, T.; Markelc, B.; Sersa, G.; Coer, A.; Stimac, M.; Lavrencak, J.; Brozic, A.; Kranjc, S.; Cemazar, M. Multiple delivery of siRNA against endoglin into murine mammary adenocarcinoma prevents angiogenesis and delays tumor growth. *PLoS One* **2013**, *8*, e58723, doi:10.1371/journal.pone.0058723.

259. Duwel, A.; Eleno, N.; Jerkic, M.; Arevalo, M.; Bolanos, J.P.; Bernabeu, C.; Lopez-Novoa, J.M. Reduced tumor growth and angiogenesis in endoglin-haploinsufficient mice. *Tumour Biol* **2007**, *28*, 1-8, doi:10.1159/000097040.

260. Zhang, L.; Yang, B.; Li, X.; Zhang, Y.; Zhao, J.; Wang, W.; Yu, X.; Zhai, Z.; Sun, H. The targeting of endoglin on vascular endothelial cells affects the infiltration of M2 macrophages into the breast cancer microenvironment by modulating the interleukin-6 (IL-6) level. *Translational Cancer Research* **2018**, *7*, 912-921.

261. Romero, D.; O'Neill, C.; Terzic, A.; Contois, L.; Young, K.; Conley, B.A.; Bergan, R.C.; Brooks, P.C.; Vary, C.P. Endoglin regulates cancer-stromal cell interactions in prostate tumors. *Cancer Res* **2011**, *71*, 3482-3493, doi:10.1158/0008-5472.CAN-10-2665.

262. Hawinkels, L.J.; Kuiper, P.; Wiercinska, E.; Verspaget, H.W.; Liu, Z.; Pardali, E.; Sier, C.F.; ten Dijke, P. Matrix metalloproteinase-14 (MT1-MMP)-mediated endoglin shedding inhibits tumor angiogenesis. *Cancer Res* **2010**, *70*, 4141-4150, doi:10.1158/0008-5472.CAN-09-4466.

263. Castonguay, R.; Werner, E.D.; Matthews, R.G.; Presman, E.; Mulivor, A.W.; Solban, N.; Sako, D.; Pearsall, R.S.; Underwood, K.W.; Seehra, J., et al. Soluble endoglin specifically binds bone morphogenetic proteins 9 and 10 via its orphan domain, inhibits blood vessel formation, and suppresses tumor growth. *J Biol Chem* **2011**, *286*, 30034-30046, doi:10.1074/jbc.M111.260133.

264. Takahashi, N.; Kawanishi-Tabata, R.; Haba, A.; Tabata, M.; Haruta, Y.; Tsai, H.; Seon, B.K. Association of serum endoglin with metastasis in patients with colorectal, breast, and other solid tumors, and suppressive effect of chemotherapy on the serum endoglin. *Clin Cancer Res* **2001**, *7*, 524-532.

265. Li, C.; Guo, B.; Wilson, P.B.; Stewart, A.; Byrne, G.; Bundred, N.; Kumar, S. Plasma levels of soluble CD105 correlate with metastasis in patients with breast cancer. *Int J Cancer* **2000**, *89*, 122-126, doi:10.1002/(sici)1097-0215(20000320)89:2<122::aid-ijc4>3.0.co;2-m.

266. Hromada, C.; Muhleder, S.; Grillari, J.; Redl, H.; Holnthoner, W. Endothelial Extracellular Vesicles-Promises and Challenges. *Front Physiol* **2017**, *8*, 275, doi:10.3389/fphys.2017.00275.

267. Grange, C.; Tapparo, M.; Collino, F.; Vitillo, L.; Damasco, C.; Deregibus, M.C.; Tetta, C.; Bussolati, B.; Camussi, G. Microvesicles released from human renal cancer stem cells stimulate angiogenesis and formation of lung premetastatic niche. *Cancer Res* **2011**, *71*, 5346-5356, doi:10.1158/0008-5472.CAN-11-0241.

268. Douglas, S.R.; Yeung, K.T.; Yang, J.; Blair, S.L.; Cohen, O.; Eliceiri, B.P. Identification of CD105+ Extracellular Vesicles as a Candidate Biomarker for Metastatic Breast Cancer. *J Surg Res* **2021**, *268*, 168-173, doi:10.1016/j.jss.2021.06.050.

269. Liu, Y.; Paauwe, M.; Nixon, A.B.; Hawinkels, L. Endoglin Targeting: Lessons Learned and Questions That Remain. *Int J Mol Sci* **2020**, *22*, doi:10.3390/ijms22010147.

270. Nolan-Stevaux, O.; Zhong, W.; Culp, S.; Shaffer, K.; Hoover, J.; Wickramasinghe, D.; Ruefli-Brasse, A. Endoglin requirement for BMP9 signaling in endothelial cells reveals new mechanism of action for selective anti-endoglin antibodies. *PLoS One* **2012**, *7*, e50920, doi:10.1371/journal.pone.0050920.

271. Rosen, L.S.; Hurwitz, H.I.; Wong, M.K.; Goldman, J.; Mendelson, D.S.; Figg, W.D.; Spencer, S.; Adams, B.J.; Alvarez, D.; Seon, B.K., et al. A phase I first-in-human study of TRC105 (Anti-Endoglin Antibody) in patients with advanced cancer. *Clin Cancer Res* **2012**, *18*, 4820-4829, doi:10.1158/1078-0432.CCR-12-0098.

272. Apolo, A.B.; Karzai, F.H.; Trepel, J.B.; Alarcon, S.; Lee, S.; Lee, M.J.; Tomita, Y.; Cao, L.; Yu, Y.; Merino, M.J., et al. A Phase II Clinical Trial of TRC105 (Anti-Endoglin Antibody) in Adults With Advanced/Metastatic Urothelial Carcinoma. *Clin Genitourin Cancer* **2017**, *15*, 77-85, doi:10.1016/j.clgc.2016.05.010.

273. Karzai, F.H.; Apolo, A.B.; Cao, L.; Madan, R.A.; Adelberg, D.E.; Parnes, H.; McLeod, D.G.; Harold, N.; Peer, C.; Yu, Y., et al. A phase I study of TRC105 anti-endoglin (CD105) antibody in metastatic castration-resistant prostate cancer. *BJU Int* **2015**, *116*, 546-555, doi:10.1111/bju.12986.

274. Duffy, A.G.; Ulahannan, S.V.; Cao, L.; Rahma, O.E.; Makarova-Rusher, O.V.; Kleiner, D.E.; Fioravanti, S.; Walker, M.; Carey, S.; Yu, Y., et al. A phase II study of TRC105 in patients with hepatocellular carcinoma who have progressed on

sorafenib. *United European Gastroenterol J* **2015**, *3*, 453-461, doi:10.1177/2050640615583587.

275. Attia, S.; Sankhala, K.K.; Riedel, R.F.; Robinson, S.I.; Conry, R.M.; Boland, P.M.; Barve, M.A.; Fritchie, K.; Seon, B.K.; Alvarez, D., et al. A phase 1B/ phase 2A study of TRC105 (Endoglin Antibody) in combination with pazopanib (P) in patients (pts) with advanced soft tissue sarcoma (STS). *Journal of Clinical Oncology* **2016**, *34*, 11016-11016, doi:10.1200/JCO.2016.34.15_suppl.11016.
276. Mehta, C.R.; Liu, L.; Theuer, C. An adaptive population enrichment phase III trial of TRC105 and pazopanib versus pazopanib alone in patients with advanced angiosarcoma (TAPPAS trial). *Ann Oncol* **2019**, *30*, 103-108, doi:10.1093/annonc/mdy464.
277. Levine, E.G.; Forero, A.; O'Connor, T.; Seon, B.K.; Jivani, M.A.; Adams, B.J.; Theuer, C.P. A phase Ib dose-escalation study of TRC105 (anti-endoglin antibody) in combination with capecitabine for advanced solid tumors (including patients with progressive or recurrent HER2-negative metastatic breast cancer). *Journal of Clinical Oncology* **2013**, *31*, 3057-3057, doi:10.1200/jco.2013.31.15_suppl.3057.
278. Ahluwalia, M.S.; Rogers, L.R.; Chaudhary, R.T.; Newton, H.B.; Seon, B.K.; Jivani, M.A.; Adams, B.J.; Shazer, R.L.; Theuer, C.P. A phase 2 trial of TRC105 with bevacizumab for bevacizumab refractory glioblastoma. *Journal of Clinical Oncology* **2016**, *34*, 2035-2035, doi:10.1200/JCO.2016.34.15_suppl.2035.
279. Gordon, M.S.; Robert, F.; Matei, D.; Mendelson, D.S.; Goldman, J.W.; Chiorean, E.G.; Strother, R.M.; Seon, B.K.; Figg, W.D.; Peer, C.J., et al. An open-label phase Ib dose-escalation study of TRC105 (anti-endoglin antibody) with bevacizumab in patients with advanced cancer. *Clin Cancer Res* **2014**, *20*, 5918-5926, doi:10.1158/1078-0432.CCR-14-1143.
280. Choueiri, T.K.; Zakharia, Y.; Pal, S.; Kocsis, J.; Pachynski, R.; Poprach, A.; Nixon, A.B.; Liu, Y.; Starr, M.; Lyu, J., et al. Clinical Results and Biomarker Analyses of Axitinib and TRC105 versus Axitinib Alone in Patients with Advanced or Metastatic Renal Cell Carcinoma (TRAXAR). *Oncologist* **2021**, *26*, 560-e1103, doi:10.1002/onco.13777.
281. Barrett, S.D.; Bridges, A.J.; Dudley, D.T.; Saltiel, A.R.; Fergus, J.H.; Flamme, C.M.; Delaney, A.M.; Kaufman, M.; LePage, S.; Leopold, W.R., et al. The discovery of the benzhydroxamate MEK inhibitors CI-1040 and PD 0325901. *Bioorg Med Chem Lett* **2008**, *18*, 6501-6504, doi:10.1016/j.bmcl.2008.10.054.
282. Ghadimi, M.P.; Young, E.D.; Belousov, R.; Zhang, Y.; Lopez, G.; Lusby, K.; Kivlin, C.; Demicco, E.G.; Creighton, C.J.; Lazar, A.J., et al. Survivin is a viable target for

the treatment of malignant peripheral nerve sheath tumors. *Clin Cancer Res* **2012**, *18*, 2545-2557, doi:10.1158/1078-0432.CCR-11-2592.

283. Graña, O.; Rubio-Camarillo, M.; Fdez-Riverola, F.; Pisano, D.G.; Glez-Peña, D. Nextpresso: Next Generation Sequencing Expression Analysis Pipeline. *Current Bioinformatics* **2018**, *13*, 583-591, doi:http://dx.doi.org/10.2174/1574893612666170810153850.
284. Trapnell, C.; Roberts, A.; Goff, L.; Pertea, G.; Kim, D.; Kelley, D.R.; Pimentel, H.; Salzberg, S.L.; Rinn, J.L.; Pachter, L. Differential gene and transcript expression analysis of RNA-seq experiments with TopHat and Cufflinks. *Nat Protoc* **2012**, *7*, 562-578, doi:10.1038/nprot.2012.016.
285. Langmead, B.; Trapnell, C.; Pop, M.; Salzberg, S.L. Ultrafast and memory-efficient alignment of short DNA sequences to the human genome. *Genome Biol* **2009**, *10*, R25, doi:10.1186/gb-2009-10-3-r25.
286. Li, H.; Handsaker, B.; Wysoker, A.; Fennell, T.; Ruan, J.; Homer, N.; Marth, G.; Abecasis, G.; Durbin, R.; Genome Project Data Processing, S. The Sequence Alignment/Map format and SAMtools. *Bioinformatics* **2009**, *25*, 2078-2079, doi:10.1093/bioinformatics/btp352.
287. Love, M.I.; Huber, W.; Anders, S. Moderated estimation of fold change and dispersion for RNA-seq data with DESeq2. *Genome Biol* **2014**, *15*, 550, doi:10.1186/s13059-014-0550-8.
288. Subramanian, A.; Tamayo, P.; Mootha, V.K.; Mukherjee, S.; Ebert, B.L.; Gillette, M.A.; Paulovich, A.; Pomeroy, S.L.; Golub, T.R.; Lander, E.S., et al. Gene set enrichment analysis: a knowledge-based approach for interpreting genome-wide expression profiles. *Proc Natl Acad Sci U S A* **2005**, *102*, 15545-15550, doi:10.1073/pnas.0506580102.
289. Conway, T.; Wazny, J.; Bromage, A.; Tymms, M.; Sooraj, D.; Williams, E.D.; Beresford-Smith, B. Xenome--a tool for classifying reads from xenograft samples. *Bioinformatics* **2012**, *28*, i172-178, doi:10.1093/bioinformatics/bts236.
290. Williams, K.B.; Largaespada, D.A. New Model Systems and the Development of Targeted Therapies for the Treatment of Neurofibromatosis Type 1-Associated Malignant Peripheral Nerve Sheath Tumors. *Genes (Basel)* **2020**, *11*, doi:10.3390/genes11050477.
291. Hanahan, D.; Weinberg, R.A. Hallmarks of cancer: the next generation. *Cell* **2011**, *144*, 646-674, doi:10.1016/j.cell.2011.02.013.
292. Narasimhan, P.; Liu, J.; Song, Y.S.; Massengale, J.L.; Chan, P.H. VEGF Stimulates the ERK 1/2 signaling pathway and apoptosis in cerebral endothelial

cells after ischemic conditions. *Stroke* **2009**, *40*, 1467-1473, doi:10.1161/STROKEAHA.108.534644.

293. Xu, J.; Liu, X.; Jiang, Y.; Chu, L.; Hao, H.; Liua, Z.; Verfaillie, C.; Zweier, J.; Gupta, K.; Liu, Z. MAPK/ERK signalling mediates VEGF-induced bone marrow stem cell differentiation into endothelial cell. *J Cell Mol Med* **2008**, *12*, 2395-2406, doi:10.1111/j.1582-4934.2008.00266.x.
294. Yao, Z.; Torres, N.M.; Tao, A.; Gao, Y.; Luo, L.; Li, Q.; de Stanchina, E.; Abdel-Wahab, O.; Solit, D.B.; Poulikakos, P.I., et al. BRAF Mutants Evade ERK-Dependent Feedback by Different Mechanisms that Determine Their Sensitivity to Pharmacologic Inhibition. *Cancer Cell* **2015**, *28*, 370-383, doi:10.1016/j.ccell.2015.08.001.
295. Lito, P.; Pratilas, C.A.; Joseph, E.W.; Tadi, M.; Halilovic, E.; Zubrowski, M.; Huang, A.; Wong, W.L.; Callahan, M.K.; Merghoub, T., et al. Relief of profound feedback inhibition of mitogenic signaling by RAF inhibitors attenuates their activity in BRAFV600E melanomas. *Cancer Cell* **2012**, *22*, 668-682, doi:10.1016/j.ccr.2012.10.009.
296. Dituri, F.; Cossu, C.; Mancarella, S.; Giannelli, G. The Interactivity between TGFbeta and BMP Signaling in Organogenesis, Fibrosis, and Cancer. *Cells* **2019**, *8*, doi:10.3390/cells8101130.
297. Zhang, L.; Ye, Y.; Long, X.; Xiao, P.; Ren, X.; Yu, J. BMP signaling and its paradoxical effects in tumorigenesis and dissemination. *Oncotarget* **2016**, *7*, 78206-78218, doi:10.18632/oncotarget.12151.
298. Dhillon, A.S.; Hagan, S.; Rath, O.; Kolch, W. MAP kinase signalling pathways in cancer. *Oncogene* **2007**, *26*, 3279-3290, doi:10.1038/sj.onc.1210421.
299. Berra, E.; Milanini, J.; Richard, D.E.; Le Gall, M.; Vinals, F.; Gothie, E.; Roux, D.; Pages, G.; Pouyssegur, J. Signaling angiogenesis via p42/p44 MAP kinase and hypoxia. *Biochem Pharmacol* **2000**, *60*, 1171-1178, doi:10.1016/s0006-2952(00)00423-8.
300. Guo, Y.J.; Pan, W.W.; Liu, S.B.; Shen, Z.F.; Xu, Y.; Hu, L.L. ERK/MAPK signalling pathway and tumorigenesis. *Exp Ther Med* **2020**, *19*, 1997-2007, doi:10.3892/etm.2020.8454.
301. Puerto-Camacho, P.; Amaral, A.T.; Lamhamedi-Cherradi, S.E.; Menegaz, B.A.; Castillo-Ecija, H.; Ordonez, J.L.; Dominguez, S.; Jordan-Perez, C.; Diaz-Martin, J.; Romero-Perez, L., et al. Preclinical Efficacy of Endoglin-Targeting Antibody-Drug Conjugates for the Treatment of Ewing Sarcoma. *Clin Cancer Res* **2019**, *25*, 2228-2240, doi:10.1158/1078-0432.CCR-18-0936.

302. Maleki, M.; Ghanbarvand, F.; Reza Behvarz, M.; Ejtemaei, M.; Ghadirkhomi, E. Comparison of mesenchymal stem cell markers in multiple human adult stem cells. *Int J Stem Cells* **2014**, *7*, 118-126, doi:10.15283/ijsc.2014.7.2.118.
303. Bai, S.; Zhu, W.; Coffman, L.; Vlad, A.; Schwartz, L.E.; Elishaev, E.; Drapkin, R.; Buckanovich, R.J. CD105 Is Expressed in Ovarian Cancer Precursor Lesions and Is Required for Metastasis to the Ovary. *Cancers (Basel)* **2019**, *11*, doi:10.3390/cancers11111710.
304. Henry, L.A.; Johnson, D.A.; Sarrio, D.; Lee, S.; Quinlan, P.R.; Crook, T.; Thompson, A.M.; Reis-Filho, J.S.; Isacke, C.M. Endoglin expression in breast tumor cells suppresses invasion and metastasis and correlates with improved clinical outcome. *Oncogene* **2011**, *30*, 1046-1058, doi:10.1038/onc.2010.488.
305. Lakshman, M.; Huang, X.; Ananthanarayanan, V.; Jovanovic, B.; Liu, Y.; Craft, C.S.; Romero, D.; Vary, C.P.; Bergan, R.C. Endoglin suppresses human prostate cancer metastasis. *Clin Exp Metastasis* **2011**, *28*, 39-53, doi:10.1007/s10585-010-9356-6.
306. Barresi, V.; Branca, G.; Caffo, M.; Caltabiano, R.; Ieni, A.; Vitarelli, E.; Lanzafame, S.; Tuccari, G. Immuno-expression of endoglin and smooth muscle actin in the vessels of brain metastases. Is there a rational for anti-angiogenic therapy? *Int J Mol Sci* **2014**, *15*, 5663-5679, doi:10.3390/ijms15045663.
307. Salgado, K.B.; Toscani, N.V.; Silva, L.L.; Hilbig, A.; Barbosa-Coutinho, L.M. Immunoexpression of endoglin in brain metastasis secondary to malignant melanoma: evaluation of angiogenesis and comparison with brain metastasis secondary to breast and lung carcinomas. *Clin Exp Metastasis* **2007**, *24*, 403-410, doi:10.1007/s10585-007-9077-7.
308. Paauwe, M.; Schoonderwoerd, M.J.A.; Helderman, R.; Harryvan, T.J.; Groenewoud, A.; van Pelt, G.W.; Bor, R.; Hemmer, D.M.; Versteeg, H.H.; Snaar-Jagalska, B.E., et al. Endoglin Expression on Cancer-Associated Fibroblasts Regulates Invasion and Stimulates Colorectal Cancer Metastasis. *Clin Cancer Res* **2018**, *24*, 6331-6344, doi:10.1158/1078-0432.CCR-18-0329.
309. Graham, D.S.; Russell, T.A.; Eckardt, M.A.; Motamedi, K.; Seeger, L.L.; Singh, A.S.; Bernthal, N.M.; Kalbasi, A.; Dry, S.M.; Nelson, S.D., et al. Oncologic Accuracy of Image-guided Percutaneous Core-Needle Biopsy of Peripheral Nerve Sheath Tumors at a High-volume Sarcoma Center. *Am J Clin Oncol* **2019**, *42*, 739-743, doi:10.1097/COC.0000000000000591.
310. Wasa, J.; Nishida, Y.; Tsukushi, S.; Shido, Y.; Sugiura, H.; Nakashima, H.; Ishiguro, N. MRI features in the differentiation of malignant peripheral nerve sheath

tumors and neurofibromas. *AJR Am J Roentgenol* **2010**, *194*, 1568-1574, doi:10.2214/AJR.09.2724.

311. Cescon, D.W.; Bratman, S.V.; Chan, S.M.; Siu, L.L. Circulating tumor DNA and liquid biopsy in oncology. *Nature Cancer* **2020**, *1*, 276-290, doi:10.1038/s43018-020-0043-5.
312. Nogues, A.; Gallardo-Vara, E.; Zafra, M.P.; Mate, P.; Marijuan, J.L.; Alonso, A.; Botella, L.M.; Prieto, M.I. Endoglin (CD105) and VEGF as potential angiogenic and dissemination markers for colorectal cancer. *World J Surg Oncol* **2020**, *18*, 99, doi:10.1186/s12957-020-01871-2.
313. Svatek, R.S.; Karam, J.A.; Roehrborn, C.G.; Karakiewicz, P.I.; Slawin, K.M.; Shariat, S.F. Preoperative plasma endoglin levels predict biochemical progression after radical prostatectomy. *Clin Cancer Res* **2008**, *14*, 3362-3366, doi:10.1158/1078-0432.CCR-07-4707.
314. Karam, J.A.; Svatek, R.S.; Karakiewicz, P.I.; Gallina, A.; Roehrborn, C.G.; Slawin, K.M.; Shariat, S.F. Use of preoperative plasma endoglin for prediction of lymph node metastasis in patients with clinically localized prostate cancer. *Clin Cancer Res* **2008**, *14*, 1418-1422, doi:10.1158/1078-0432.CCR-07-0901.
315. Vidal, A.C.; Duong, F.; Howard, L.E.; Wiggins, E.; Freedland, S.J.; Bhowmick, N.A.; Gong, J. Soluble Endoglin (sCD105) as a Novel Biomarker for Detecting Aggressive Prostate Cancer. *Anticancer Res* **2020**, *40*, 1459-1462, doi:10.21873/anticanres.14088.
316. Bernabeu, C.; Lopez-Novoa, J.M.; Quintanilla, M. The emerging role of TGF-beta superfamily coreceptors in cancer. *Biochim Biophys Acta* **2009**, *1792*, 954-973, doi:10.1016/j.bbadis.2009.07.003.
317. David, L.; Mallet, C.; Mazerbourg, S.; Feige, J.J.; Bailly, S. Identification of BMP9 and BMP10 as functional activators of the orphan activin receptor-like kinase 1 (ALK1) in endothelial cells. *Blood* **2007**, *109*, 1953-1961, doi:10.1182/blood-2006-07-034124.
318. Santibanez, J.F.; Perez-Gomez, E.; Fernandez, L.A.; Garrido-Martin, E.M.; Carnero, A.; Malumbres, M.; Vary, C.P.; Quintanilla, M.; Bernabeu, C. The TGF-beta co-receptor endoglin modulates the expression and transforming potential of H-Ras. *Carcinogenesis* **2010**, *31*, 2145-2154, doi:10.1093/carcin/bgq199.
319. Luo, K. Signaling Cross Talk between TGF-beta/Smad and Other Signaling Pathways. *Cold Spring Harb Perspect Biol* **2017**, *9*, doi:10.1101/cshperspect.a022137.
320. Javelaud, D.; Mauviel, A. Crosstalk mechanisms between the mitogen-activated protein kinase pathways and Smad signaling downstream of TGF-beta:

implications for carcinogenesis. *Oncogene* **2005**, *24*, 5742-5750, doi:10.1038/sj.onc.1208928.

321. Zhou, Q.; Heinke, J.; Vargas, A.; Winnik, S.; Krauss, T.; Bode, C.; Patterson, C.; Moser, M. ERK signaling is a central regulator for BMP-4 dependent capillary sprouting. *Cardiovasc Res* **2007**, *76*, 390-399, doi:10.1016/j.cardiores.2007.08.003.
322. Izumi, M.; Masaki, M.; Hiramoto, Y.; Sugiyama, S.; Kuroda, T.; Terai, K.; Hori, M.; Kawase, I.; Hirota, H. Cross-talk between bone morphogenetic protein 2 and leukemia inhibitory factor through ERK 1/2 and Smad1 in protection against doxorubicin-induced injury of cardiomyocytes. *J Mol Cell Cardiol* **2006**, *40*, 224-233, doi:10.1016/j.yjmcc.2005.11.007.
323. Ahsan, S.; Ge, Y.; Tainsky, M.A. Combinatorial therapeutic targeting of BMP2 and MEK-ERK pathways in NF1-associated malignant peripheral nerve sheath tumors. *Oncotarget* **2016**, *7*, 57171-57185, doi:10.18632/oncotarget.11036.
324. Zhang, J.; Yuan, B.; Zhang, H.; Li, H. Human epithelial ovarian cancer cells expressing CD105, CD44 and CD106 surface markers exhibit increased invasive capacity and drug resistance. *Oncol Lett* **2019**, *17*, 5351-5360, doi:10.3892/ol.2019.10221.
325. Kokaji, E.; Shimomura, A.; Minamisaka, T.; Nakajima, T.; Miwa, S.; Hatta, H.; Nishida, T.; Kiya, C.; Imura, J. Endoglin (CD105) and SMAD4 regulate spheroid formation and the suppression of the invasive ability of human pancreatic cancer cells. *Int J Oncol* **2018**, *52*, 892-900, doi:10.3892/ijo.2018.4262.
326. Hu, J.; Guan, W.; Liu, P.; Dai, J.; Tang, K.; Xiao, H.; Qian, Y.; Sharrow, A.C.; Ye, Z.; Wu, L., et al. Endoglin Is Essential for the Maintenance of Self-Renewal and Chemoresistance in Renal Cancer Stem Cells. *Stem Cell Reports* **2017**, *9*, 464-477, doi:10.1016/j.stemcr.2017.07.009.
327. Pal, K.; Pletnev, A.A.; Dutta, S.K.; Wang, E.; Zhao, R.; Baral, A.; Yadav, V.K.; Aggarwal, S.; Krishnaswamy, S.; Alkharfy, K.M., et al. Inhibition of endoglin-GIPC interaction inhibits pancreatic cancer cell growth. *Mol Cancer Ther* **2014**, *13*, 2264-2275, doi:10.1158/1535-7163.MCT-14-0291.
328. Fujiwara, K.; Ohuchida, K.; Ohtsuka, T.; Mizumoto, K.; Shindo, K.; Ikenaga, N.; Cui, L.; Takahata, S.; Aishima, S.; Tanaka, M. Migratory activity of CD105+ pancreatic cancer cells is strongly enhanced by pancreatic stellate cells. *Pancreas* **2013**, *42*, 1283-1290, doi:10.1097/mpa.0b013e318293e7bd.
329. Ziebarth, A.J.; Nowsheen, S.; Steg, A.D.; Shah, M.M.; Katre, A.A.; Dobbin, Z.C.; Han, H.D.; Lopez-Berestein, G.; Sood, A.K.; Conner, M., et al. Endoglin (CD105) contributes to platinum resistance and is a target for tumor-specific therapy in

epithelial ovarian cancer. *Clin Cancer Res* **2013**, *19*, 170-182, doi:10.1158/1078-0432.CCR-12-1045.

330. Wong, V.C.; Chan, P.L.; Bernabeu, C.; Law, S.; Wang, L.D.; Li, J.L.; Tsao, S.W.; Srivastava, G.; Lung, M.L. Identification of an invasion and tumor-suppressing gene, Endoglin (ENG), silenced by both epigenetic inactivation and allelic loss in esophageal squamous cell carcinoma. *Int J Cancer* **2008**, *123*, 2816-2823, doi:10.1002/ijc.23882.
331. Perez-Gomez, E.; Villa-Morales, M.; Santos, J.; Fernandez-Piqueras, J.; Gamallo, C.; Dotor, J.; Bernabeu, C.; Quintanilla, M. A role for endoglin as a suppressor of malignancy during mouse skin carcinogenesis. *Cancer Res* **2007**, *67*, 10268-10277, doi:10.1158/0008-5472.CAN-07-1348.
332. Paauwe, M.; Heijkants, R.C.; Oudt, C.H.; van Pelt, G.W.; Cui, C.; Theuer, C.P.; Hardwick, J.C.; Sier, C.F.; Hawinkels, L.J. Endoglin targeting inhibits tumor angiogenesis and metastatic spread in breast cancer. *Oncogene* **2016**, *35*, 4069-4079, doi:10.1038/onc.2015.509.
333. Adigbli, G.; Menoret, S.; Cross, A.R.; Hester, J.; Issa, F.; Anegon, I. Humanization of Immunodeficient Animals for the Modeling of Transplantation, Graft Versus Host Disease, and Regenerative Medicine. *Transplantation* **2020**, *104*, 2290-2306, doi:10.1097/TP.0000000000003177.
334. Shultz, L.D.; Goodwin, N.; Ishikawa, F.; Hosur, V.; Lyons, B.L.; Greiner, D.L. Human cancer growth and therapy in immunodeficient mouse models. *Cold Spring Harb Protoc* **2014**, *2014*, 694-708, doi:10.1101/pdb.top073585.
335. Darzi, S.; Deane, J.A.; Nold, C.A.; Edwards, S.E.; Gough, D.J.; Mukherjee, S.; Gurung, S.; Tan, K.S.; Vashi, A.V.; Werkmeister, J.A., et al. Endometrial Mesenchymal Stem/Stromal Cells Modulate the Macrophage Response to Implanted Polyamide/Gelatin Composite Mesh in Immunocompromised and Immunocompetent Mice. *Sci Rep* **2018**, *8*, 6554, doi:10.1038/s41598-018-24919-6.
336. Hu, Z.; Van Rooijen, N.; Yang, Y.G. Macrophages prevent human red blood cell reconstitution in immunodeficient mice. *Blood* **2011**, *118*, 5938-5946, doi:10.1182/blood-2010-11-321414.
337. Schoonderwoerd, M.J.A.; Koops, M.F.M.; Angela, R.A.; Koolmoes, B.; Toitou, M.; Paauwe, M.; Barnhoorn, M.C.; Liu, Y.; Sier, C.F.M.; Hardwick, J.C.H., et al. Targeting Endoglin-Expressing Regulatory T Cells in the Tumor Microenvironment Enhances the Effect of PD1 Checkpoint Inhibitor Immunotherapy. *Clin Cancer Res* **2020**, *26*, 3831-3842, doi:10.1158/1078-0432.CCR-19-2889.

338. Tsujie, M.; Uneda, S.; Tsai, H.; Seon, B.K. Effective anti-angiogenic therapy of established tumors in mice by naked anti-human endoglin (CD105) antibody: differences in growth rate and therapeutic response between tumors growing at different sites. *Int J Oncol* **2006**, *29*, 1087-1094.

339. Tsujie, M.; Tsujie, T.; Toi, H.; Uneda, S.; Shiozaki, K.; Tsai, H.; Seon, B.K. Anti-tumor activity of an anti-endoglin monoclonal antibody is enhanced in immunocompetent mice. *Int J Cancer* **2008**, *122*, 2266-2273, doi:10.1002/ijc.23314.

340. Nagabushan, S.; Lau, L.M.S.; Barahona, P.; Wong, M.; Sherstyuk, A.; Marshall, G.M.; Tyrrell, V.; Wegner, E.A.; Ekert, P.G.; Cowley, M.J., et al. Efficacy of MEK inhibition in a recurrent malignant peripheral nerve sheath tumor. *NPJ Precis Oncol* **2021**, *5*, 9, doi:10.1038/s41698-021-00145-8.

341. Castellsague, J.; Gel, B.; Fernandez-Rodriguez, J.; Llatjos, R.; Blanco, I.; Benavente, Y.; Perez-Sidelnikova, D.; Garcia-Del Muro, J.; Vinals, J.M.; Vidal, A., et al. Comprehensive establishment and characterization of orthoxenograft mouse models of malignant peripheral nerve sheath tumors for personalized medicine. *EMBO Mol Med* **2015**, *7*, 608-627, doi:10.15252/emmm.201404430.

342. Kim, R.; Tan, E.; Wang, E.; Mahipal, A.; Chen, D.T.; Cao, B.; Masawi, F.; Machado, C.; Yu, J.; Kim, D.W. A Phase I Trial of Trametinib in Combination with Sorafenib in Patients with Advanced Hepatocellular Cancer. *Oncologist* **2020**, *25*, e1893-e1899, doi:10.1634/theoncologist.2020-0759.

343. Lim, H.Y.; Merle, P.; Weiss, K.H.; Yau, T.; Ross, P.; Mazzaferro, V.; Blanc, J.F.; Ma, Y.T.; Yen, C.J.; Kocsis, J., et al. Phase II Studies with Refametinib or Refametinib plus Sorafenib in Patients with RAS-Mutated Hepatocellular Carcinoma. *Clin Cancer Res* **2018**, *24*, 4650-4661, doi:10.1158/1078-0432.CCR-17-3588.

344. Shroff, R.T.; Yarchoan, M.; O'Connor, A.; Gallagher, D.; Zahurak, M.L.; Rosner, G.; Ohaji, C.; Sartorius-Mergenthaler, S.; Parkinson, R.; Subbiah, V., et al. The oral VEGF receptor tyrosine kinase inhibitor pazopanib in combination with the MEK inhibitor trametinib in advanced cholangiocarcinoma. *Br J Cancer* **2017**, *116*, 1402-1407, doi:10.1038/bjc.2017.119.

345. Tai, W.M.; Yong, W.P.; Lim, C.; Low, L.S.; Tham, C.K.; Koh, T.S.; Ng, Q.S.; Wang, W.W.; Wang, L.Z.; Hartano, S., et al. A phase Ib study of selumetinib (AZD6244, ARRY-142886) in combination with sorafenib in advanced hepatocellular carcinoma (HCC). *Ann Oncol* **2016**, *27*, 2210-2215, doi:10.1093/annonc/mdw415.

346. Adjei, A.A.; Richards, D.A.; El-Khoueiry, A.; Braiteh, F.; Becerra, C.H.; Stephenson, J.J., Jr.; Hezel, A.F.; Sherman, M.; Garbo, L.; Leffingwell, D.P., et al.

A Phase I Study of the Safety, Pharmacokinetics, and Pharmacodynamics of Combination Therapy with Refametinib plus Sorafenib in Patients with Advanced Cancer. *Clin Cancer Res* **2016**, *22*, 2368-2376, doi:10.1158/1078-0432.CCR-15-1681.

347. Lim, H.Y.; Heo, J.; Choi, H.J.; Lin, C.Y.; Yoon, J.H.; Hsu, C.; Rau, K.M.; Poon, R.T.; Yeo, W.; Park, J.W., et al. A phase II study of the efficacy and safety of the combination therapy of the MEK inhibitor refametinib (BAY 86-9766) plus sorafenib for Asian patients with unresectable hepatocellular carcinoma. *Clin Cancer Res* **2014**, *20*, 5976-5985, doi:10.1158/1078-0432.CCR-13-3445.
348. Subbiah, V.; Meyer, C.; Zinner, R.; Meric-Bernstam, F.; Zahurak, M.L.; O'Connor, A.; Roszik, J.; Shaw, K.; Ludwig, J.A.; Kurzrock, R., et al. Phase Ib/II Study of the Safety and Efficacy of Combination Therapy with Multikinase VEGF Inhibitor Pazopanib and MEK Inhibitor Trametinib In Advanced Soft Tissue Sarcoma. *Clin Cancer Res* **2017**, *23*, 4027-4034, doi:10.1158/1078-0432.CCR-17-0272.
349. Liu, Y.; Starr, M.D.; Brady, J.C.; Dellinger, A.; Pang, H.; Adams, B.; Theuer, C.P.; Lee, N.Y.; Hurwitz, H.I.; Nixon, A.B. Modulation of circulating protein biomarkers following TRC105 (anti-endoglin antibody) treatment in patients with advanced cancer. *Cancer Med* **2014**, *3*, 580-591, doi:10.1002/cam4.207.
350. Liu, Y.; Starr, M.D.; Brady, J.C.; Rushing, C.; Pang, H.; Adams, B.; Alvarez, D.; Theuer, C.P.; Hurwitz, H.I.; Nixon, A.B. Modulation of Circulating Protein Biomarkers in Cancer Patients Receiving Bevacizumab and the Anti-Endoglin Antibody, TRC105. *Mol Cancer Ther* **2018**, *17*, 2248-2256, doi:10.1158/1535-7163.MCT-17-0916.

APPENDIX

1. Supplementary tables

Supplementary Table 1. Differentially expressed genes in shENG vs shScramble STS26T cells

shENG vs shScramble							
Down-regulated genes							
RRS1	TTC35	TIPIN	HCFC2	ACOX2	PURA	PRKRIR	HDAC9
DDX39A	SLC25A43	LOC339290	DLX1	HIPK1	ZC3H12C	LY6K	DUSP7
NSUN2	HSPA13	MND1	SETD7	TRIM35	DNTTIP2	EIF4E3	RIMS2
HIPK2	USP12	CENPC1	MLF1IP	AOX1	GATA2	IL11	ZFP1
LAMB3	ARPC5	ELP3	UTP15	SGPP1	PHLDA1	AMMECR1	C15orf48
NUP50	C3orf64	KBTBD2	ZNF639	C20orf20	PCNA	ACAT1	MARS2
CALD1	PIK3CB	IGFN1	LAPTM5	CCDC86	MME	SLCO1B3	AGPAT9
NMD3	STK39	UAP1	IPMK	SH3BGRL	IER2	TMEM156	EP400NL
RBBP8	CDC42EP2	C9orf5	ZNF480	STC1	TUSC1	SLC16A6	NCEH1
PDGFC	RFWD3	TMEM192	ATP2B1	CD83	KLF10	C16orf87	ZNF597
NOP56	GPBP1L1	ANXA3	MZT1	FABP5	PPM1A	ZBTB34	FAM111B
TBC1D15	CKAP2L	KLHL2	TMEM64	FOXD1	ZNF468	AMMECR1L	LOC730755
HMGA1	CCNA2	FAM214B	LOC654433	ZNF238	PAK3	MPP4	FAIM3
TPM4	CKAP2	TMPRSS15	NUFIP2	PLK3	ZBTB41	NEDD4L	ZNF823
C1GALT1	SLC35B1	C1orf55	APOOL	SERTAD2	MYEF2	PAWR	ZNF280B
NUCKS1	CEP152	ODC1	C16orf52	SLC14A1	ANTXR2	FOSL1	ZNF567
RANBP1	EID2	ZNF146	ADCY7	NGF	LARP1B	IER5L	CASP3
PARP4	ABCE1	NEDD4	ENOX2	PPP1R18	OSGIN1	ICK	CHAC1
IFRD1	ALPK2	CEP170	EMP1	ARHGAP11A	C10orf88	NAV3	C1orf51
NQO1	KAT6A	YEATS4	C5orf30	SEPSECS	EREG	PHF13	VSTM1
METAP2	KIAA0020	SLC39A10	MYPN	GRPEL2	TEF	ATG5	FBP1
KLHL5	SLC7A11	ZMYND11	CTNNAL1	B3GNT2	SLC7A5	ARPP19	C1D
MAGOHB	CD55	LOC647979	FOXG1	LIG4	TOB1	NGFR	RFX8
MOK	SAMD4A	OSTF1	RAB11FIP2	TIPARP	ZNF778	ZFP161	ID3
ENOPH1	PHLDA2	C9orf41	VDAC1	RFK	IKZF5	PCLO	HBEGF
MTMR6	PAK1IP1	TRAPPC6B	HIPK3	KLHL8	IKBKAP	AKAP2	ZNF284
LPXN	EIF1B	ECHS1	FBXO5	SPRY4	CCP110	LPAR1	FGF1
AMIGO2	DCAF12	ZBTB11	PAICS	GAN	OTUD6B	SERTAD3	ELAVL2
TMPO	MB21D1	TAF1A	ZSCAN12	ZNF449	E2F3	FBXL3	WDR69
LTN1	BNC1	TAF4B	LOC96610	FAM107B	FZD8	SMEK3P	ID1
LTV1	HTATSF1	ANKRD50	GAS2L3	ZNF193	SIX4	WDR66	ELTD1
AIMP1	VEGFA	RAD1	DYRK3	SDR42E1	STARD13	FAM217B	ZIC2
PCID2	FGF2	CD274	ZNF200	FAM19A2	PER3	EIF5A2	DDIT4
SRGN	RRP15	CDKN2D	ZNF569	GDNF	SOX7	G0S2	MCTP1
SRGAP1	RELB	MCL1	FANCE	SLC25A25	BIRC3	FOXN2	FAM196B
C4orf43	B4GALT6	C4orf32	NT5E	KLF2	ZFP28	SP140	TMEM71
BRIX1	MTR	PPAT	ZNF594	RAB28	BRIP1	TOB2	MAPRE1
CWC27	STYX	APOO	USPL1	CCDC80	PLD6	MYBL1	ZC4H2
ATP8B1	MIDN	LRRCC1	ESF1	TOMM5	DSP	ZNF28	RAB3A
DHX33	PLAUR	TICAM1	KCTD6	MESDC1	ZNF25	KBTBD6	IL24
OTUD4	TRIM11	ZNF215	RAP2A	SLC16A7	E2F8	FAM129A	ENG
RALBP1	HMGB2	BTG3	RNF219	FASTKD3	ZNF225	ZNF503	BCHE
SLC3A2	FOSL2	BARD1	COL13A1	ZNF574	ZNF48	RNF182	
SNX24	NANP	ZNF263	NLRP3	SDHAP1	FNDC3A	C10orf116	
POLR3F	THUMPD1	MAPK6	SNAPC1	CPOX	KLHL11	CMAS	
AP1AR	TRMU	PIM3	CHIC2	CYB5R2	RP9	ZNF420	

shENG vs shScramle

Up-regulated genes							
GAGE10	MST4	PLEKHN1	CREB3L1	PDE4A	F11R	FAM101B	IRF2BPL
COL3A1	CHST15	NRP2	CELSR2	LIPG	STARD10	CPA4	DDR1
FRZB	MFAP2	PROS1	PHLDB3	FSTL5	PBX1	IGSF3	ITFG3
OLR1	OR7E12P	CEND1	C9orf116	IL1R1	DHCR7	SAMD9	LEPREL1
CD69	S1PR2	HCAR1	COLEC12	LOC100216545	ZNF608	ALDH4A1	OSBPL1A
CACNA2D1	ANKLE1	C4orf39	PFKFB4	LOC100134868	FBLN1	RELN	CLSTN3
PDPN	HLA-DOB	EPHB4	LOC388692	GPRC5B	PRUNE2	PSD4	MAN2A1
NTF3	LOC728392	C16orf5	LYPD3	GCHFR	SERPINH1	LOC149773	NNMT
NEDD9	MAP3K8	FAM26E	LFNG	TMEM150A	SLC17A9	FN1	STK38
LYPD6B	TOX	GPRC5C	BTN3A3	IPW	SORBS1	MAP3K5	SORT1
HTRA3	FHL1	KIAA1377	LOC401320	PODXL	ATP11A	NFIA	PDLIM1
ITM2A	ABHD15	NFKBIA	CAPN5	C12orf76	LMBR1L	NLGN2	SFMBT2
C10orf81	DISP2	SULF2	TSPAN9	COL5A1	DNAJB4	SHROOM2	BHLHE41
RNF128	KIAA1161	KIAA1522	LINC00263	KLF7	CLCN6	HLA-H	MFGE8
HAVCR2	CCL2	LOX	IL6	LIMCH1	SPTBN2	BBS9	TK2
SLC1A1	GLIPR2	FADS2	ARID5B	SGK1	TBC1D8B	F2RL1	CTSF
ALX4	NID2	ANGPTL2	C1QTNF1	CARD11	SGK223	ARL14	GBP1
MEST	IFI27	KLK6	ITGB8	TGFBR3	MGC21881	FBXL19	CRISPLD2
PPP1R14C	ZNF558	FLT1	IFITM1	TRIM55	MT1E	PLCE1	CDK14
ROPN1L	ANK1	BEND4	TRIM47	MEIS3P1	LOC730091	ZBTB47	DBN1
TNF	CYBRD1	RGS2	OAS2	ARHGAP28	ALDOC	AR	SPARC
RRAD	TNFSF10	TNFRSF11B	PBXIP1	SCD	REPS2	LEPREL2	LPCAT1
SEPT4	HSPA12A	SLC12A8	PDGFB	AMOT	DAB2IP	SLC25A23	C14orf133
MEGF10	ZNF518B	FLJ35776	KIAA1462	GSN	TRIM45	ARHGEF3	UBE2L6
RAB26	HBE1	FSTL3	DCDC2	PDGFRB	KCNN4	RGS14	TIMP4
MSC	PTGS1	ORAI3	CELSR1	SLC16A4	S100A3	PTGFRN	LIMK1
DAPK1	LLGL2	PLXND1	MCTP2	FAM84B	MAGEC1	SDC3	DPCD
ADC	FNDC4	CDKN2B	TTC39B	ADRA1B	CLDN11	CADM1	FBN1
MMP11	DMD	DNAJA4	HDAC11	BMF	CLIP2	COL4A5	PCYT2
FAM110B	PCOLCE	PIGZ	KLHDC8B	EMR1	EHHADH	NES	SNX18
C10orf10	GFRA1	IFIT1	PTPRR	CTGF	TMEM51	TNFRSF19	ACAP3
LINC00511	TPTEP1	NUAK2	ARHGAP27	PTK2B	NACC2	INHBA	CYBA
OASL	RASD2	TNIK	GREM1	SSC5D	CNTNAP1	RNF170	WNT5A
MN1	COL5A2	MMP15	TBX15	TMEM133	NRBP2	TTYH3	PCYOX1
LRRN4	LOC100129534	NFKBIZ	IGFBP4	TUBA1A	PAFAH2	SPPL2B	RAB3B
FAP	HAPLN3	VAT1L	FOXO4	CYR61	GNAO1	ECE1	SEMA4B
ATF3	RTN2	CCDC74A	DEM1	MPP2	LYST	PGPEP1	SIPA1
DMRT2	C3	PLAT	TRANK1	TSPAN15	SLC46A3	MOV10	IRF1
MX2	CGN	LOC644656	CPT1C	PCYOX1L	ENGASE	KRT15	CMTM3
KCNK6	FLNC	PNRC1	TRIB1	UST	PAPSS2	SEPT6	PEX6
DNM3OS	RGAG4	RNF157	LRRC17	SLC17A5	NAT14	GABARAPL1	ODZ2
EDN1	NBR2	KIAA1199	GALM	C20orf194	ITGA11	PLXNB1	FADS1
CD70	SLC25A42	C1QTNF6	PDGFRL	CCDC28B	FGF13	NME3	LGALS3
NXN	ATP7B	PIK3C2B	APCDD1L	SPATA6	SPOCK1	DHCR24	SYT11
QPRT	PADI1	SLC27A3	IRF5	PHLDA3	SIX5	FAM53B	APOL6
IFI44L	FLRT3	F2RL3	ASPHD1	AMIGO1	DNAJC4	BTN3A2	CHPF
SEL1L3	TM7SF2	CEBPD	GMIP	ZHX2	SERINC2	COL7A1	WDTC1
PAEP	MT1F	FRMD4B	HOOK2	C7orf41	MSMO1	CCDC71L	GADD45A
CD24	IRF9	OLFML2B	MMP17	MAPK8IP1	SCG2	NAPRT1	PRIC285
VGLL2	ARHGEF16	ST3GAL5	OCEL1	CXXC5	SLAMF7	NCOA7	TNK2
ACCN2	NTNG1	SARDH	TMEM102	S100A4	ULK1	DHRS1	LPIN1
LOC100216546	LOC158257	SIPA1L2	HKDC1	SFXN5	BANP	DRAM1	ATG9A
LOC728643	ELOVL2	LAMA5	TCEA2	LOC642852	MIB2	PPP1R3B	TNS3
ATP6V0D2	GATSL3	PLCXD3	P4HA2	PTPRU	SDK1	CALHM2	DPYSL3
TCN1	OAS1	SAMD9L	MRAS	IFIT3	GALK1	NCOA1	EFHC1
CTXN1	CITED2	EFNA1	MLLT3	PLD1	UBA7	HMGCS1	SPTLC2
DACT1	C14orf45	OLFML2A	KAZN	C14orf79	SMAD7	PARP10	ARMC9
EPHA4	SLC16A13	AFAP1L2	ESRG	ZC3H12A	ITPK1	ACBD7	GRB10
ATF7IP2	PGM2L1	P2RX6	SLC12A7	SECTM1	MFI2	TNFRSF9	PLXNB2
GDA	C1orf226	TTC30B	TFEB	ARHGEF4	PDE5A	ATP13A2	LAMB2
MX1	MMP13	IFIT2	CDKL5	HES6	NRN1	PAM	JUND
SMAD6	EGR1	XAF1	AQP1	MARCKSL1	PXDN	TRIM65	GABARAP
PARM1	PTGER4	ADORA1	BMP1	SH3TC1	PITPNM1	STAT2	F3
ADORA2A	HAVCR1	DIXDC1	HTR1D	CERCAM	ADA	DYNC2H1	KLF6
TMEM45A	FLRT2	CKB	ZNF385A	DOCK2	GPX3	RHBDF1	PLOD1
TMCC2	CCDC69	SPIRE2	OPLAH	STK32C	PACS1	GRAMD3	IDH1
L1CAM	STRA6	LOC100505817	SERPINA5	HSPA1A	WEE1	ERCC6	MYO18A
GJA3	ADAMTS15	VAV3	SAMD12	ENPP2	ING4	FASN	DAG1
EPHB6	MYO1D	LOC338799	CEP112	SYTL2	NDRG4	CD82	F2R
SEMA3B	KSR1	TNFAIP3	SLC6A9	TMEM117	TMEM67	SOX12	PGD
ACSS1	EPS8L2	ACTBL2	CMBL	TOR2A	TGFB1	COL12A1	MARCKS
JUP	EFEMP1	C1orf150	TMEM180	SLC43A2	CSMD2	COL1A1	
DPP4	CYP2S1	BST2	DUSP1	LTBP4	GPR126	COL6A1	
PCOLCE2	ABCA7	ZNF699	BCL6	TCF7	GBP2	PKP3	

Supplementary Table 2. Differentially expressed genes in anti-ENG-treated STS26T xenografts compared to control IgG-treated STS26T xenografts.

Anti-ENG vs IgG		
Down-regulated genes		**Up-regulated genes**
NFATC4	ITGA1	PKIB
AHRR	POSTN	C7
MAN1A1	RFX8	ATP5G1
FIBIN	AHSA2	PCNA
HMCN1	THBS2	ABLIM1
SEMA5A	PLXDC1	
FLT1	BMF	
SLC25A27	IGFBP2	

2. Publications

- **González Muñoz T**, Amaral AT, Puerto-Camacho P, Peinado H, de Álava E. Endoglin in the Spotlight to Treat Cancer. *International Journal of Molecular Sciences*. 2021; 22(6):3186. https://doi.org/10.3390/ijms22063186.

- **González-Muñoz T**, Kim, A., Ratner, N., Peinado, H. The need for new treatments targeting MPNST: filling in the gaps. *Clinical Cancer Research*, under review.

3. Oral presentations

- **TRACON SAB Annual Meeting**. San Diego, California, US, November 2018.
- **Congreso Médico Anual de Neurofibromatosis**. Madrid, Spain, June 2018.
- **6th and 8th CNIO Lab Day**. Madrid, Spain, December 2016 and 2018.
- **3er GEIVEX International Symposium**. San Sebastián, Spain, September 2016.

4. Poster presentations

- **2nd ASEICA Educational Symposium**. Madrid, Spain, November 2019.
- **2018 Joint Global Neurofibromatosis Conference**. Paris, France, November 2018.
- **2018 ISEV International Symposium**. Barcelona, Spain, May 2018.
- **1st ASEICA Educational Symposium**. Madrid, Spain, November 2017.
- **2017 NF Conference**. Washington DC, US, June 2017.